

**LOW MOLECULAR WEIGHT
CONTROLLED STRUCTURE
POLYETHYLENE SYNTHESIS**

**SYNTHESIS OF NARROWLY DISTRIBUTED
LOW MOLECULAR WEIGHT
POLYETHYLENE AND POLYETHYLENE MIMICS WITH
CONTROLLED STRUCTURES AND FUNCTIONALITIES**

By LAI CHI SO, B.A.Sc. (NANOTECHNOLOGY ENGINEERING)

A Thesis Submitted to the School of Graduate Studies in Partial Fulfilment of the
Requirements for the Degree of Master of Applied Science

McMaster University © Copyright by Lai Chi So, December 2012

MASTER OF APPLIED SCIENCE (2012)

McMaster University

(Chemical Engineering)

Hamilton, Ontario

TITLE: Synthesis of Narrowly Distributed Low Molecular Weight Polyethylene and Polyethylene Mimics with Controlled Structures and Functionalities

AUTHOR: Lai Chi So, B.A.Sc.
(University of Waterloo, Waterloo, ON, Canada)

SUPERVISORS: Dr. Shiping Zhu (McMaster University)
Dr. Santiago Faucher (Xerox Research Centre of Canada)
Dr. Hwee Ng (Xerox Research Centre of Canada)

NUMBER OF PAGES: xvii, 176

Abstract

The controlled synthesis of functional low molecular weight polyethylene and polyethylene mimics is important in tuning polymer properties and is of great industrial interests. Living polymerization is a method that allows for precise control in polymer structure. Although high molecular weight polymers with controlled structures can be efficiently produced via living polymerization, the production of low molecular weight polymers faces the challenges of the use of large amounts of expensive catalyst and the broadening of polydispersity.

The synthesis of well-defined functional low molecular weight polyethylene and polyethylene mimics is studied. Promising polymerization systems, including living ring opening metathesis polymerization (ROMP), living coordination polymerization, coordinative chain transfer polymerization (CCTP), and living C1 polymerization, are identified and are analyzed based on product properties, efficiency, cost, and safety.

Within the identified systems, living ROMP is selected for study due to the industrial relevance of ROMP polymers, the availability of raw materials, and the ease of reaction setup. The efficiency of ROMP is challenged by polydispersity broadening resulting from slow initiation and poor reactor volume efficiency due to its implementation as a solution polymerization process. The challenges are addressed by the use of excess phosphine and the realization of ROMP as a bulk polymerization process.

Experimental results demonstrate that bulk ROMP with and without phosphines yield product with similar or enhanced molecular weight distribution control as solution ROMP. Kinetic studies confirm living polymerization behaviour of bulk ROMP. A mathematical model is developed for the first time using method of moments to describe the kinetics and development of molecular weight distribution of ROMP. The model is a useful tool in preliminary research and commercialization of ROMP. The success of bulk ROMP and the development of a representative model yield ROMP as a promising method for the production of low molecular weight polymers with controlled architecture.

Acknowledgements

This Master's thesis opportunity was made possible thanks to my supervisors. To Dr. Shiping Zhu, for his knowledgeable insights and guidance. To Dr. Santiago Faucher, whose constant hunt for new adventures, unconventional thinking, and mentorship are only a few of the many traits that have made an impact on my life. I would like to thank Dr. Hwee Ng for taking me under his supervisor in the midst of my studies. I would also like to acknowledge Natural Sciences and Engineering Research Council of Canada (NSERC) and Xerox Research Centre of Canada (XRCC) for financial support through the NSERC Industrial Postgraduate Scholarships Program.

I would like to thank the research staff of XRCC, especially the analytical team whose expertise enabled the progress of this project and Kimberly Nosella whose mentorship is treasured. To the members of Dr. Shiping Zhu's research group, especially Dr. Dapeng Zhou, Cameron Derry, Weifeng Liu, and Chad Smithson, your friendships have made this experience memorable.

Finally, I would like to thank my friends and family for their encouragement throughout my studies. To my brother, for setting the standards high. To my dad, for his support. And mom, words cannot express my appreciation and gratitude.

Table of Contents

Abstract	iii
Acknowledgements	v
List of Schemes	ix
List of Figures	xi
List of Tables	xiii
List of Abbreviations and Symbols	xv
1. Introduction	1
1.1. Synthesis of Narrowly Distributed Low Molecular Weight Polymers	1
1.2. Research Objectives	4
1.3. References	8
2. Pathways for Synthesis of Low Molecular Weight Polymers with Controlled Structures	10
2.1. Living Ring Opening Metathesis Polymerization.....	10
2.1.1. Mechanism	10
2.1.2. Catalysts	12
2.1.3. Monomers.....	15
2.1.4. Living Ring-Opening Metathesis Polymerization Reactions.....	17
2.1.5. Summary	21
2.2. Living Coordination Polymerization	23
2.2.1. Mechanism	23
2.2.2. Catalysts and Co-Catalysts.....	26
2.2.3. Living Coordination Polymerization Reactions.....	34
2.2.4. Summary	41
2.3. Living Coordination Polymerization via Coordinative Chain Transfer.....	42
2.3.1. Mechanism	42
2.3.2. Catalyst, Co-Catalysts, and Chain Transfer Agents.....	45
2.3.3. Living Coordinative Chain Transfer Polymerization Reactions.....	49
2.3.4. Summary	54
2.4. Living C1 Polymerization via Polyhomologation.....	56
2.4.1. Mechanism	56
2.4.2. Catalysts	58
2.4.3. Monomers.....	60

2.4.4.	Living Polyhomologation Reactions.....	62
2.4.5.	Summary	65
2.5.	Application Concerns.....	66
2.6.	Conclusions.....	77
2.7.	References.....	79
3.	Bulk Synthesis of Narrowly Distributed Low Molecular Weight Polymers via Living Ring Opening Metathesis Polymerization.....	91
3.1.	Introduction.....	91
3.2.	Experimental	94
3.2.1.	Materials.....	94
3.2.2.	NMR Measurements	94
3.2.3.	GPC Measurements.....	94
3.2.4.	DSC Measurements.....	95
3.2.5.	Solution Polymerization.....	96
3.2.6.	Bulk Polymerization.....	97
3.2.7.	Kinetic Studies	97
3.3.	Results and Discussion.....	98
3.3.1.	Solution and Bulk Polymerization in the Absence of Phosphine.....	100
3.3.2.	Solution and Bulk Polymerization in the Presence of Phosphine	104
3.3.3.	Living Behaviour of Bulk Polymerization in the Presence of Phosphine	108
3.4.	Conclusions.....	112
3.5.	References.....	114
4.	Mathematical Modelling of Living Ring Opening Metathesis Polymerization	117
4.1.	Introduction.....	117
4.2.	Model Development.....	119
4.2.1.	Reaction Scheme	119
4.2.2.	Mass Balance Equations.....	122
4.2.3.	Method of Moments	123
4.3.	Model Validation	130
4.3.1.	Case I: Bulk Polymerization of 1,5-Cyclooctadiene via Grubbs' "First Generation" Catalyst and Triphenylphosphine	131
4.3.2.	Case II: Solution Polymerization of Cyclopentene via Grubbs' "First Generation" Catalyst and Tricyclohexylphosphine.....	137
4.4.	Results and Discussion.....	144

4.4.1. Effects of Catalyst Decomposition.....	146
4.4.2. Effects of Catalyst Activation and Deactivation	149
4.4.3. Effects of Intermolecular Chain Transfer Reactions.....	151
4.5. Conclusions.....	153
4.6. References.....	155
Appendices to Chapter 4.....	157
A.4.1. Reaction Mechanism.....	157
A.4.2. Mass Balance Equations.....	163
A.4.3. Mathematical Approximations for Generation of Species with Active Catalyst Centers via Chain Transfer Reactions.....	165
A.4.4. Mathematical Approximations for Generation of Species without Active Catalyst Centers via Chain Transfer Reactions	167
5. Conclusions and Recommendations	171
5.1. Conclusions.....	171
5.2. Recommendations.....	174

List of Schemes

- Scheme 2.1. A general reaction mechanism for living ROMP [1]. Note: L_n , M, and R represent the ligand, metal center, and pendent group on the catalyst. X and Y represent functional groups of the quenching reagent. k_p is the rate of propagation. 11
- Scheme 2.2. Mechanism for (a) increased initiation efficiency of biphosphine ruthenium catalysts and (b) decreased propagation rate via addition of more labile phosphine during polymerization [7]. Note: k_f , k_b , and k_p are the rates of catalyst activation, catalyst deactivation, and propagation, respectively..... 14
- Scheme 2.3. Cossee-Arlman mechanism for coordination polymerization of olefin monomers [41]. Note: M, P, and R represent the metal center of the catalyst, the propagating polymer chain, and the functional group of the monomer, respectively. 25
- Scheme 2.4. Proposed mechanism for metallocene/aluminum/boron ternary catalyst system [46]. Note: L_n , M, and Me represent the ligand, metal center, and methyl groups on the catalyst. BX_3 , AlR_3 , LA, and P represent the boron species, aluminum species, Lewis acid, and propagating polymer chain. x represents the number of LA..... 25
- Scheme 2.5. Mechanism for living CCTP [86], [87], [89] 2008. Note: L_n and M represent the ligand and metal center on the catalyst. P^1 and P^2 represent two different polymer chains. MGM represent the main-group metal alkyls used as CTA. n and $n-1$ represent the number of polymer chains attached to the MGM alkyl. R represents the functional group on the monomer. k_p is the rate of chain propagation and k_{ct} is the rate of chain transfer. 44
- Scheme 2.6. Proposed mechanism for living CCTP via a hafnium-based catalyst, an aluminum-based primary chain transfer agent, and a zinc-based secondary chain transfer agent [88]. Note: L_n represents the ligand on the catalyst. P_n represents polymer chains with n repeating units. k_p is the rate of chain propagation, $k_{ct[Al,Hf]}$ is the rate of chain transfer between chain growth state and primary chain transfer state, $k_{ct[Zn,Al]}$ is the rate of chain transfer between primary chain transfer state and secondary chain transfer state, and $k_{ct[Zn,Hf]}$ is the rate of chain transfer between chain growth state and secondary chain transfer state. 44
- Scheme 2.7. Proposed mechanism for polyhomologation [110]. Note: B and R are boron and alkyl functional groups on the borane catalyst. $Me_2(O)SCH_2$ is the ylide monomer and DMSO is dimethyl sulfoxide. R' is the functional group

incorporated onto the final polymer during boron-carbon bond cleavage and post-polymerization functionalization reactions.....	57
Scheme 3.1. Reaction scheme for living ROMP of 1,5-cyclooctadiene using a Grubbs' "first generation" ruthenium catalyst [9]. Note: k_f , k_b , k_p , and k_d are the rates of catalyst activation, catalyst deactivation, propagation, and depropagation, respectively.	99
Scheme 4.1. General living ROMP reaction scheme used in model development [3], [7].	121

List of Figures

Figure 3.1. Representative ^1H NMR spectrum of poly(1,5-cyclooctadiene) synthesized via bulk polymerization.	101
Figure 3.2. Comparison of the number average molecular weight (M_n) (diamond symbols) and polydispersities (PDI) (triangular symbols) of poly(1,5-cyclooctadiene) in solution ROMP (filled symbols) and bulk ROMP (empty symbols) via Grubbs' "first generation" catalyst in the absence of phosphine.	103
Figure 3.3. Comparison of (a) number average molecular weight (M_n), (b) polydispersity (PDI), and (c) conversion (x) of poly(1,5-cyclooctadiene) in solution ROMP (filled symbols) and bulk ROMP (empty symbols) with Grubbs' "first generation" catalyst in the presence of triphenylphosphine.	107
Figure 3.4. Time evolution of molecular weight distributions for room temperature bulk ROMP of 1,5-cyclooctadiene with Grubbs' "first generation" catalyst in the presence of triphenylphosphine with $[\text{M}]_0$ of 8.2 M, $[\text{M}]_0/[\text{I}]$ of 150, and $[\text{P}]_0/[\text{I}]$ of 10.	110
Figure 3.5. (a) Number-average molecular weight (M_n) versus conversion (x) plot, (b) polydispersity (PDI) versus conversion (x) plot, and (c) first-order rate plot for room temperature bulk ROMP of 1,5-cyclooctadiene with Grubbs' "first generation" catalyst in the presence of triphenylphosphine with $[\text{M}]_0$ of 8.2 M, $[\text{M}]_0/[\text{I}]$ of 150, and $[\text{P}]_0/[\text{I}]$ of 10. Conversion was determined by GPC.	111
Figure 4.1. Comparison of experimentally determined (filled symbols) and model simulations (solid and dashed lines) of (a) number-average molecular weight (M_n) versus conversion (x) plot, (b) polydispersity (PDI) versus conversion (x) plot, and (c) first-order rate plot for bulk ROMP of 1,5-cyclooctadiene.	136
Figure 4.2. Comparison of time evolution of experimentally determined molecular weight (M_n) (filled symbols) and polydispersity (PDI) (empty symbols) with model predictions of M_n (solid line) and PDI (dashed line) for the polymerization of cyclopentene. Experimental data was reported by Myers and Register [1].	141
Figure 4.3. Comparison of time evolution of experimentally determined true conversion (filled symbols) and apparent conversion (empty symbols) with model predictions (solid line) for the polymerization of cyclopentene. True conversion was determined by GPC and apparent conversion was calculated from M_n assuming that each catalyst results in the growth of one chain. Experimental data was reported by Myers and Register [1].	141

Figure 4.4. Effects of catalyst decomposition on the time evolution of (a) conversion and number-average molecular weight and (b) polydispersity in living ROMP. k_{de} values of 10^{-4} s^{-1} (solid line), 10^{-5} s^{-1} (dashed line), and 10^{-6} s^{-1} (dotted line) were used in simulation.	148
Figure 4.5. Effects of catalyst activation and deactivation on the time evolution of (a) conversion and number-average molecular weight and (b) polydispersity in living ROMP. k_b/k_f values of 100 (solid line), 1000 (dashed line), and 10,000 (dotted line) were used in simulation.	150
Figure 4.6. Effects of intermolecular chain transfer reactions on the time evolution of (a) conversion and number-average molecular weight and (b) polydispersity in living ROMP. $k_{tr, inter}$ values of $10^{-3} \text{ L mol}^{-1} \text{ s}^{-1}$ (solid line), $10^{-4} \text{ L mol}^{-1} \text{ s}^{-1}$ (dashed line), and $10^{-5} \text{ L mol}^{-1} \text{ s}^{-1}$ (dotted line) were used in simulation.	152

List of Tables

Table 2.1. Catalysts for living ROMP.	14
Table 2.2. Monomers for living ROMP.....	16
Table 2.3. Ring strain of living ROMP monomers.	16
Table 2.4. Selected examples of living ROMP reactions.	20
Table 2.5. Metallocene-based catalysts for living coordination polymerization.	28
Table 2.6. Co-catalysts for living coordination polymerization.	29
Table 2.7. Non-metallocene-based catalyst for living coordination polymerization.....	32
Table 2.8. Selected examples of living coordination polymerization reactions via metallocene-type catalysts.	38
Table 2.9. Selected examples of living coordination polymerization reactions via non-metallocene-type catalysts.	40
Table 2.10. Catalysts for living CCTP.....	47
Table 2.11. Chain transfer agents for living CCTP.	48
Table 2.12. Selected examples of living CCTP reactions.....	52
Table 2.13. Catalysts for living polyhomologation.	59
Table 2.14. Monomers for living polyhomologation.....	61
Table 2.15. Selected examples of living polyhomologation reactions.	64
Table 2.16. Polymer molecular weight produced via polymerization reactions.....	67
Table 2.17. Polydispersities of polymer produced via polymerization reactions.	68
Table 2.18. Turnover frequency of polymerization reactions.....	70
Table 2.19. Comparison of reactor volume efficiency and catalyst cost efficiency of polymerization reactions.	74
Table 2.20. Prices for transition metals present in catalysts.	76
Table 3.1. Solution and bulk ROMP of 1,5-cyclooctadiene with Grubbs' "first generation" catalyst in the absence of phosphine.	103
Table 3.2. Solution and bulk ROMP of 1,5-cyclooctadiene with Grubbs' "first generation" catalyst in the presence of triphenylphosphine.....	106
Table 4.1. Chain species resulting from the living ROMP mechanism used in model development.	122
Table 4.2. j^{th} order moment equations for chain species in living ROMP.....	125
Table 4.3. Reaction conditions used for reactions and in simulated model for bulk living ROMP of 1,5-cyclooctadiene.....	132
Table 4.4. Kinetic parameters used in simulated models for bulk living ROMP of 1,5-cyclooctadiene.....	132

Table 4.5. Reaction conditions used for reactions and in simulated model, and kinetic parameters used in simulated model for solution living ROMP of cyclopentene.	138
Table A.4.1.1. Detailed living ROMP mechanism used in model development [3], [7].	158
Table A.4.2.1. Mass balance equations for chain species formation in living ROMP. ...	163

List of Abbreviations and Symbols

[I]₀	Initial catalyst concentration (mol L ⁻¹)
[M]₀	Initial monomer concentration (mol L ⁻¹)
[M]_{eff}	Effective monomer concentration defined as [M] ₀ – [M] _{eq} (mol L ⁻¹)
[M]_{eq}	Equilibrium monomer concentration (mol L ⁻¹)
[P]₀	Initial triphenylphosphine (PPh ₃) concentration (mol L ⁻¹)
•I	Active catalyst species
•IM_i	Chain species with <i>i</i> monomers and 1 active catalyst center
•IM_iI	Chain species with <i>i</i> monomers, 1 active catalyst center, and 1 dormant catalyst center
•IM_iI^D	Chain species with <i>i</i> monomers, 1 active catalyst center, and 1 decomposed catalyst center
1,5-COD	1,5-cyclooctadiene
Ar	2,6-(<i>i</i> -Pr) ₂ Ph
B-C	Boron-carbon bond
BHT	2,6-di- <i>tert</i> -butyl-4-methylphenol (butylated hydroxytoluene)
Bz	Benzene
C=C	Carbon-carbon double bond
CB	Chlorobenzene
CCTP	Catalytic chain transfer polymerization
CGS	Chain growth state
CP	Cyclopentene
Cp	Cyclopentadienyl
Cp*	Pentamethylcyclopentadienyl
CTA	Chain transfer agent
CTM	Chain transfer mediator
CTS	Chain transfer state
Cy	Cyclohexyl
D	1-decene
DCB	Dichlorobenzene
DCM	Dichloromethane
DEE	Diethyl ether
DMSO	Dimethyl sulfoxide
DSC	Differential scanning calorimetry
E	Ethylene

<i>f</i>	Initiator efficiency calculated as $([M]_0 / [I]) \times (x / (M_n / (\text{monomer molecular weight})))$
Flu	Fluorenyl
GI	Bis(tricyclohexylphosphine)benzylidene ruthenium(IV) dichloride (Grubbs' "first generation" catalyst)
GPC	Gel permeation chromatography
H	1-hexene
H₂IMes	1,3-dimesityl-imidazolidine-2-ylidene
HD	1,5-hexadiene
I	Dormant catalyst (Catalyst after phosphine exchange)
I⁰	Initial catalyst species
I^DM_i	Chain species with <i>i</i> monomers and 1 decomposed catalyst center
I^DM_iI^D	Chain species with <i>i</i> monomers and 2 decomposed catalyst centers
IM_i	Chain species with <i>i</i> monomers and 1 dormant catalyst center
IM_iI	Chain species with <i>i</i> monomers and 2 dormant catalyst centers
IM_iI^D	Chain species with <i>i</i> monomers, 1 dormant catalyst center, and 1 decomposed catalyst center
Ind	Indenyl
IP	Isoprene
<i>k_b</i>	Rate constant for catalyst deactivation (s ⁻¹)
<i>k_d</i>	Rate constant for depropagation (s ⁻¹)
<i>k_{de}</i>	Rate constant for catalyst decomposition (s ⁻¹)
<i>k_f</i>	Rate constant for catalyst activation (s ⁻¹)
<i>k_p</i>	Rate constant for propagation (L mol ⁻¹ s ⁻¹)
<i>k_{tr, inter}</i> (<i>k_{tr}</i>)	Rate constant for intermolecular chain transfer (L mol ⁻¹ s ⁻¹)
M	Monomer species
MGM	Main-group metal
M_i	Chain species with <i>i</i> monomers and no catalyst centers
<i>M_n</i>	Number-average molecular weight (g/mol)
<i>M_{n,th}</i>	Theoretical number-average molecular weight calculated as (monomer molecular weight) $\times x \times [M]_0 / [I]$
<i>M_w</i>	Weight-average molecular weight (g/mol)
N	Norborene
NCN	Nitrogen-carbon-nitrogen ligand
NHC	<i>N</i> -heterocyclic carbenes
NMR	Nuclear magnetic resonance
O	1-octene

<i>o</i>-DCB	<i>Ortho</i> -dichlorobenzene
ODE	Ordinary differential equation
P	Triphenylphosphine (PPh ₃) added to the reaction
p(1,5-COD)	Poly(1,5-cyclooctadiene)
p(CP)	Polycyclopentene
P⁰	Tricyclohexylphosphine (PCy ₃) dissociated from the initial catalyst
PCy₃	Tricyclohexylphosphine
PDI	Polydispersity index
PE	Polyethylene
Ph	Phenyl
PL	Propylene
P_M	Monomer pressure (atm)
PPh₃	Tricyclohexylphosphine
<i>Rac</i>-(Et)Ind₂	<i>Racemic</i> -ethylenebis(indenyl)
<i>r_n</i>	Number-average chain length
ROMP	Ring opening metathesis polymerization
RT	Room temperature
Ru	Ruthenium
<i>r_w</i>	Weight-average chain length
St	Styrene
<i>T_g</i>	Glass transition temperature (°C)
THF	Tetrahydrofuran
<i>T_{m, midpoint}</i>	Midpoint melting temperature (°C)
<i>T_{m, offset}</i>	Offset melting temperature (°C)
<i>T_{m, onset}</i>	Onset melting temperature (°C)
TMS	Tetramethylsilane
TOF	Turnover frequency (mol mol ⁻¹ h ⁻¹ for liquid monomers; mol mol ⁻¹ h ⁻¹ atm ⁻¹ for gaseous monomers)
Tol	Toluene
Tol-<i>d</i>8	Deuterated toluene
<i>T_p</i>	Temperature of polymerization reaction (°C)
<i>t_p</i>	Time of polymerization reaction
<i>T_R</i>	Reaction temperature (°C)
VCH	Vinylcyclohexane
vers	Versatate
<i>x</i>	Conversion

1. Introduction

1.1. Synthesis of Narrowly Distributed Low Molecular Weight Polymers

The precise control of molecular weight and chain microstructure is critically important in the control of polymer chemical and physical properties and is a topic of fundamental importance in polymer synthesis [1]. For the simplest polymer chain – polyethylene (PE) – polymer morphology, chemical properties, phase properties, and mechanic properties can be adjusted by changing the physical and chemical characteristics of the polymer, including molecular weight, molecular weight distribution, branching, and chain-end functionality. Specifically, the synthesis of narrowly distributed, low molecular weight, and functional PEs is of great industrial interest. Low molecular weight PEs and PE mimics are used in various applications, including lubricants, adhesives, inks, and polymer additives. The uniformity of narrowly distributed polymers allows for consistent material performance and tailored functionalization allows for polymer processing and applications in different media.

Low molecular weight PEs and PE mimics can be industrially obtained via thermal cracking processes [2]. However, these inexpensive polymers lack microstructure, polydispersity, and functionalization control [3]. As a result, commercial low molecular

weight polymers are not suitable for technologically advanced applications, such as printing inks, where defined chemical and physical properties are required.

Polymerization reactions can also be used to obtain low molecular weight PEs and PE mimics. Living or controlled alkene polymerization, the use of chain transfer reactions, and the controlled copolymerization of alkenes with functional monomers are various methods for controlling physical and chemical properties of PEs in its synthesis. Living or controlled polymerization is a method that allows for high degrees of control in molecular weight and polymer architectures [1]. In an ideal living polymerization system, the reaction proceeds to complete monomer conversion, the number of active centers remains constant during polymerization, there is fast and complete initiation, there are no chain transfer reactions or polymer chain termination, there is a linear relationship between degree of polymerization (or number-average molecular weight, M_n) and monomer consumption, the polydispersity indices (PDI) are of less than 1.5, and chain-end functionalization can be synthesized [1], [4]. Since often one active catalytic center mediates the growth of one polymer chain, the polymerization of low molecular weight product poses the challenge of the use of large amounts of expensive catalysts.

However, in reality, slow initiation and polymer chain termination result in a lack of ideal living behaviour. For the synthesis of high molecular weight polymers, the non-idealities are dissimulated by the majority of the population, that is late initiated or early terminated polymer chains will not greatly affect the polydispersity of high molecular weight

polymers produced by living polymerization. Contrarily, in the synthesis of low molecular weight polymers via living polymerization, Poisson broadening of the molecular weight distribution plays a significant role and the non-idealities can have a profound impact on the properties of the product. Therefore, the production of narrowly distributed low molecular weight polymers via living polymerization systems is challenged by polydispersity broadening.

1.2. Research Objectives

In this thesis, the synthesis of narrowly distributed low molecular weight polymers, specifically of simple PE structure, is studied. Polymers with molecular weights in the order of 10^3 g/mol and polydispersities of less than 1.20 are of specific interest. Chain-end and backbone functionalization, reaction efficiency, reaction cost, and industrial applications are also of interest.

A review of reported polymerization systems that allow for the synthesis of narrowly distributed low molecular weight PEs and PE mimics is provided in **Chapter 2**. Polymerization systems, including living ring-opening metathesis polymerization (ROMP), living coordination polymerization, living coordination polymerization via coordinative chain transfer, and living C1 polymerization via polyhomologation, have been identified as promising polymerization systems. The mechanisms of these polymerization systems are discussed in detail, along with the availability and ease of preparation of the raw materials required for these systems. Reported reactions for the synthesis of PEs and PE mimics with low molecular weights and polydispersities are summarized. Comparisons of reaction efficiency, cost, and safety are also presented.

From the review in **Chapter 2**, living ROMP is selected for study due to the industrial relevance of ROMP polymers, the availability of raw materials, and the ease of polymerization setup [5]. Living ROMP is a coordination-type living chain growth

polymerization process, which has been studied considerably [4], [6]. Living ROMP converts cyclic olefins into narrowly distributed polymeric materials with periodic carbon-carbon double bond (C=C) unsaturations. The periodic C=C unsaturations can be exploited via post-polymerization reactions to obtain polymers with various controlled architectures. Post-polymerization hydrogenation or functionalization reactions can be employed to yield PE mimics or functional polymers, respectively [7–9].

There are numerous experimental studies in living ROMP as a solution polymerization process using various reagents. Due to the large volume of solvents used in solution polymerization, the polymer product generally contributes to less than 50 wt. % of the reactor solution, leading to poor reactor volume efficiencies [10–20]. Although successful bulk polymerizations of cyclopentene and cycloheptene have been reported, detailed studies of the behaviour and products of bulk ROMP have not been reported [10]. In **Chapter 3**, the behaviour and products of bulk ROMP of 1,5-cyclooctadiene with a ruthenium-based catalyst and phosphine-based polymerization regulator are presented and contrasted with that of solution ROMP. It is demonstrated that bulk ROMP yields similar, if not improved, molecular weight control as compared to solution ROMP. In addition, the living behaviour of the solution process is maintained when the process is converted into a bulk process.

The behaviour and products of ROMP obtained in experimental work can be explained and predicted by modelling the ROMP process. A simple kinetic model for the ROMP of

cyclopentene using a ruthenium-based catalyst enhanced by the addition of tricyclohexylphosphine as a polymerization regulator has been reported [10], [11]. The model is based on the assumption that the rate of monomer consumption is first-order in monomer concentration and initiator concentration. This highly simplistic model does not consider non-idealities, including but not limited to chain transfer reactions and catalyst decomposition, which are present in the real system. The model only allows for determining number-average molecular weight and conversion and does not provide any information on molecular weight distribution.

In **Chapter 4**, a model to describe the reaction kinetics and molecular weight distribution of phosphine-enhanced ruthenium-based living ROMP is presented. The method of moments is applied in model development, such that non-idealities, including intermolecular chain transfer reactions and catalyst decomposition, can be considered. The model is validated with experimental data obtained for the bulk ROMP of 1,5-cyclooctadiene and published literature data obtained for the solution ROMP of cyclopentene. The effects of catalyst decomposition, catalyst activation and deactivation, and intermolecular chain transfer reactions on reaction kinetics and molecular weight distribution are also discussed. It is demonstrated that the model provides new insights into the ROMP mechanism and may be applied in new experiment design and as a predictive model.

Finally, the research of the thesis is summarized in **Chapter 5**. The contributions of the research to the field of polymer synthesis and recommendations for future research are presented.

1.3. References

- [1] G. J. Domski, J. M. Rose, G. W. Coates, A. D. Bolig, and M. Brookhart, “Living Alkene Polymerization: New Methods for the Precision Synthesis of Polyolefins,” *Progress in Polymer Science*, vol. 32, pp. 30–92, 2007.
- [2] P. S. Umare, K. Rao, G. L. Tembe, D. A. Dhoble, and B. Trivedi, “Controlled Synthesis of Low-Molecular-Weight Polyethylene Waxes by Titanium – Biphenolate – Ethylaluminum Sesquichloride Based Catalyst Systems,” *Journal of Applied Polymer Science*, vol. 104, pp. 1531–1539, 2007.
- [3] C. R. Luo, F. Ding, H. R. Zhang, L. Xiong, H. J. Guo, and X. D. Chen, “Wax Formation Study by the Pyrolysis of High Density Polyethylene,” *Advanced Materials Research*, vol. 418–420, pp. 1673–1676, Dec. 2012.
- [4] C. W. Bielawski and R. H. Grubbs, “Living Ring-Opening Metathesis Polymerization,” *Progress in Polymer Science*, vol. 32, pp. 1–29, 2007.
- [5] S. Sutthasupa, M. Shiotsuki, and F. Sanda, “Recent Advances in Ring-Opening Metathesis Polymerization, and Application to Synthesis of Functional Materials,” *Polymer Journal*, vol. 42, pp. 905–915, 2010.
- [6] C. Slugovc, “The Ring Opening Metathesis Polymerisation Toolbox,” *Macromolecular Rapid Communications*, vol. 25, pp. 1283–1297, 2004.
- [7] M. A. Hillmyer, S. T. Nguyen, and R. H. Grubbs, “Utility of a Ruthenium Metathesis Catalyst for the Preparation of End-Functionalized Polybutadiene,” *Macromolecules*, vol. 30, pp. 718–721, 1997.
- [8] O. J. Kwon, H. T. Vo, S. B. Lee, T. K. Kim, H. S. Kim, and H. Lee, “Ring-Opening Metathesis Polymerization and Hydrogenation of Ethyl-Substituted Tetracyclododecene,” *Bulletin of the Korean Chemical Society*, vol. 32, pp. 2737–2742, 2011.
- [9] M. P. McGrath, E. D. Sall, and S. J. Tremont, “Functionalization of Polymers by Metal-Mediated Processes,” *Chemical Reviews*, vol. 95, pp. 381–398, 1995.
- [10] A. Hejl, O. A. Scherman, and R. H. Grubbs, “Ring-Opening Metathesis Polymerization of Functionalized Low-Strain Monomers with Ruthenium-Based Catalysts,” *Macromolecules*, vol. 38, pp. 7214–7218, 2005.

- [11] S. B. Myers and R. A. Register, "Synthesis of Narrow-Distribution Polycyclopentene Using a Ruthenium Ring-Opening Metathesis Initiator," *Polymer*, vol. 49, pp. 877–882, 2008.
- [12] S. T. Trzaska, L. W. Lee, and R. A. Register, "Synthesis of Narrow-Distribution 'Perfect' Polyethylene and Its Block Copolymers by Polymerization of Cyclopentene," *Macromolecules*, vol. 33, pp. 9215–9221, 2000.
- [13] G. C. Bazan et al., "Living Ring-Opening Metathesis Polymerization of 2,3-Difunctionalized Norbornenes by $\text{Mo}(\text{CH-t-Bu})(\text{N-2,6-C}_6\text{H}_3\text{-i-Pr}_2)(\text{O-t-Bu})_2$," *Journal of the American Chemical Society*, vol. 112, pp. 8378–8387, 1990.
- [14] G. C. Bazan, S. R., H.-N. Cho, and V. C. Gibson, "Polymerization of Functionalized Norbornenes Employing $\text{Mo}(\text{CH-t-Bu})(\text{NAr})(\text{O-t-Bu})_2$ as the Initiator," *Macromolecules*, vol. 24, pp. 4495–4502, 1991.
- [15] C. W. Bielawski and R. H. Grubbs, "Increasing the Initiation Efficiency of Ruthenium-Based Ring-Opening Metathesis Initiators: Effect of Excess Phosphine," *Macromolecules*, vol. 34, pp. 8838–8840, 2001.
- [16] T.-L. Choi and R. H. Grubbs, "Controlled Living Ring-Opening-Metathesis Polymerization by a Fast-Initiating Ruthenium Catalyst," *Angewandte Chemie International Edition*, vol. 42, pp. 1743 – 1746, 2003.
- [17] L.-B. W. Lee and R. A. Register, "Hydrogenated Ring-Opened Polynorbornene : A Highly Crystalline Atactic Polymer," *Macromolecules*, vol. 38, pp. 1216–1222, 2005.
- [18] B. R. Maughon and R. H. Grubbs, "Ruthenium Alkylidene Initiated Living Ring-Opening Metathesis Polymerization (ROMP) of 3-Substituted Cyclobutenes," *Macromolecules*, vol. 30, pp. 3459–3469, 1997.
- [19] J. S. Murdzek and R. R. Schrock, "Low Polydispersity Homopolymers and Block Copolymers by Ring Opening of 5,6-Dicarbomethoxynorbornene," *Macromolecules*, vol. 20, pp. 2640–2642, 1987.
- [20] R. Singh, C. Czekelius, and R. R. Schrock, "Living Ring-Opening Metathesis Polymerization of Cyclopropenes," *Macromolecules*, vol. 39, pp. 1316–1317, 2006.

2. Pathways for Synthesis of Low Molecular Weight Polymers with Controlled Structures

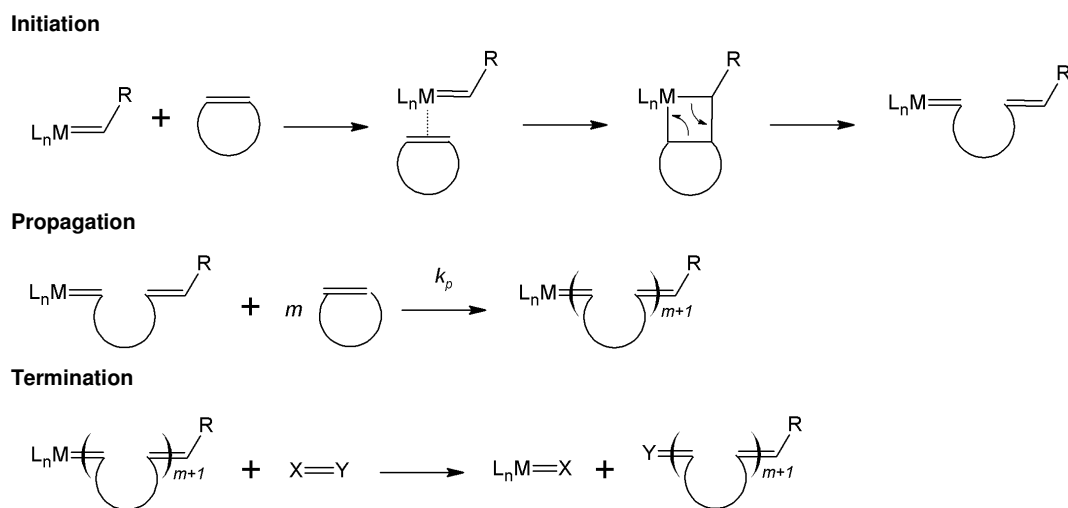
This chapter is based on the manuscript authored by Lai Chi So, Santiago Faucher, and Shiping Zhu entitled “Synthesis of Low Molecular Weight Polyethylene Polymers with Controlled Structures” prepared for submission for publication. Lai Chi So carried out the literature review under the guidance of Dr. Faucher. Dr. Faucher and Dr. Zhu aided in manuscript revision.

2.1. Living Ring Opening Metathesis Polymerization

2.1.1. Mechanism

Living ring opening metathesis polymerization (ROMP) is a chain growth polymerization process, which converts cyclic olefins into polymers with low polydispersities [1]. A general mechanism for ROMP is shown in **Scheme 2.1** [1]. The polymerization mechanism is based on olefin metathesis reaction, where two carbon-carbon double bonds (C=C) are removed and two new C=C are created [2]. ROMP is catalyzed by transition metal centers with associated ligands. In initiation, the monomer coordinates to the metal center of the metal alkylidene catalyst. [2+2]-cycloaddition followed by cycloreversion forms a new metal alkylidene containing the first polymer chain unit. The driving force for polymerization is the strain of the ring between the metal center and the alkylidene ligand [1], [2]. Propagation follows the same steps as initiation. Polymerization stops

when all the monomer is consumed, a reaction equilibrium is reached, or the reaction is terminated with a known agent to remove the metal from the polymer chain [1].



Scheme 2.1. A general reaction mechanism for living ROMP [1]. Note: L_n , M , and R represent the ligand, metal center, and pendent group on the catalyst. X and Y represent functional groups of the quenching reagent. k_p is the rate of propagation.

2.1.2. Catalysts

Catalysts with various metal centers and ligands, which provide tunability of reaction characteristics, have been reported for living ROMP. The molybdenum (Mo) based Schrock's catalysts and the ruthenium (Ru) based Grubbs' catalysts are two common groups of catalysts. Most of the catalysts shown in **Table 2.1** are commercially available. **Mo-1** and **Ru-2** can be synthesized according to literature procedures [3–5].

The Schrock's catalysts and their derivatives, **Mo-1**, **Mo-2**, and **Mo-3**, shown in **Table 2.1**, are suitable for living ROMP due to their rapid initiation and propagation rates [6]. Catalyst activities are tuned by modifying the alkoxide ligand, where more electron withdrawing ligands allow for increased activities [1]. However, these catalysts have restricted functional-group tolerance and sensitivity towards protic solvents and air [2].

Grubbs' "first generation" catalyst, **Ru-1** demonstrates enhanced tolerances to functional groups, protic solvents, and air [3]. To enhance the application of biphosphine ruthenium alkylidene catalysts, such as **Ru-1**, **Ru-2**, and **Ru-3**, the use of excess phosphine has been reported. Catalyst initiation involves the dissociation of phosphine ligand from biphosphine ruthenium alkylidene catalysts to create a monomer coordination site. The rate of phosphine exchange (i.e. the exchange of the original phosphine ligand with the added excess phosphine) is faster than the rates of reactions with olefins for the ruthenium catalysts [1], [7]. The use of relatively labile phosphines to the ruthenium catalysts leads

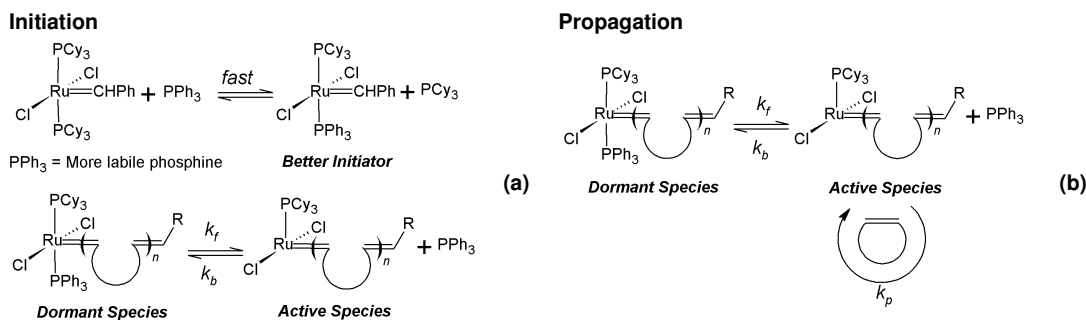
to the formation of a ruthenium-based catalyst with enhanced initiation efficiency, as illustrated in **Scheme 2.2 (a)**. The added phosphine also competes with monomer for the metal center and lowers the rate of propagation, as illustrated in **Scheme 2.2 (b)**. This concept is similar to controlled living free radical polymerization, in which specific chemical species are added to favour the probability of radical deactivation over monomer propagation [8]. The molecular weight distributions of the resulting polymers are closer to theoretical values. It has also been reported that the addition of phosphine does not affect the polymerization of functional monomers, such as monomers consisting of amino ester and alcohol groups [7].

As discussed, increased initiation efficiency enhances living polymerization behaviour. By tuning the nature of the phosphine ligand and the ligand environment of ruthenium-based catalysts, not only can initiation rate be increased, ROMP activity can also be improved [9]. In ROMP, phosphine dissociation from the metal center is required prior to olefin coordination. Stabilization of the intermediates is necessary to prevent premature catalyst decomposition. *N*-heterocyclic carbenes (NHC) are strong σ -donors but are less labile than the phosphines in **Ru-1** [10], [11]. They are less likely to dissociate from the catalyst but provide increased electron density to stabilize the intermediates. By changing the phosphine ligands to a combination of strongly ligating NHCs and weakly coordinating pyridines, such as Grubbs' "third generation" catalyst, **Ru-3**, fast initiation and high activities for ROMP has been demonstrated.

Table 2.1. Catalysts for living ROMP.

Catalyst	Ref.
Mo-1 Mo(NAr)[CH(<i>t</i> -Bu)][O(<i>t</i> -Bu)] ₂	[4], [5]
Mo-2 Mo(NAr)[CH(CH ₃) ₂ Ph][OC(CH ₃) ₃] ₂	Strem Chemical
Mo-3 Mo(NAr)[CH(CH ₃) ₂ Ph][OC(CH ₃)(CF ₃) ₂] ₂	Strem Chemical
Ru-1 (PCy ₃) ₂ (Cl) ₂ Ru=CHPh (Grubbs' "first generation" catalyst)	Sigma-Aldrich
Ru-2 (PCy ₃) ₂ (Cl) ₂ Ru=(CH) ₂ CPh ₂ ,	[3]
Ru-3 (H ₂ IMes)(3-Br-py) ₂ (Cl) ₂ Ru=CHPh, (Grubbs' "third generation" catalyst)	Sigma-Aldrich

Ar = 2,6-(*i*-Pr)₂Ph; Cy = cyclohexyl; H₂IMes = 1,3-dimesityl-imidazolidine-2-ylidene



Scheme 2.2. Mechanism for (a) increased initiation efficiency of biphosphine ruthenium catalysts and (b) decreased propagation rate via addition of more labile phosphine during polymerization [7]. Note: k_f , k_b , and k_p are the rates of catalyst activation, catalyst deactivation, and propagation, respectively.

2.1.3. Monomers

Living ROMP has been demonstrated for a variety of cyclic olefinic monomers. High ring strain monomers, such as functionalized cyclopropene, functionalized cyclobutene, norbornene and its functionalized derivatives, and *trans*-cyclooctene, have been successfully polymerized to greater than approximately 80% yield. Lower ring strain monomers, including cyclopentene, cycloheptene, and 1,5-cyclooctadiene, are also possible candidates and have been polymerized with lower yields. The types and availability of the cyclic olefinic monomers used in literature are given in **Table 2.2**.

The driving force of ROMP is the release of ring strain energy associated with ring opening. Therefore, polymerization reactions can easily reach high conversions for high ring strain monomers. However, for low ring strain monomers, the gain in enthalpy of ring opening is countered by a loss of entropy in polymerization. There exists an equilibrium between monomeric and polymeric form and any monomer below the equilibrium monomer concentration is not converted to polymer [12]. To avoid molecular weight distribution broadening through propagation-depropagation equilibrium, the monomer concentration should remain above the equilibrium monomer concentration [13]. The equilibrium monomer concentrations for cyclopentene and 1,5-cyclooctadiene at room temperature were reported to be 1.3 mol/L and 0.25 mol/L respectively [13], [14]. **Table 2.3** summarizes the ring strain of various cyclic olefinic monomers used for living ROMP.

Table 2.2. Monomers for living ROMP.

Monomer		Ref.
<i>f</i> -CPr	3,3-disubstituted cyclopropene	[15], [16]
<i>f</i> -CB	Functionalized cyclobutene	[17]
CP	Cyclopentene	Sigma-Aldrich
<i>f</i> -CP	Functionalized cyclopentene	[12]
N	Norbornene	Sigma-Aldrich
<i>f</i> -N	Functionalized norbornene	[18], [19], and Sigma-Aldrich
<i>f</i> -CHp	Functionalized cycloheptene	[12]
<i>t</i> -CO	<i>Trans</i> -cyclooctene	[20]
<i>f-t</i> -Co	Functionalized <i>trans</i> -cyclooctene	[21]
COD	1,5-cyclooctadiene	Sigma-Aldrich

Table 2.3. Ring strain of living ROMP monomers.

Monomer	Number of C in ring	Ring strain (kcal/mol)	Ref.
Cyclopropene	3	55.1	[22]
Cyclobutene	4	28.0	[22]
Norbornene	5	23.62	[23]
<i>Trans</i> -cyclooctene	8	17.85	[23]
1,5-cyclooctadiene	8	13.28	[23]
Cycloheptene	7	7.35	[23]
Cyclopentene	5	6.93	[23]

2.1.4. Living Ring-Opening Metathesis Polymerization Reactions

The synthesis of living ROMP polymers using various combinations of catalysts and monomers have been reported in literature. **Table 2.4** provides a summary of reported living ROMP reactions which yield low molecular weight polyethylene (PE) mimics with low polydispersities.

The living ROMP of high ring strain monomers yield products with low molecular weights and polydispersities. Singh et al. from the Schrock group studied the polymerization of functionalized cyclopropene using molybdenum-based catalysts (reactions **ROMP-1** to **ROMP-3**) [16]. Products with molecular weights between 8,210 g/mol to 11,900 g/mol, polydispersities of less than 1.05 to 1.50, and over 90% yield was obtained in one hour via solution polymerization at room temperature. Similarly, solution ROMP of functionalized cyclobutene at room temperature and at 45 °C yielded narrowly distributed low molecular weight polymers with yields above 79% (reactions **ROMP-4** and **ROMP-5**) [17]. *Trans*-cyclooctene and its derivatives are also monomers of high ring strain. However, the larger ring structure of cyclooctene renders the synthesis of low molecular weight more challenging. Walker et al. from the Grubbs group reported polymerization of *trans*-cyclooctene and its derivatives using ruthenium-based catalysts and excess phosphines yielding polymers with molecular weights in the range of 10^4 g/mol to 10^5 g/mol, polydispersities of 1.02 to 1.60, and yields ranging from 66% to 99%

under mild solution polymerization conditions for less than 10 min (reactions **ROMP-6** and **ROMP-7**) [21].

Although monomers with high ring strain can yield narrowly dispersed low molecular weight polymers, the monomers are not readily available, have limited shelf-lives, and are difficult to handle [15]. Norbornene is a high ring strain monomer, is commercially available, and has been intensively studied in its application in ROMP by both the Schrock and Grubbs groups (reactions **ROMP-8** to **ROMP-12**) [4], [18], [24–27]. However, similar to *trans*-cyclooctene, the polymerization of norbornene does not yield products with very low molecular weights due to the higher molecular weight of norbornene. In addition, the structure of norbornene does not allow for the synthesis of linear PE structure.

Low ring-strain monomers, including 1,5-cyclooctadiene, cycloheptene, and cyclopentene, are not only commercially available, but they also yield products that better mimic the PE structure than norbornene. Bielawski and Grubbs demonstrated the synthesis of poly(1,5-cyclooctadiene) with molecular weight of 8,000 g/mol, polydispersity of 1.19, and yield of 91% using Grubbs' "first generation" catalyst and excess phosphine via a room temperature solution polymerization process (reaction **ROMP-13**) [7]. Bulk and solution ROMP of cycloheptene and cyclopentene and their derivatives using ruthenium-based catalysts have been demonstrated (reactions **ROMP-14** to **ROMP-17**) [12], [13]. Products with molecular weights in the range of 10^3 g/mol to

10^4 g/mol, polydispersities of greater than 1.3, and yields ranging from 24% to 92% was obtained. In general, bulk polymerization yielded products with higher molecular weight than solution polymerization. However, no significant differences in the polydispersities of the polymers produced in bulk and in solution were observed. To address the high polydispersities obtained by Hejl et al., Myers and Register reported that polymer molecular weight distribution can be controlled by the addition of excess phosphine in the room temperature solution polymerization of cyclopentene with Grubbs' "first generation" catalyst. However, polymer yield was greatly suppressed, with reported conversions of less than 32% [13].

For all of the aforementioned living ROMP polymers, chain-end and backbone functionalization can be obtained. Chain-end functionalized polymers can be produced by using catalysts and terminating agents with various functionalities. The use of *cis*-olefins as post-polymerization chain transfer agents yield various chain-end functional groups, including alcohols, acetates, and bromides [28–31]. To obtain functionalization along the polymeric backbone, direct polymerization of functionalized monomers can be employed. Post-polymerization functionalization that exploits the unsaturated polymeric backbone is also possible [32]. The unsaturated backbone can also be hydrogenation via conventional post-polymerization catalytic hydrogenation, tandem ROMP-hydrogenation via a ruthenium catalyst, and non-catalytic diimide hydrogenation to obtain PE mimics [29], [33–37].

Table 2.4. Selected examples of living ROMP reactions.

Reaction Ref. No.	Monomer	Catalyst	Reaction condition	Solvent	t_p	T_p	M_n	PDI	TOF	Ref.
ROMP-1	<i>f</i> -CPt	Mo-1	100	THF	1 h	RT	11,900	< 1.05	10 ¹	[16]
ROMP-2	<i>f</i> -CPt	Mo-2	76	THF	1 h	RT	8,210	< 1.05	10 ¹	[16]
ROMP-3	<i>f</i> -CPt	Mo-3	70, 100	THF	1 h	RT	8,890 – 8,990	1.05 – 1.5	10 ¹	[16]
ROMP-4	<i>f</i> -CB	Ru-1	25 – 161	THF	2 h	RT	4,200 – 23,300	1.11 – 1.20	10 ¹	[17]
ROMP-5	<i>f</i> -CB	Ru-2	25.7 – 152	Tol	1 h – 1.5 h	45	4,900 – 21,300	1.15 – 1.18	10 ¹	[17]
ROMP-6	<i>t</i> -CO	Ru-1	194 – 3,842 (PPh ₃ :Ru = 0 – 60)	DCM or THF	10 min	23	31,000 – 390,000	1.06 – 1.60	10 ² – 10 ³	[21]
ROMP-7	<i>f</i> - <i>t</i> -Co	Ru-1	200 – 1,000 (PPh ₃ :Ru = 0 – 60)	DCM or THF	5 min	23	41,000 – 321,000	1.02 – 1.06	10 ² – 10 ⁴	[21]
ROMP-8	N	Mo-1	50 – 200	Tol	5 min	RT	13,500 – 48,600	1.04 – 1.11	10 ²	[4], [18]
ROMP-9	N	Mo-2	640 (PMe ₃ :Mo = 5)	Tol	1 h	RT	60,000	1.11	10 ² – 10 ³	[24], [25]
ROMP-10	N	Ru-4	100 – 200	DCM	30 min	-20	9,000 – 22,000	1.06 – 1.10	10 ²	[26]
ROMP-11	<i>f</i> -N	Ru-4	50 – 400	DCM	30 min	23	11,500 – 114,000	1.05 – 1.10	10 ²	[26]
ROMP-12	<i>f</i> -N	Mo-1	51 – 723	Tol	30 min – 24 h	22	7,740 – 152,150	1.04 – 1.22	10 ¹ – 10 ²	[18], [27]
ROMP-13	COD	Ru-1	100 (PPh ₃ :Ru = 2)	DCM	5 h – 24 h	23	8,000	1.19	10 ⁰ – 10 ¹	[7]
ROMP-14	<i>f</i> -CHp	Ru-4	214	DCM	24 h	25	66,800	1.2	10 ⁰	[12]
ROMP-15	CP	Ru-4	500	DCM	24 h	25	13,300	1.3	10 ¹	[12]
ROMP-16	CP	Ru-1	3,000 – 20,000 (PCy ₃ :Ru = 0 – 67)	Tol	15 min – 6 h	RT	4,700 – 64,750	1.10 – 1.63	10 ¹ – 10 ³	[13]
ROMP-17	<i>f</i> -CP	Ru-4	150	DCM	24 h	25	16,600	1.3	10 ⁰	[12]

Reaction condition = monomer to catalyst molar ratio (phosphine to catalyst molar ratio); DCM = dichloromethane; PCy₃ = tricyclohexylphosphine; PMe₃ = trimethylphosphine; PPh₃ = triphenylphosphine; THF = Tetrahydrofuran; Tol = Toluene

2.1.5. Summary

Living ROMP polymerizes cyclic olefins into narrowly distributed, low molecular weight, functional PE mimics. Living ROMP is advantageous in the respect that many of the catalysts and monomers are commercially available and that the reactions are carried out at relatively mild conditions. Further, the presence of C=C in the polymer chains allows for great flexibility in chain-end and backbone functionalization.

Although many of the monomers are easily accessible, they are more expensive than conventional ethylene and α -olefin monomers that are used in industrial olefin polymerizations. In addition, high catalyst loadings are needed in the production of low molecular weight products. Residual catalyst in the final product can affect the product's chemical and physical properties. Post-polymerization catalyst removal methods, including the use of heterogeneous functionalized particles as catalyst scavengers and the use of small molecules as catalyst solubility modifiers, have been shown as possible pathways for effective removal of Grubbs' "third generation" catalyst from polymers prepared via solution polymerization [38]. Supporting catalyst is another simple catalyst removal technique and is also a potential catalyst recycling method to improve cost effectiveness. The preparation of Grubbs' "first generation" catalyst supported on polystyrene beads and the use of the supported catalyst in the tandem ROMP-hydrogenation of norbornene were successfully demonstrated [39]. However, the

decreased catalytic reactivity of the heterogeneous system had significant influence on the molecular weight and molecular weight distribution of the product.

There have been numerous developments into improving the performance (i.e. enhanced catalytic activities and functional group compatibilities) and the cost effectiveness (i.e. via catalyst support and recycling) of living ROMP catalysts [40]. However, since cyclic olefin monomers are more expensive than conventional olefin monomers, living ROMP may be limited to specialty chemical applications. Regardless, living ROMP is a versatile pathway for the production of narrowly distributed, low molecular weight, functional PE mimics.

2.2. Living Coordination Polymerization

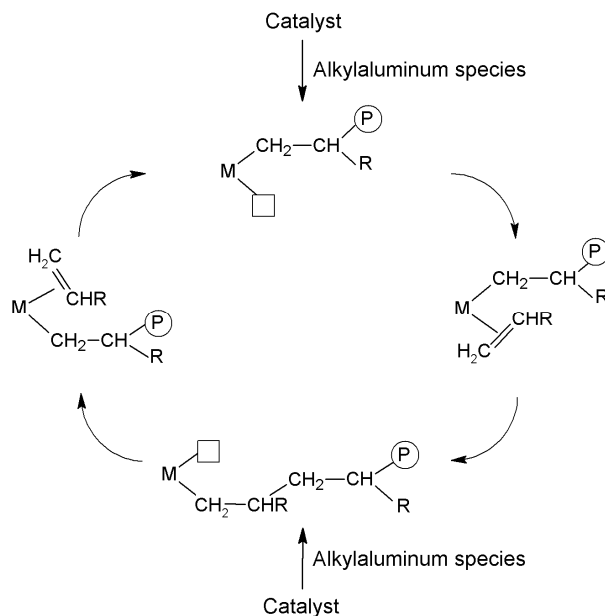
2.2.1. Mechanism

Coordination polymerization is a chain growth polymerization process which involves the addition of monomers to a macromolecule through an organometallic active center. The Cossee-Arlman mechanism for coordination polymerization of olefin monomers is shown in **Scheme 2.3** [41]. The catalyst is first activated with an alkylaluminum species, which also acts as a scavenger for impurities, including oxygen and water. The metal center of the catalyst has two coordination sites for the propagating polymer chain end and the incoming monomer. The orientation of the monomer is dictated by monomer coordination at the vacant coordination site. The coordination bond between the metal center and the propagating chain is broken and new bonds between the chain end and the new monomer unit, and between the metal center and the new monomer unit are formed. Chain propagation occurs by the continuing insertion of monomer units between the catalyst metal center and the propagating polymer chain end [42]. Acidic hydrogen is commonly used to quench the polymerization reaction by cleaving the metal-alkyl bond [43].

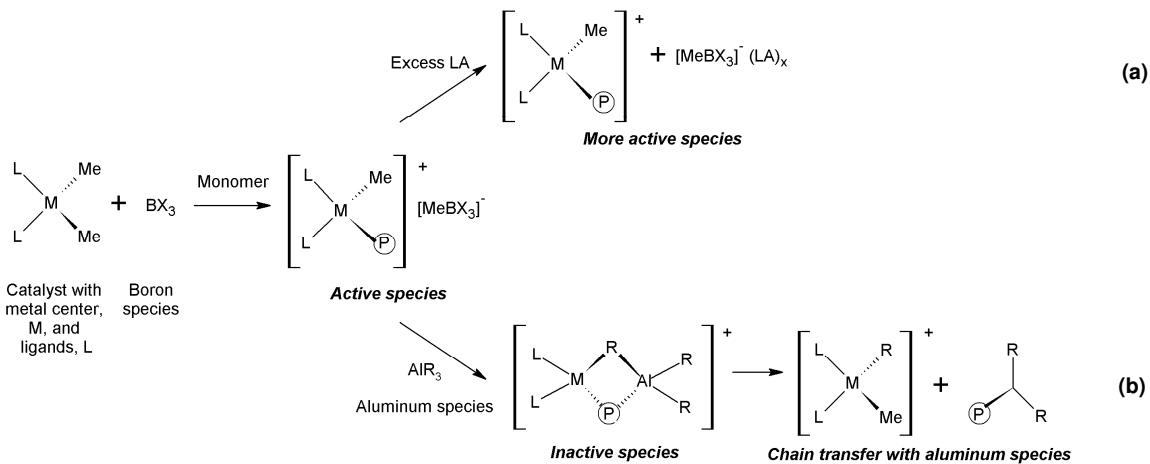
Coordination polymerization via traditional metallocene-based catalyst, which are usually transition metal complexes bearing metallocene-based ligands, is a popular route for olefin polymerization but is unsuitable for the production of narrowly distributed functional polymers. Chain termination by β -hydrogen (β -H) transfer or transfer to

alkylaluminum species is common and results in polydispersity broadening [44]. Further, polymerization of functional monomers often results in catalyst deactivation due to strong complexation between the Lewis acid components of the catalyst and the non-bonded electron pairs on nitrogen, oxygen, and halides of functional monomers [45].

To control molecular weight distribution, living polymerization via metallocene-based catalyst can be employed. In the metallocene/aluminum-species binary system at low temperatures, β -H transfer can be suppressed. With the addition of boron (B) species, the ternary metallocene/aluminum-species/boron-species system also demonstrates living polymerization characteristics [44]. As shown in the proposed mechanism in **Scheme 2.4**, the active species of the ternary system is the coordinatively unsaturated cationic metal species. With the addition of a boron-based co-catalyst, the active species become the cationic-metallic-species/anionic-boron-species ion pair. The aluminum species can interact with either ionic species. As depicted in **Scheme 2.4 (a)**, the coordination of the aluminum species (or excess boron species as a Lewis acid) to the anionic species assists ion pair separation, enhances monomer coordination, and enhances propagation rate. As indicated in **Scheme 2.4 (b)**, in the interaction of the aluminum species with the cationic species, if the complexation is strong enough to prevent monomer coordination, catalyst activity is lowered. If the complexation is loose, propagation is lowered and chain transfer to the aluminum species is increased. The interactions between the three components are dependent on the structures of the component and reaction temperature [46].



Scheme 2.3. Cossee-Arlman mechanism for coordination polymerization of olefin monomers [41]. Note: M, P, and R represent the metal center of the catalyst, the propagating polymer chain, and the functional group of the monomer, respectively.



Scheme 2.4. Proposed mechanism for metallocene/aluminum/boron ternary catalyst system [46]. Note: L_n , M, and Me represent the ligand, metal center, and methyl groups on the catalyst. BX_3 , AlR_3 , LA, and P represent the boron species, aluminum species, Lewis acid, and propagating polymer chain. x represents the number of LA.

2.2.2. Catalysts and Co-Catalysts

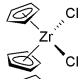
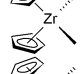
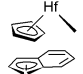
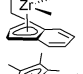
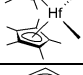
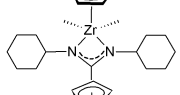
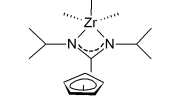
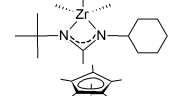
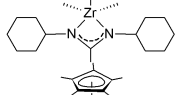
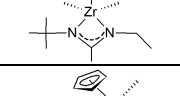
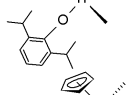
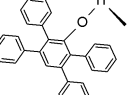
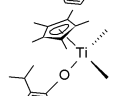
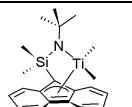
Several groups have shown successful living homopolymerization and copolymerizations of α -olefins via metallocene-based catalysts [47–57]. Metallocene-based catalysts and co-catalysts that have been reported for living coordination polymerization are summarized in **Table 2.5** and **Table 2.6**.

The use of sandwich-type biscyclopentadienyl (bis-Cp) catalysts with commercially available aluminum and boron-based species for the polymerization and copolymerization of α -olefins at low reaction temperatures of less than 0°C have been studied [47], [48]. Many of the bis-Cp catalysts, such as **Zr-1**, **Zr-2**, and **Hf-1**, are readily available. Since polymerization kinetics and polymer molecular weight distribution are affected by the steric and electronic features of the catalyst ligands, modifications of the simple bis-Cp catalyst ligands into racemic-ethylenebis(indenyl) (*rac*-(*et*)Ind₂) and *bis*(*pentamethylcyclopentadienyl*) (bis-Cp*) ligands, resulting in **Zr-3** and **Hf-2**, were investigated [47], [48], [58]. Higher propagation rates were reported for bis-Cp* compared to bis-Cp catalysts, suggesting that the electron-releasing or bulky nature of Cp* induces propagation reaction [48].

Further modifications of the simple metallocene catalyst structure and the application of these catalysts have been studied by groups such as Sita et al., Abu-Omar et al., Nomura et al, and Shiono et al. Successful living polymerization reactions using half-sandwich

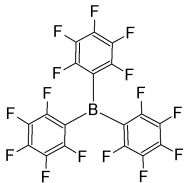
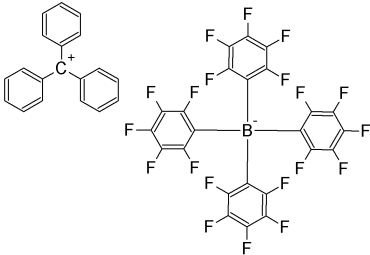
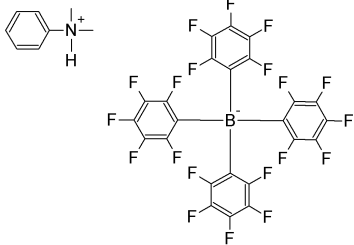
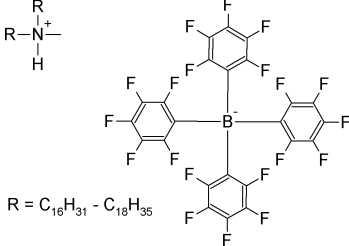
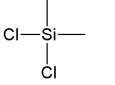
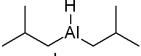
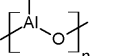
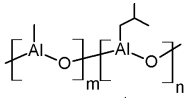
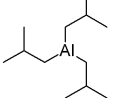
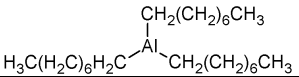
metallocene catalysts that can be synthesized in relatively few steps from non-exotic starting materials have been reported [49–52], [59–61]. The mono-Cp amidinate catalysts, **Zr-4**, **Zr-5**, **Zr-6**, **Zr-7**, and **Zr-8**, and mono-Cp aryloxide catalysts, **Ti-1**, **Ti-2**, and **Ti-3**, and their derivatives are capable of polymerizing 1-hexene, while a non-Cp *ansa*-fluorenyl catalyst **Ti-4** is able to produce stereospecific living polymers. The use of amidinate and aryloxide ligands is advantageous because ligands with different steric and electronic behaviour can be commercially obtained or readily synthesized to tune the molecular weight distribution and the stereospecificity of the polymer product [51]. In the case of the mono-Cp aryloxides, the stability of the catalytically active species increases when the ligand size increases, allowing for increased reaction temperature range up to room temperature. Bulky ligands also allow for lower polydispersity and higher molecular weight due to suppressed chain termination and chain transfer reactions. However, bulky ligands hinder polymerization and lowers catalyst activity [51].

Table 2.5. Metallocene-based catalysts for living coordination polymerization.

	Catalyst		Ref.
Bis-Cp	Zr-1 Cp_2ZrCl_2		Sigma-Aldrich
	Zr-2 Cp_2ZrMe_2		Sigma-Aldrich
	Hf-1 Cp_2HfMe_2		Strem Chemicals
	Zr-3 <i>Rac</i> -(Et)Ind ₂ ZrMe ₂		[47]
	Hf-2 Cp^*HfMe_2		[48], [58]
Mono-Cp amidinate	Zr-4 $\text{CpZrMe}_2[\text{NCyC}(\text{Me})\text{NCy}]$		[49]
	Zr-5 $\text{CpZrMe}_2[\text{N}(i\text{-Pr})\text{C}(\text{Me})\text{N}(i\text{-Pr})]$		[49]
	Zr-6 $\text{CpZrMe}_2[\text{N}(i\text{-Pr})\text{C}(\text{Me})\text{NCy}]$		[49]
	Zr-7 $\text{Cp}^*\text{ZrMe}_2[\text{NCyC}(\text{Me})\text{NCy}]$		[50], [59]
	Zr-8 $\text{Cp}^*\text{ZrMe}_2[\text{N}(t\text{-Bu})\text{C}(\text{Me})\text{NEt}]$		[50], [59]
Mono-Cp aryloxiide	Ti-1 $\text{CpTiMe}_2(\text{O}-2,6\text{-}i\text{-Pr}_2\text{C}_6\text{H}_3)$		[51]
	Ti-2 $\text{CpTiMe}_2(\text{O}-2,3,5,6\text{-Ph}_4\text{C}_6\text{H})$		[51]
	Ti-3 $\text{Cp}^*\text{TiMe}_2(\text{O}-2,6\text{-}i\text{-Pr}_2\text{C}_6\text{H}_3)$		[53]
Ansa-fluorenyl	Ti-4 $[\text{t-BuNSiMe}_2\text{Flu}]\text{TiMe}_2$		[52], [61]

Rac-(Et)Ind₂ = *racemic*-ethylenebis(indenyl); Cp = cyclopentadienyl; Cp* = pentamethylcyclopentadienyl; Cy = cyclohexyl; Flu = fluorenyl

Table 2.6. Co-catalysts for living coordination polymerization.

	Catalyst		Ref.
B-1	Tris(pentafluorophenyl)borane, $(C_6F_5)_3B$		Sigma-Aldrich
B-2	Trityltetra(pentafluorophenyl)borate, $Ph_3CB(C_6F_5)_4$		Strem Chemicals
B-3	N,N-Dimethylanilinium tetra(pentafluorophenyl)borate, $[PhNMe_2H][B(C_6F_5)_4]$		Strem Chemicals
B-4	N,N,N-trialkylammonium (tetrakis(pentafluorophenyl)borate, $[R_2NMeH][B(C_6F_5)_4]$, $R = C_{16}H_{31} - C_{18}H_{35}$		DOW Chemicals
DMDCS	Dimethyldichlorosilane, $Si(CH_3)_2Cl_2$		Sigma-Aldrich
DIBAH	<i>Diisobutyl</i> aluminum hydride, $(i-Bu)_2AlH$		Sigma-Aldrich
MAO	Methylaluminoxane		Sigma-Aldrich
MMAO	Modified methylaluminoxane		AkzoNobel
TIBA	Triisobutylaluminum, $Al(i-Bu)_3$		Sigma-Aldrich
TOA	Trioctylaluminum, $AlOct_3$		Sigma-Aldrich

Due to the extensive research into metallocene-based catalysts which resulted in numerous publications and patents in this field, there has also been great interest in the development of new non-metallocene-based catalyst for living coordination polymerization [62–75]. **Table 2.7** lists several non-metallocene-based catalysts that have been reported for living coordination polymerization.

Titanium catalysts with diamide, phenoxy-imine, or indolide-imine chelate ligands have been reported for living coordination polymerization of α -olefins. Living polymerization of simple α -olefins into atactic polymers has been reported for diamide complexes of titanium, **Ti-5** and **Ti-6** [62], [63]. When activated using MAO, chain transfer to aluminum was shown to be the source of chain termination. Chain transfer reactions were eliminated and living behaviour was demonstrated when boron-species were used in lieu of MAO [64]. Living ethylene polymerization is possible with phenoxy-imine complexes of titanium, **Ti-7**, **Ti-8**, **Ti-9**, **Ti-10**, **Ti-11**, and **Ti-12**, and indolide-imine complexes of titanium, **Ti-13**, **Ti-14**, and **Ti-15**. Phenoxy-imine complexes **Ti-8** and **Ti-9** can also produce living polypropylene with high syndiotacticity [65–67]. The living polymerization using fluorine containing phenoxy-imine titanium complexes at temperatures ranging from 0°C to 75°C was demonstrated by the Fujita group. The presence of the fluorine atom adjacent to the imine nitrogen atom in the ligand was suggested to be necessary for high temperature living polymerization and to suppress β -H transfer. However, complexes with a fluorine atom adjacent to the imine nitrogen also

yielded lower activities [68]. Titanium catalysts with indolide-imine ligands with and without fluorine also allow for living ethylene polymerization at and above room temperature. Unlike phenoxy-imine complexes, it is the bulky rigid indolide-imine ligands and not the presence of fluorine atoms that suppresses chain termination reactions. The presence of fluorine atoms influences the catalytic activity by increasing the electron withdrawing properties of the ligands and the electrophilicity of the titanium center, and hence, enhances the catalytic activity [67], [68].

There are various non-metallocene catalysts, such as nickel and palladium diimine catalysts, that have also been reported for uses in living olefin polymerization. Since chain walking, or consecutive β -hydride elimination followed by olefin reinsertion with opposite regiochemistry, is a mechanistic feature of these catalysts, polymerization of olefins, especially of ethylene, results in highly branched products [64]. Therefore, nickel and palladium diimine catalyst will not be discussed.

Table 2.7. Non-metallocene-based catalyst for living coordination polymerization.

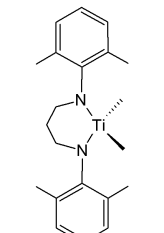
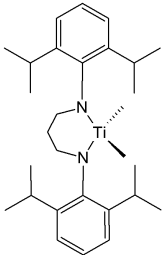
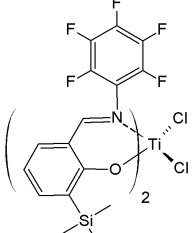
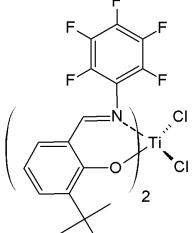
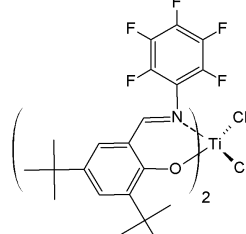
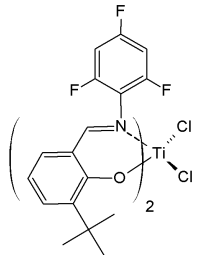
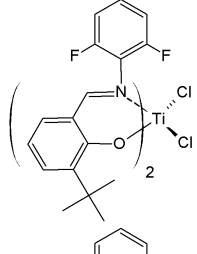
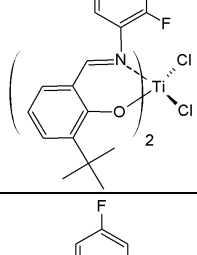
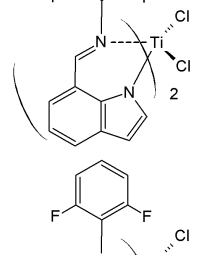
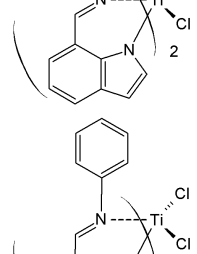
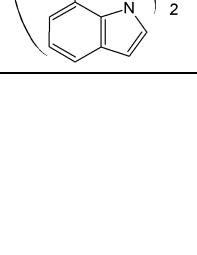
	Catalyst		Ref.	
Diamide ligand	Ti-5	$[(2,6\text{-Me}_2\text{C}_6\text{H}_3)\text{N}(\text{CH}_2)_3\text{N}(2,6\text{-Me}_2\text{C}_6\text{H}_3)]\text{TiMe}_2$		[63], [69]
	Ti-6	$[(2,6\text{-}i\text{-Pr}_2\text{C}_6\text{H}_3)\text{N}(\text{CH}_2)_3\text{N}(2,6\text{-}i\text{-Pr}_2\text{C}_6\text{H}_3)]\text{TiMe}_2$		[63], [69]
Phenoxy-imine ligand	Ti-7	$\{\eta^2\text{-1-[C(H)=N}(2,3,4,5,6\text{-F(Ph))]\text{-2-O-3-SiMe}_3\text{C}_6\text{H}_3\}_2\text{TiCl}_2$		[65]
	Ti-8	$\{\eta^2\text{-1-[C(H)=N}(2,3,4,5,6\text{-F(Ph))]\text{-2-O-3-}t\text{-BuC}_6\text{H}_3\}_2\text{TiCl}_2$		[68]
	Ti-9	$\{\eta^2\text{-1-[C(H)=N}(2,3,4,5,6\text{-F(Ph))]\text{-2-O-3,5-}t\text{-Bu}_2\text{C}_6\text{H}_3\}_2\text{TiCl}_2$		[65]

Table 2.7. Continued

	Catalyst		Ref.	
Phenoxy-imine ligand	Ti-10	$\{\eta^2\text{-1-[C(H)=N(2,4,6-F(Ph))]-2-O-3-}t\text{-BuC}_6\text{H}_3\}_2\text{TiCl}_2$		[68]
	Ti-11	$\{\eta^2\text{-1-[C(H)=N(2,6-F(Ph))]-2-O-3-}t\text{-BuC}_6\text{H}_3\}_2\text{TiCl}_2$		[68]
	Ti-12	$\{\eta^2\text{-1-[C(H)=N(6-F(Ph))]-2-O-3-}t\text{-BuC}_6\text{H}_3\}_2\text{TiCl}_2$		[68]
Indolide-imine ligand	Ti-13	$[7\text{-}(2,4,6\text{-F(Ph)N=CH)C}_8\text{H}_5\text{N}]_2\text{TiCl}_2$		[70]
	Ti-14	$[7\text{-}(2,6\text{-F(Ph)N=CH)C}_8\text{H}_5\text{N}]_2\text{TiCl}_2$		[70]
	Ti-15	$[7\text{-}(PhN=CH)C}_8\text{H}_5\text{N}]_2\text{TiCl}_2$		[70]

2.2.3. Living Coordination Polymerization Reactions

Living homopolymerization of propylene, 1-hexene, 1-octene, 1-decene, norbornene, vinylcyclohexane, and copolymerization of 1-hexene and vinylcyclohexane, ethylene and norbornene, and propylene and norbornene have been reported using different binary and ternary catalyst systems and are summarized in **Table 2.8** and **Table 2.9**.

Metallocene catalysts can produce narrowly distributed low molecular weight PE mimics at temperatures ranging from -78°C to 40°C . Atactic polypropylene with molecular weights of 1,000 g/mol to 50,000 g/mol and polydispersities of 1.04 to 1.55 can be obtained using a ternary bis-Cp catalyst system (reactions **M-1** to **M-4**) [47], [48]. Atactic block copolymers of ethylene and propylene can also be produced via a ternary bis-Cp catalyst system (reactions **M-6** and **M-7**) [48]. The aforementioned processes using bis-Cp catalysts resulted in low yields of less than 35%. Under similar reaction conditions, Bis-Cp* catalyst **Hf-2**, which demonstrates higher propagation rates than bis-Cp catalysts, has been demonstrated to give higher yields in shorter reaction times without compromising polymer molecular weight distribution and stereochemistry (reactions **M-5** and **M-8**) [48]. As indicated, the reported processes involving bis-Cp and bis-Cp* catalysts do not demonstrate polymer tacticity control. However, tacticity control can be achieved using a bis-Cp-like rac-(et)Ind₂ catalyst **Zr-3** (reaction **M-9**) [47].

Evidently, the requirement for low temperatures is a challenge for reactions using sandwich-type metallocene catalysts. Nomura et al. reported that atactic poly(1-hexene) with molecular weights of 5,000 g/mol to 186,500 g/mol and polydispersities of 1.09 to 2.02 can be synthesized using half-sandwich aryloxy catalysts in a wide temperature range of -50°C to 25°C (reactions **M-10** to **M-12**) [51], [53]. Similar to sandwich-type metallocene catalysts, polymer tacticity is not well controlled.

Polymerization reactions via half-sandwich metallocene catalysts that allow for improved polymer tacticity control were reported. Highly isotactic polymers with molecular weights of 11,032 g/mol to 69,544 g/mol, polydispersities of 1.03 to 1.50, and conversions of greater than 95% were obtained using mono-Cp amidinate catalysts activated with boron-species at temperatures ranging from -10°C to 25°C (reactions **M-13** to **M-19**) [49], [50]. The use of a half-sandwich *ansa*-fluorenyl catalyst in solution polymerization to produce syndio-rich polypropylene and poly(1-hexene) with molecular weights of 5,500 g/mol to 176,000 g/mol, polydispersities of 1.07 to 1.40, and conversion of 95% to 100% was also reported (reactions **M-20** to **M-22**) [52], [54].

Non-metallocene catalysts have shown successful living homopolymerization of ethylene and various α -olefins, and can operate at higher reaction temperature ranges than the reported living polymerization via metallocene catalysts. Titanium catalysts bearing diamide ligands have been reported for polymerizations of propylene, 1-hexene, 1-octene, and 1-decene [62], [63]. Atactic polymers with molecular weights of 4,100 g/mol to

164,000 g/mol, polydispersities of 1.05 to 1.16, and a yield of approximately 30% were produced at 0° C and room temperature (reactions **NM-1** to **NM-3**). The Fujita group has reported the synthesis of syndiotactic polypropylene using titanium catalysts with phenoxy-imine ligands activated with MAO at reaction temperatures ranging from 0°C to 50°C (reactions **NM-4** to **NM-8**) [65–67]. Not only do titanium catalysts with phenoxy-imine pose the advantages of tacticity control and increased reaction temperature range, they also allow for ethylene homopolymerization (reactions **NM-9** to **NM-12**) [68]. The reported PEs have molecular weights of 13,000 g/mol to 424,000 g/mol and polydispersities of 1.05 to 1.25. The Fujita group also studied the application of titanium catalyst with indolide-imine ligands in living ethylene polymerization, which produced similar products as polymerizations using titanium catalysts with phenoxy-imine ligands (reactions **NM-13** to **NM-15**) [70].

Polymers in a similar molecular weight range can also be prepared using titanium catalysts with aryloxy ligands, nickel catalysts bearing salicylaldimine ligands, and palladium catalysts bearing diimine ligands [71–75]. However, the molecular weight distribution of the product is not well controlled, with polydispersities greater than 1.30. As such, these polymerization systems are not discussed.

The polymerization pathways discussed mainly involves the polymerization of ethylene and/or α -olefins, yielding saturated polymers with no functionalization. Polymerization of functional monomers or post-polymerization reactions can be employed for polymer

functionalization. As discussed, polymerization of functional monomers using metallocene-based catalysts often results in catalyst poisoning [45]. To address this issue, the use of monomers with sterically protected functional groups is possible. Hakala et al. demonstrated the polymerization of oxygen-functionalized olefins where the spacer between the double bond and the oxygen atom is large and the oxygen atom is shielded by sterically bulky groups [76]. The pretreatment of polar monomers with excess alkylaluminum compounds to mask the functional group was also shown to be successful [77], [78]. With post-polymerization reaction, it is possible to obtain chain-end and backbone functionalized polymers. β -H elimination reactions in metallocene catalyzed polymerization yield terminally unsaturated groups, which can be functionalized via various chemistries [79], [80]. For backbone functionalization, reaction sites can first be created on the backbones of the saturated polymers by breaking stable carbon-hydrogen (C-H) bonds via treatment with radical initiators, followed by reactions with functional compounds. However, undesirable side reactions, such as crosslinking and degradation, are possible [79].

Table 2.8. Selected examples of living coordination polymerization reactions via metallocene-type catalysts.

Reaction Ref. No.	Catalyst	Co-catalyst	Monomer	Reaction condition	Solvent	t_p	T_p	M_n	PDI	TOF	Ref.
Bis-Cp											
M-1	Zr-1	TOA/B-1	PL	P:Al:B:Zr = 2,075:20:1:1	Tol	6 h – 12 h	-78	1,100 – 3,900	1.20 – 1.23	10^1	[48]
M-2	Zr-2	TIBA/B-1	PL	P:Al:B:Zr = 2,075:20:1:1	Tol	3 h – 12 h	-78	2,700 – 10,300	1.04 – 1.23	10^0	[48]
M-3	Zr-2	TOA/B-1	PL	P:Al:B:Zr = 2,079:20:1:1	Tol	3 h – 12 h	-78 or -50	9,400 – 46,300	1.06 – 1.55	$10^1 - 10^2$	[47]
M-4	Hf-1	TOA/B-1	PL	P:Al:B:Hf = 2,079:20:1:1	Tol	3 h – 24 h	-50	6,000 – 34,300	1.04 – 1.08	10^1	[47]
M-5	Hf-2	TOA/B-1	PL	P:Al:B:Hf = 2,075:20:1:1	Tol	2 h – 10 h	-78	27,700 – 104,000	1.06 – 1.10	10^2	[48]
M-6	Zr-2	TOA/B-1	E/PL block copolymer	P:E:Al:B:Zr = 2,075:512:20:1:1	Tol	15 h	-78	71,000	1.16	10^1	[48]
M-7	Hf-1	TOA/B-1	E/PL block copolymer	P:E:Al:B:Hf = 2,075:512:20:1:1, 2,075:1,025:20:1:1	Tol	27 h – 30 h	-50	69,000 – 155,000	1.07	10^1	[48]
M-8	Hf-2	TOA/B-1	E/PL block copolymer	P:E:Al:B:Hf = 2,075:512:20:1:1	Tol	3 h	-78	90,000	1.30	10^2	[48]
M-9	Zr-3	TOA/B-1	H	H:Al:B:Zr = 2,083:20:1:1	Tol	5 h – 14 h	-78	2,300 – 5,400	1.22 – 1.29	10^1	[47]
Mono-Cp aryloxyde											
M-10	Ti-3	TIBA/B-2, or TOA/B-2	H	H:Al:B:Ti = 239,900:500:3:1	<i>n</i> -Hexane	5 min – 60 min	-50, -40, -30	30,900 – 186,500	1.20 – 2.02	10^4	[53]
M-11	Ti-1	B-1	H	H:B:Ti = 100:1:1	Tol-d8	5 min – 2 h	-20, 0, 25	5,000 – 6,800	1.24 – 1.60	$10^1 - 10^2$	[51]
M-12	Ti-2	B-1	H	H:B:Ti = 100:1:1	Tol-d8	5 min – 2 h	-20, 0, 25	12,100 – 12,600	1.09 – 1.14	$10^2 - 10^3$	[51]

Table 2.8. Continued

Reaction Ref. No.	Catalyst	Co-catalyst	Monomer	Reaction condition	Solvent	t_p	T_p	M_n	PDI	TOF	Ref.
Mono-Cp amidinate											
M-13	Zr-4	B-3	H	H:B:Zr = 200:1:1	CB	1 h	-10	23,500	1.06	10^2	[49]
M-14	Zr-4	B-3	VCH	VCH:B:Zr = 200:1:1	CB	2 h	-10	20,400	1.10	10^1	[49]
M-15	Zr-4	B-3	H/VCH block copolymer	H:VCH:B:Zr = 154:78:1:1	CB	5 h	-10	24,400	1.08	10^1	[49]
M-16	Zr-5	B-3	H	H:B:Zr = 200:1:1	CB	1 h	-10	20,800	1.03	10^2	[49]
M-17	Zr-6	B-3	H	H:B:Zr = 200:1:1	CB	1 h	-10	21,700	1.09	10^2	[49]
M-18	Zr-7	B-3	H	H:B:Zr = 12,800:1:1	CB	30 min	0	11,032	1.10	10^2	[50]
M-19	Zr-8	B-3	H	H:B:Zr = 12,800:1:1, 800:1:1	CB	15 min – 30 min	-10, 0, 25	32,572 – 69,544	1.03 – 1.50	$10^2 – 10^3$	[50]
Ansa-fluorenyl											
M-20	Ti-4	Dried MMAO (no TMA)	PL	P:Al:Ti = 380:400:1, 749:400:1, 1,497:400:1	Heptane, Tol, CB, or <i>o</i> -DCB	1 h	0	24,300 – 176,000	1.14 – 1.39	$10^2 – 10^3$	[54]
M-21	Ti-4	TOA/B-1	PL	P:Al:B:Ti = 2,083:20:1:1	Tol	2 h – 16 h	-50	2,100 – 19,900	1.15 – 1.40	10^1	[52]
M-22	Ti-4	TOA/B-1	H	P:Al:B:Ti = 2,002:20:1:1	Tol	16 h – 72 h	-50	5,500 – 26,000	1.07 – 1.12	10^0	[52]
M-23	Ti-4	Dried MAO (no TMA)	N	N:Al:Ti = 1,800:400:1:0	Tol	5 min, 2 h	0, 20, 40	18,700 – 29,600	1.13 – 1.48	$10^2 – 10^4$	[55]
M-24	Ti-4	Dried MAO (no TMA)	E/N random copolymer	N:E:Al:Ti = 252:180:400:1 – 3,900:300:400:1	Tol	2 min, 30 min	0, 20	71,000 – 103,000	1.16 – 1.75	$10^3 – 10^4$	[56]
M-25	Ti-4	Dried MAO (no TMA)	PL/N random copolymer	N:P:Al:Ti = 255:127:400:1 – 255:850:400:1	Tol	2 min – 12 min	20	61,000 – 156,000	1.11 – 1.18	10^4	[57]

Reaction condition = molar ratios of reagents; CB = chlorobenzene; E = ethylene; H = 1-hexene; MAO = methylaluminoxane; MMAO = modified methylaluminoxane; N = norbornene; *o*-DCB = *ortho*-dichlorobenzene; PL = propylene; TIBA = triisobutylaluminum; TMA = trimethylaluminum; TOA = trioctylaluminum; Tol = toluene; Tol-*d*8 = Deuterated toluene; VCH = vinylcyclohexane

Table 2.9. Selected examples of living coordination polymerization reactions via non-metallocene-type catalysts.

Reaction Ref. No.	Catalyst	Co-catalyst	Monomer	Reaction condition (P_M)	Solvent	t_p	T_p	M_n	PDI	TOF	Ref.
Diamide ligand											
NM-1	Ti-5	B-1	O or D	(O or D):B:Ti = 5,000:1:1 – 6,000:1:1	Pentane	30 min	RT	17,300 – 20,900	1.05 – 1.11	10^2 – 10^3	[63]
NM-2	Ti-6	B-1	H, O, or D	(H, O, or D):B:Ti = 5,000:1:1 – 7,500:1:1	Pentane, Tol, or DCM	10 min – 30 min	RT	4,100 – 164,200	1.05 – 1.09	10^2	[63]
NM-3	Ti-6	Dried MMAO	PL	Al:Ti = 400 (1)	Heptane	25 min	0	29,200	1.16	10^3	[62]
Phenoxy-imine ligand											
NM-4	Ti-7	MAO	PL	Al:Ti = 250 (1)	Tol	3 h – 5 h	0, 25, 50	24,700 – 47,000	1.05 – 1.23	10^1 – 10^2	[65]
NM-5	Ti-8	MAO	PL	Al:Ti = 250 (1)	Tol	5 h	0, 25	23,600 – 28,500	1.05 – 1.11	10^1	[65]
NM-6	Ti-8	MAO	PL	Al:Ti = 50 – 125 (100 L/h flow rate)	Tol	15 min – 5 h	25	2,000 – 28,500	1.08 – 1.11	10^1	[66]
NM-7	Ti-9	MAO	PL	Al:Ti = 250 (1)	Tol	5 h	0, 25	19,200 – 29,800	1.05 – 1.15	10^1 – 10^2	[65]
NM-8	Ti-9	MAO	PL	Al:Ti = 150 (3)	Tol	15 min – 24 h	0, 20	11,100 – 102,500	1.08 – 1.13	10^1 – 10^2	[67]
NM-9	Ti-8	MAO	E	Al:Ti = 1,250 – 2,500 (1)	Tol	1 min	25, 50, 75	329,000 – 424,000	1.13 – 1.15	10^5 – 10^6	[68]
NM-10	Ti-10	MAO	E	Al:Ti = 3,125 (1)	Tol	5 min	50	145,000	1.25	10^4	[68]
NM-11	Ti-11	MAO	E	Al:Ti = 2,500 (1)	Tol	5 min	50	64,000	1.05	10^4	[68]
NM-12	Ti-12	MAO	E	Al:Ti = 12,500 (1)	Tol	5 min	50	13,000	1.06	10^3	[68]
Indolide-imine ligand											
NM-13	Ti-13	MAO	E	Al:Ti = 250 (1)	Tol	10 min	25, 50	41,900 – 53,300	1.11 – 1.24	10^4	[70]
NM-14	Ti-14	MAO	E	Al:Ti = 250 (1)	Tol	10 min	25	11,000	1.13	10^3	[70]
NM-15	Ti-15	MAO	E	Al:Ti = 250 (1)	Tol	10 min	25	12,100	1.14	10^3	[70]

Reaction condition = molar ratios of reagents (P_M = monomer pressure given in atm); D = 1-decene; DCM = dichloromethane; E = ethylene; H = 1-hexene; MAO = methylaluminoxane; MMAO = modified methylaluminoxane; O = 1-octene; PL = propylene; Tol = toluene

2.2.4. Summary

Living coordination polymerization via metallocene and non-metallocene-based catalysts stems from Ziegler-Natta catalysts and single-site metallocene catalysts development for commercial polyolefin production. As such, the use of conventional monomer sources and the potential application in commercial polyolefin production processes are attractive. There has been progress into the development of supported metallocene and non-metallocene-based catalysts, which can transform these homogenous solution processes into commercially applicable slurry or gas-phased processes. Metallocene-based bis-Cp catalysts supported on conventional silica, mesoporous silica, and clay, and non-metallocene-based phenoxy-imine titanium catalysts supported on silica nanoparticles are examples of supported living coordination polymerization catalysts [81–84].

This polymerization system is challenged by the availability of catalysts, the pyrophoric nature of metal alkyl co-catalysts, and the low reaction temperatures required for polydispersity control. Further, there is less functionalization flexibility in living coordination polymerization compared to living ROMP. Development into less expensive synthesis routes for non-metallocene-based catalysts, which require milder reaction temperatures than metallocene-based catalysts, would further commercialization possibilities of living coordination polymerization. However, living coordination polymerization remains better suited for the production of PEs and end functionalized PEs than for backbone functionalized PEs.

2.3. Living Coordination Polymerization via Coordinative Chain Transfer

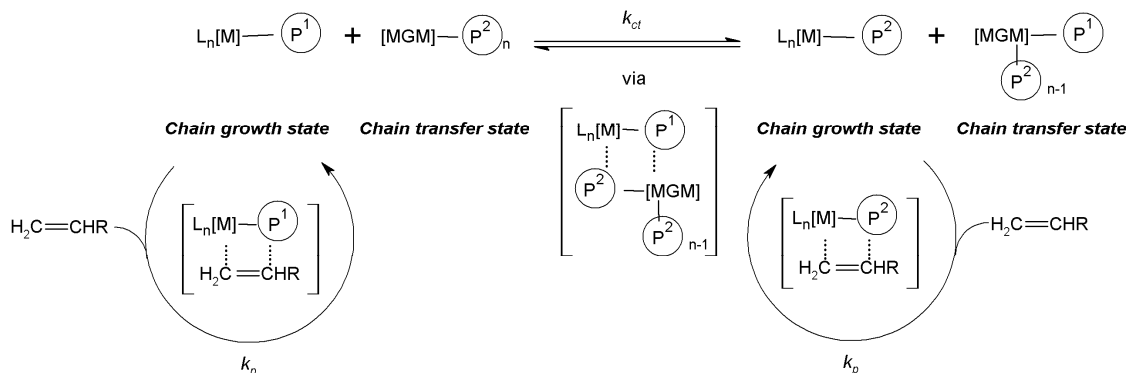
2.3.1. Mechanism

Chain propagation in living coordination polymerization, as discussed in **Chapter 2.2**, is limited to one polymer chain per active catalyst center. For controlled oligomerization, high catalyst to monomer ratio (to decrease polymer molecular weight) and low reaction temperatures (to achieve low polydispersities by suppressing chain transfer and termination reactions) are necessary. Coordinative chain transfer polymerization (CCTP) addresses the intrinsic limitation of living coordination polymerization, where the number of polymer chains is determined by the amount of catalysts. Polymerization is catalyzed by a transition metal or lanthanide catalyst via the coordination mechanism and main-group metal (MGM) alkyls are used as a “surrogate” metal chain-growth site or a chain transfer agent (CTA). The quantity of polymer product is not determined by the amount of catalyst but by the amount of the less expensive CTA [85], [86].

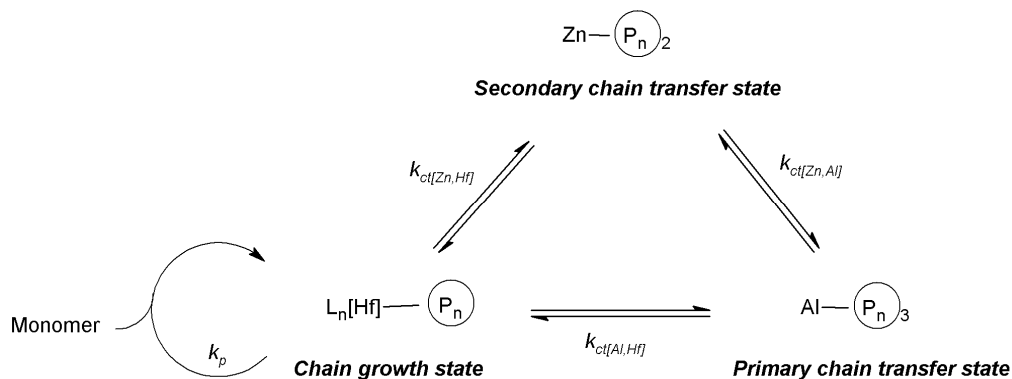
CCTP is a degenerative transfer polymerization that relies on very fast, reversible, chain transfer between an active chain growth state (CGS) and inactive chain transfer state (CTS), as illustrated in **Scheme 2.5**. Chain growth occurs only via the active metal centers of the catalysts. When the polymer chains are transferred to the MGM centers, the chains “rest” at the inactive centers where chain termination processes are limited. The equilibrium between CGS and CTS is critical. CGS is responsible for the growth of one

polymer chain. If excess CTA is present, chain transfer are faster than chain growth and chain termination processes are suppressed, then all polymer chains will grow with similar rates and narrowly distributed MGM terminated polymers are produced. Strong coordination of the active metal centers with MGM centers results in low concentrations of CGS and limited chain growth. Very strong coordination can result in the growth of only a few chains and polydispersity broadening. Contrarily, CGS dominates when coordination is weak, resulting in a conventional coordination polymerization where the CTA act as scavengers and chain termination reactions are not negligible [87].

The Sita group has also studied the use of two CTA to enhance the overall rate of chain transfer in **Scheme 2.5** and to produce low molecular weight polymers (< 1,000 g/mol) with extremely narrow polydispersities (< 1.10). A proposed mechanism is outlined in **Scheme 2.6** [88]. Chain transfer occurs between the active CGS and the inactive primary CTS, as a result of the use of the primary CTA. The secondary CTA acts as a chain-transfer mediator (CTM) between the CGS and the primary CTS. The rate of chain transfer between CGS and secondary CTS ($k_{ct[Zn,Hf]}$) and the rate of chain transfer between the primary CTS and the secondary CTS ($k_{ct[Zn,Al]}$) must be faster than the rate of chain transfer between CGS and the primary CTS ($k_{ct[Al,Hf]}$). Further, $k_{ct[Al,Hf]}$ must be faster than the rate of chain propagation (k_p).



Scheme 2.5. Mechanism for living CCTP [86], [87], [89] 2008. Note: L_n and M represent the ligand and metal center on the catalyst. P^1 and P^2 represent two different polymer chains. MGM represent the main-group metal alkyls used as CTA. n and $n-1$ represent the number of polymer chains attached to the MGM alkyl. R represents the functional group on the monomer. k_p is the rate of chain propagation and k_{ct} is the rate of chain transfer.



Scheme 2.6. Proposed mechanism for living CCTP via a hafnium-based catalyst, an aluminum-based primary chain transfer agent, and a zinc-based secondary chain transfer agent [88]. Note: L_n represents the ligand on the catalyst. P_n represents polymer chains with n repeating units. k_p is the rate of chain propagation, $k_{ct[Al,Hf]}$ is the rate of chain transfer between chain growth state and primary chain transfer state, $k_{ct[Zn,Al]}$ is the rate of chain transfer between primary chain transfer state and secondary chain transfer state, and $k_{ct[Zn,Hf]}$ is the rate of chain transfer between chain growth state and secondary chain transfer state.

2.3.2. Catalyst, Co-Catalysts, and Chain Transfer Agents

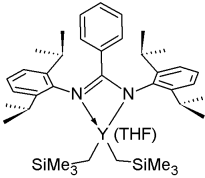
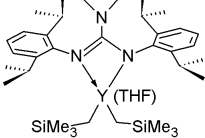
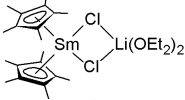
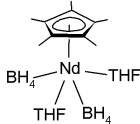
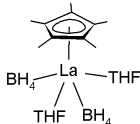
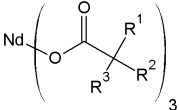
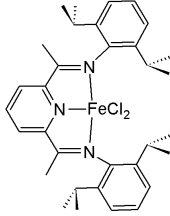
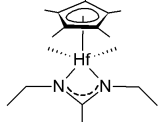
CCTP is catalyzed by organo-lanthanide or transition-metal catalysts and requires the presence of readily available and relatively inexpensive magnesium (Mg), aluminum (Al), or zinc (Zn) based main-group metal alkyl chain transfer agents. **Table 2.10** and **Table 2.11** summarize catalysts and CTA that have been reported. Catalysts activation via co-catalysts similar to those used in living coordination polymerization, shown in **Table 2.6**, is sometimes necessary.

CCTP via organo-lanthanide catalysts bearing samarium (Sm), yttrium (Y), neodymium (Nd), and lanthanum (La) have been reported. A samarium-based catalyst **Sm-1**, which can be synthesized relatively easily, was reported for the synthesis of PEs at high reaction temperatures of 80°C [87], [90], [91]. The weak interaction and coordination of MGM alkyls with the CTS and low activity of neutral lanthanide species yields this catalyst as non-optimal for efficient synthesis of narrowly dispersed low molecular weight polymers [87]. The cationic yttrium-based species bearing stronger electron donating nitrogen-carbon-nitrogen (NCN) ligands, **Y-1** and **Y-2**, demonstrated enhanced chain transfer, improved molecular weight distribution control, and higher polymerization activities under similar reaction conditions [92]. Synthesis of the yttrium-based catalysts is outlined in literature and involves the use of commercially available reagents. Neodymium and lanthanum-based half-lanthanidocene borohydrides, **Nd-1** and **La-1**, are also examples of easily synthesized catalysts. The bulky and electron-rich Cp* ligand not only limits β -H

elimination to yield narrow polydispersities, but also enables syndioselective polymerization of polystyrene [93], [94]. Commercially available catalyst systems also exist for CCTP. A ternary catalyst system consisting of neodymium versatate **Nd-2** as the catalyst, dichlorodimethylsilane (DMDCS) as the co-catalyst, and alkylaluminum as the CTA was reported for the polymerization of *cis*-1,4 polyisoprene [95].

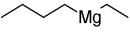
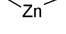
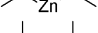
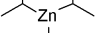
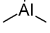
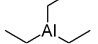
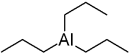
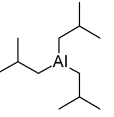
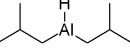
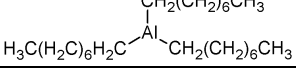
In addition to organo-lanthanide catalysts, transition-metal catalysts can be used for CCTP. Transition-metal catalysts for CCTP are mainly based on iron, zirconocene, and hafnocene complexes and require activation by aluminum or boron-based species. Britovsek et al. and Chen et al. reported the use of a readily synthesized bis(imino)pyridine iron catalyst **Fe-1** and a commercially available zirconocene dichloride catalyst **Zr-1** to produce low molecular weight PEs with polydispersities of less than 1.4 [96], [97]. A half hafnocene catalyst **Hf-3** with increased monomer versatility and enhanced molecular weight distribution control was demonstrated to yield various low molecular weight polyolefins with polydispersities under 1.10 [85], [88], [98].

Table 2.10. Catalysts for living CCTP.

	Catalyst		Ref.	
Lanthanide-based	Y-1	$(\text{ArNC}(\text{C}_6\text{H}_5)\text{NAr})\text{Y}(\text{CH}_2\text{SiMe}_3)(\text{THF})^+$		[92]
	Y-2	$(\text{ArNC}(\text{NMe}_2)\text{NAr})\text{Y}(\text{CH}_2\text{SiMe}_3)(\text{THF})^+$		[92]
	Sm-1	$\text{Cp}^*_2\text{SmCl}_2\text{Li}(\text{OEt})_2$		[90], [91]
	Nd-1	$\text{Cp}^*\text{Nd}(\text{BH}_4)_2(\text{THF})_2$		[99], [100]
	La-1	$\text{Cp}^*\text{La}(\text{BH}_4)_2(\text{THF})_2$		[101], [102]
	Nd-2	$\text{Nd}(\text{vers})_3$		Rhodia
Transition-metal-based	Fe-1	$\{2,6-(\text{MeC}=\text{N}-2,6-i\text{-Pr}_2\text{C}_6\text{H}_3)_2\text{C}_5\text{H}_3\text{N}\}\text{FeCl}_2$		[103], [104]
	Hf-3	$\text{Cp}^*\text{Hf}(\text{Me})_2[\text{N}(\text{Et})\text{C}(\text{Me})\text{N}(\text{Et})]$		[98], [105]

Ar = 2,6-(*i*-Pr)₂Ph; Cp* = pentamethylcyclopentadienyl; vers = versatate

Table 2.11. Chain transfer agents for living CCTP.

	Catalyst		Ref.
BEM	Butylethylmagnesium, MgBuEt		AkzoNobel
DMZ	Dimethylzinc, ZnMe ₂		Sigma-Aldrich
DEZ	Diethylzinc, ZnEt ₂		Sigma-Aldrich
DIPZ	Diisopropylzinc, Zn(<i>i</i> -Pr) ₂		Sigma-Aldrich
TMA	Trimethylaluminum, AlMe ₃		Sigma-Aldrich
TEA	Triethylaluminum, AlEt ₃		Sigma-Aldrich
TPA	Tripropylaluminum, AlPr ₃		Sigma-Aldrich
TIBA	Triisobutylaluminum, Al(<i>i</i> -Bu) ₃		Sigma-Aldrich
DIBAH	Diisobutyl aluminum hydride, (<i>i</i> -Bu) ₂ AlH		Alfa Aesar
TOA	Trioctylaluminum, AlOct ₃		Sigma-Aldrich

2.3.3. Living Coordinative Chain Transfer Polymerization Reactions

Successful homopolymerization of ethylene, propylene, 1-hexene, 1-octene, 1,5-hexadiene, isoprene, and styrene, and copolymerization of styrene and isoprene, ethylene and 1-hexene, ethylene and 1-octene, and ethylene and 1,5-hexadiene have been reported. Organo-lanthanide catalysts generally operate at high temperatures of 50°C to 80°C, while transition-metal-based catalysts operate at lower temperatures of -25°C to 70°C. Synthesis of oligomers with molecular weights as low as 400 g/mol and polydispersities ranging between 1.02 and 1.40 have been reported and are summarized in **Table 2.12**.

The production of narrowly dispersed low molecular weight PEs has been demonstrated using organo-lanthanide catalysts **Sm-1**, **Y-1**, and **Y-2**. The **Sm-1** catalyst system demonstrated low catalyst activity in conditions that produced PEs with narrow polydispersities (turnover frequency of approximately 1,000 mol mol⁻¹ h⁻¹ atm⁻¹) (reaction **CCTP-1**) [87], [90]. A ternary catalyst system consisting of a yttrium-based catalyst, a boron-based co-catalyst, and an aluminum-based CTA addresses the downfalls of **Sm-1** (reactions **CCTP-2** and **CCTP-3**). Under similar reaction conditions as reaction **CCTP-1**, the yttrium-based catalyst systems produced low molecular weight PE with enhanced polydispersity control and higher turnover frequencies of up to 35,000 mol mol⁻¹ h⁻¹ atm⁻¹ [92]. Polystyrene and polyisoprene can also be produced using organo-lanthanide catalysts. Zinck et al. reported the use of **Nd-1** and **La-1** at 50°C to produce highly syndiotactic polystyrene with molecular weights of 560 g/mol to 16,000 g/mol and

polydispersities of 1.2 to 1.3 at conversions of 16% to 81% (reactions **CCTP-4** and **CCTP-5**) [93], [94]. *Cis*-1,4-polyisoprene with molecular weights of 1,200 g/mol to 7,400 g/mol and polydispersities of 1.14 to 1.23 was produced at 50°C with complete monomer conversion using a commercially available neodymium catalyst, **Nd-2** (reaction **CCTP-6**) [95].

The elevated reaction temperatures of organo-lanthanide catalyst systems allow for good solubility of PE chains and narrowly distributed polymers. For PEs produced using transition-metal-based catalysts, polydispersities are not as well controlled due to lower reaction temperatures. A zirconocene/MAO binary catalyst system produced low molecular weight PEs with polydispersities of 1.2 to 1.4 at temperatures of 40°C to 70°C (reaction **CCTP-7**) [97]. Similarly, PEs produced at room temperature using an iron-based catalyst demonstrated slightly higher polydispersities compared to reactions **CCTP-1** to **CCTP-3** (reaction **CCTP-8**) [96], [106].

Increased polydispersity control at low reaction temperatures have been demonstrated by the Sita group using a hafnocene catalyst **Hf-3**. A **Hf-3**/boron-based-co-catalyst/zinc-based-CTA ternary system was reported to polymerize ethylene and various α -olefins into narrowly distributed low molecular weight products. Room temperature polymerization of ethylene yield oligomers with molecular weights below 700 g/mol, polydispersities below 1.07, and turnover frequencies as high as 16,000 mol mol⁻¹ h⁻¹ atm⁻¹ (reaction **CCTP-9**) [85]. Atactic polypropylene with molecular weights below 33,300 g/mol and

polydispersities below 1.15 was produced with a turnover frequency of approximately 5,000 mol mol⁻¹ h⁻¹ atm⁻¹ at temperatures of -20°C to 20°C (reaction **CCTP-10**) [98]. Homopolymerization of higher α -olefins at -10°C (reactions **CCTP-11** to **CCTP-13**) and copolymerization of ethylene and higher α -olefins at room temperature (reactions **CCTP-14** to **CCTP-16**) were reported to yield polymers with molecular weights as low as 3,330 g/mol and polydispersities as low as 1.04 [85]. To further enhance polydispersity control for low molecular weight products, the Sita group studied the use of two CTA in CCTP. Using the **Hf-3** catalyst, a boron-based co-catalyst, an aluminum-based primary CTA, and a zinc-based secondary CTA, polypropylene and copolymers of propylene and 1-octene with molecular weights under 1,000 g/mol and polydispersities under 1.10 were produced at a reaction temperature of 20°C (reactions **CCTP-17** and **CCTP-18**) [88].

Chain-end functionalization of CCTP polymers can easily be achieved. The use of MGM-based CTA produces MGM-terminated polymers, which can be functionalized via post-polymerization modifications. The oxidation and hydrolysis of aluminum and zinc-terminated polymers to yield hydroxyl-terminated polymers has been reported [94], [107]. Further modification on the hydroxyl group allows for various functionalized polymers. Carboxyl-terminated polymers were also demonstrated by treatment of neodymium-catalyzed *cis*-1,4 polyisoprene with carbon dioxide and hydrochloric acid [95]. Further, chloro- and bromo-terminated PEs have been reported via oxidation of yttrium-catalyzed aluminum-terminated PEs via dry oxygen followed by reaction in chlorobenzene with phosphor pentachloride or bromide [92].

Table 2.12. Selected examples of living CCTP reactions.

Reaction Ref. No.	Catalyst	Co-catalyst	CTA	Monomer	Reaction condition (P _M)	Solvent	t _p	T _p	M _n	PDI	TOF	Ref.
Lanthanide-based												
CCTP-1	Sm-1	-	BEM	E	Mg:Sm = 10:1 – 1,000:1 (1)	Hydro-carbon solvents	5 min – 24 h	80	400 – 1,870	1.1 – 1.3	10 ³ – 10 ⁴	[87], [90]
CCTP-2	Y-1	B-4	TEA or TOA	E	Al:B:Y = 100:1:1:1 – 150:1:1.1 (5)	Tol	15 min	80	1,409 – 2,154	1.1 – 1.3	10 ⁴	[92]
CCTP-3	Y-2	B-4	TEA or TOA	E	Al:B:Y = 100:1:1:1 – 150:1:1.1 (5)	Tol	15 min	80	1,364 – 2,600	1.07 – 1.15	10 ³ – 10 ⁴	[92]
CCTP-4	Nd-1	-	BEM	St	St:Nd = 100:1 – 2,000:1 Mg:Nd = 1:1 – 10:8:1	Tol	2 h – 90 h	50	560 – 16,000	1.2 – 1.3	10 ¹	[93], [94]
CCTP-5	La-1	-	BEM	St	St:La = 100:1 – 1,000:1 Mg:La = 1:1 to 10:1	Tol	2 h – 72 h	50	830 – 12,000	1.2 – 1.3	10 ⁰	[94]
CCTP-6	Nd-2	DMDCS	DIBAH	IP	IP:Al:Cl:Nd = 100:20:4:1 – 800:20:4:1	Hexane	4 h	50	1,200 – 7,400	1.14 – 1.23	10 ¹ – 10 ²	[95]
Transition-metal-based												
CCTP-7	Zr-1	MAO	-	E	Al:Zr = 12:1 (1.5 – 2.5)	Tol	2 min	40 – 70	1,500 – 2,500	1.2 – 1.4	10 ³ – 10 ³	[97]
CCTP-8	Fe-1	MAO	DMZ, DEZ, or DIPZ	E	Zn:Al:Fe = 500:100:1 – 540:100:1 (1)	Tol	30 min	RT	600 – 800	1.1 – 1.3	10 ⁴	[96], [106]
CCTP-9	Hf-3	B-1	DEZ	E	Zn:B:Hf = 20:1:1 – 200:1:1 (0.34)	Tol	8 min – 63 min	25	449 – 665	1.03 – 1.07	10 ³ – 10 ⁴	[85]
CCTP-10	Hf-3	B-3	DEZ	PL	Zn:B:Hf = 20:1:1 – 200:1:1 (0.34)	Tol	2 h	20	1,450 – 33,300	1.04 – 1.15	10 ³	[98]
CCTP-11	Hf-3	B-3	DEZ	H	H:Zn:B:Hf = 1,670:10:1:1 – 1,670:20:1:1	Tol	15 h	-10	3,830 – 6,650	1.05 – 1.06	10 ¹	[85]
CCTP-12	Hf-3	B-3	DEZ	O	O:Zn:B:Hf = 1,000:20:1:1	Tol	18 h	-10	3,330	1.06	10 ¹	[85]
CCTP-13	Hf-3	B-3	DEZ	HD	HD:Zn:B:Hf = 1,400:10:1:1	Tol	15 h	-10	8,020	1.04	10 ¹	[85]
CCTP-14	Hf-3	B-3	DEZ	E/H random co-polymer	H:Zn:B:Hf = 1,500:20:1:1 – 1,500:50:1:1 (0.34)	Tol	1 h	25	5,910 – 13,000	1.16 – 1.24	10 ³	[85]

Table 2.12. Continued

Reaction Ref. No.	Catalyst	Co-catalyst	CTA	Monomer	Reaction condition (P_M)	Solvent	t_p	T_p	M_n	PDI	TOF	Ref.
Transition-metal-based												
CCTP-15	Hf-3	B-3	DEZ	E/O random copolymer	O:Zn:B:Hf = 1,000:20:1:1 – 1,500:20:1:1 (0.34)	Tol	1 h	25	8,870 – 12,100	1.14 – 1.25	10^3	[85]
CCTP-16	Hf-3	B-3	DEZ	E/HD random copolymer	HD:Zn:B:Hf = 1,500:20:1:1 – 1,500:50:1:1 (0.34)	Tol	1 h	25	6,220 – 14,800	1.06 – 1.11	10^3	[85]
CCTP-17	Hf-3	B-2	DEZ, TEA, TIBA, DEZ/TEA, DEZ/TPA, or DEZ/TIBA	PL	(Al or Zn):B:Hf = 20:1:1 and 100:1:1 Al:Zn:B:Hf = 10:10:1:1, 18:2:1:1, and 190:10:1:1 (0.34)	Tol	2 h – 72 h	20	580 – 7,300	1.02 – 1.21	10^2 – 10^3	[88]
CCTP-18	Hf-3	B-2	DEZ/TIBA	PL/O random copolymer	O:Al:Zn:B:Hf = 500:18:2:1:1 (0.34)	Tol	4 h	20	1,270	1.10	10^2	[88]

Reaction condition = molar ratios of reagents (P_M = monomer pressure given in atm); BEM = butylethylmagnesium; DEZ = diethylzinc; DIBAH = diisobutyl aluminum hydride; DIPZ = diisopropylzinc; DMDCS = dimethylchlorosilane; DMZ = dimethylzinc; E = ethylene; MAO = methylaluminoxane; H = 1-hexene; HD = 1,5-hexadiene; IP = isoprene; O = 1-octene; PL = propylene; St = styrene; TEA = triethylaluminum; TIBA = triisobutylaluminum; TOA = trioctylaluminum; Tol = toluene

2.3.4. Summary

Similar to living ROMP, CCTP operates under relatively mild reaction conditions. In addition, similar to living coordination polymerization via metallocene-based and non-metallocene-based catalysts, CCTP is advantageous due to the use of conventional olefin monomer sources and the potential for applications in commercial polyolefin production processes. The preparation and use of mesoporous silica supported transition metal catalyst **Fe-1** for ethylene oligomerization shows promising development in supported CCTP catalysts and slurry or gas-phased process applications [108].

Unlike the two previously discussed polymerization systems, the degenerative transfer polymerization mechanism of CCTP enables the growth of multiple polymer chains per catalyst. Since the catalyst is generally the most expensive raw material, the requirement for lower catalyst loadings in CCTP is economically advantageous. The CCTP mechanism also allows for improved molecular weight and molecular weight distribution control, resulting in product with lower molecular weights and polydispersities than those obtained via living ROMP and living coordination polymerization via metallocene-based and non-metallocene-based catalysts.

However, applications of CCTP in the production of narrowly distributed, low molecular weight, functional PEs and PE mimics faces several challenges. Firstly, development of cost effective catalyst synthesis is necessary to improve catalyst availability. Further,

scale up processes are limited by the pyrophoric nature of metal alkyl CTA. Lastly, although chain-end functionalization can be easily obtained, backbone functionalization poses a challenge. Similar to living coordination polymerization via metallocene-based and non-metallocene-based catalysts, CCTP is well suited for the production of narrowly distributed, low molecular weight PEs and end functionalized PEs.

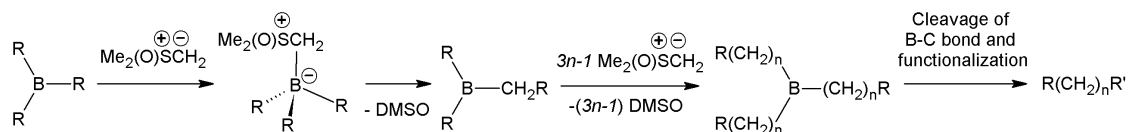
2.4. Living C1 Polymerization via Polyhomologation

2.4.1. Mechanism

Thus far, living polymerization of olefin monomers (C2 monomers) has been discussed. However, polyhomologation, which is a living polymerization of non-olefin monomers, can also yield linear saturated main-chain carbon-based polymers with controlled molecular weight, narrow molecular weight distribution, well-defined composition, and chain-end functionalities. Unlike conventional olefin polymerizations, the polymeric backbone is built one carbon at a time in polyhomologation [109], [110]. The general reaction involves the polymerization of ylide (neutral dipolar molecule containing an anionic site attached directly to a heteroatom carrying a formal positive charge) or ylide-like monomers via a Lewis acidic borane initiator or catalyst.

A proposed reaction mechanism for the polyhomologation reaction is given in **Scheme 2.7**. For illustration purposes, dimethylsulfoxonium methylide is used as the ylide monomer and a trialkyl borane is used as the catalyst. The reaction involves the nucleophilic attack of the ylide monomer on the Lewis acid borane. The complex undergoes a 1,2-migration of one of the three alkyl groups to produce the homologated alkylborane (where one of the alkyl chains is now extended by one carbon and the boron center is regenerated) and a molecule of dimethyl sulfoxide (DMSO). This process is repeated to yield polymethylene with low polydispersities, which indicates that all three

alkyl groups on the boron undergo migration with equal probability. The boron-carbon (B-C) bonds on the intermediate three-arm star polymethylene are cleaved to yield oligomeric or polymeric chains. Functionalities can be incorporated by the use of monomers bearing functionalities and/or by varying the chemistry used in B-C bond cleavage and subsequent post-polymerization reactions [110].



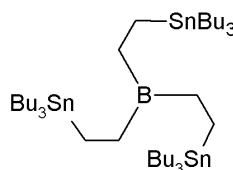
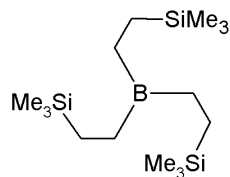
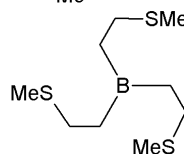
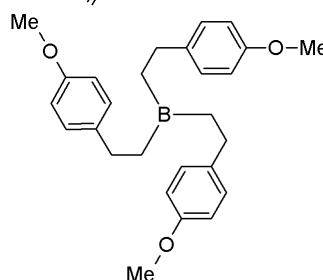
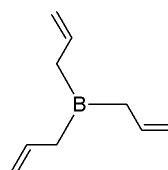
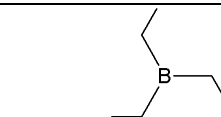
Scheme 2.7. Proposed mechanism for polyhomologation [110]. Note: B and R are boron and alkyl functional groups on the borane catalyst. $Me_2(O)SCH_2$ is the ylide monomer and DMSO is dimethyl sulfoxide. R' is the functional group incorporated onto the final polymer during boron-carbon bond cleavage and post-polymerization functionalization reactions.

2.4.2. Catalysts

Organoboranes, such as the compounds shown in **Table 2.13**, are used to catalyze or initiate polyhomologation. Based on the polyhomologation mechanism, the α -position of the polymer chain can be functionalized by the use of different functional trialkylborane catalysts. The use of commercially available triethylborane **B-5** yields a saturated α -terminal group. Various chain-end functional polymers can be synthesized using functional trialkylboranes **B-7**, **B-8**, **B-9**, and **B-10**, which can be prepared by the hydroboration of commercially available olefins [111]. The use of triallylborane **B-6** yields polymers with terminal vinyl group, which can be further functionalized via post-polymerization chemistries. It should be noted that the pyrophoric nature of organoboranes presents a limitation on the application of polyhomologation [112].

Table 2.13. Catalysts for living polyhomologation.

	Catalyst	Ref.
B-5	(Et) ₃ B Triethylborane	Sigma-Aldrich
B-6	(CH ₂ CHCH ₂) ₃ B Triallylborane	[113]
B-7	(MeOPhEt) ₃ B Tris(4-methoxyphenylethyl)borane	[111], [114], [115]
B-8	(MeSEt) ₃ B Tris[2-(methylsulfide)ethyl]borane	[111], [114], [115]
B-9	(Me ₃ SiEt) ₃ B Tris[2-(trimethylsilyl)ethyl]borane	[111], [114], [115]
B-10	(<i>n</i> -Bu ₃ SnEt) ₃ B Tris[2-(tri- <i>n</i> -butyltin)ethyl]borane	[111], [114], [115]



2.4.3. Monomers

Monomers for polyhomologation should be readily available, should have reasonable polymerization activity, should be stable under polymerization conditions, and the monomer by-product during polymerization should not inhibit polymerization [110]. Ylides of sulfoxides and ylide-like compounds, shown in **Table 2.14**, are commonly used. The unsubstituted ylide dimethylsulfonium methylide **1** has been the most common monomer reported [110]. A two-step reaction, in which DMSO first undergoes sulfur-methylation (S-methylation) to form the ylide precursor of trimethyloxosulfonium chloride and then the precursor is deprotonated with sodium hydride, has been demonstrated for the synthesis of **1** [110], [116]. S-alkylation of sulfoxides is not a general reaction and limits sulfonium ylides to the methylide group. (Dimethylamino)phenyl-oxosulfonium ylides **2** and **3** present the balance between the reactivity and stability of sulfonium ylides and the structural variations desired in polymerization products. Other ylides of sulfoxides, such as **4**, can also yield substituted polymeric backbones. Ylides of sulfoxides substituted on carbon are also potential candidates. However, they are more difficult to prepare than ylides of sulfoxides, often too unstable to isolate, and often thermally unstable under polyhomologation conditions [109], [116]. Diazoalkanes, such as trimethylsilyl diazomethane **5**, are more readily available and can serve as a polyhomologation monomer. In general, C1 monomers are more expensive than C2 monomers.

Table 2.14. Monomers for living polyhomologation.

Catalyst		Ref.
1 Dimethylsulfonium methylide		[117]
2 (Dimethylamino)aryloxosulfonium methylide		[109], [116], [118]
3 (Dimethylamino)aryloxosulfonium alkylide		[109], [116], [118]
4 (Dimethylamino)- <i>p</i> -tolylloxosulfonium cyclopropylide		[119]
5 Trimethylsilyl diazomethane		Alfa Aesar

2.4.4. Living Polyhomologation Reactions

Living polyhomologation reactions can yield polymers with molecular weights as low as 426 g/mol and polydispersities as low as 1.01. A summary of reported living polyhomologation reactions for the synthesis of narrow dispersed low molecular weight functionalized PE and PE mimics is provided in **Table 2.15**.

The Shea group have reported the homopolymerization of methylene monomers **1** and **2** via various trialkylborane catalysts to produce polymethylene with different α -position chain end functionalization (reactions **C1-1** to **C1-8**) [111], [113], [116], [120]. The use of borane catalyst **B-5** yielded polymers with no α -position functionalization, whereas the use of borane catalysts **B-6**, **B-7**, **B-8**, **B-9**, and **B-10** resulted in polymers with vinyl, 4-methoxyphenyl, methylsulfide, trimethylsilyl, and tri-*n*-butyltin functionalization at the α -position. Polymethylene with molecular weights of 426 g/mol to 13,202 g/mol, narrow polydispersities of 1.01 to 1.17, and yields ranging from 60% to 90% was produced at temperatures of 50°C to 80°C.

Side chain functionalization can be obtained by the polymerization of substituted polymethylene. Although homopolymerization of secondary and tertiary ylides **3** and **4** has been reported to be unsuccessful, the copolymerization of secondary and tertiary ylides with primary ylide **1** yield substituted polymethylene. Polymethylenes with methyl, cyclopropyl, and trimethylsilyl side chain functionalities, molecular weights of 445 g/mol

to 1,808 g/mol, and narrow polydispersities of 1.02 to 1.15 were produced at temperatures ranging from 50°C to 60°C and at yields of approximately 30% to 70% (reactions **C1-9** to **C1-11**) [116], [119], [121].

All of the aforementioned polymerization reactions are carried out in organic solvents and at slightly elevated temperatures. Recently, the Shea group have demonstrated the synthesis of polymethylene waxes with molecular weight as low as 927 g/mol at or near room temperature in aqueous conditions [122]. However, low polydispersities cannot be obtained, with the lowest reported polydispersity being 1.47. It should be noted that the optimization of polyhomologation is of great interest and may yield polyhomologation as a viable polymerization pathway in the future.

Evident from the above discussion, α -position chain end functionalization can be achieved by the use of different functional catalysts. For ω -position chain end functionalization, different B-C bond cleavage and subsequent post-polymerization chemistries can be employed. The treatment of the intermediate three-arm star polymer with *o*-xylenes and propionic acid was reported to yield saturated ω -terminal group [113]. Hydroxyl functionalization in the ω -position has been demonstrated via oxidation with trimethylamine-*N*-oxide or basic hydrogen peroxide [111].

Table 2.15. Selected examples of living polyhomologation reactions.

Reaction Ref. No.	Catalyst	Monomer	Reaction condition	ω -position functionality	Solvent	t_p	T_p	M_n	PDI	TOF	Ref.
C1-1	B-5	1	1:B = 150 – 696	-OH	Tol/THF	10 min (3 h)	60	727 – 3,287	1.04 – 1.17	$10^1 - 10^2$	[120]
C1-2	B-5	2	2:B = 60 – 150	-OH	N/A	N/A	N/A	426 – 927	1.02 to 1.11	N/A	[116]
C1-3	B-6	1	1:B = 120 – 2,400	-OH	Tol	5 min (24 h)	80	498 – 13,202	1.03 – 1.12	$10^0 - 10^2$	[113]
C1-4	B-6	1	1:B = 138 – 381	-	Tol	5 min (3 days)	80	665 – 2,426	1.03 – 1.08	10^0	[113]
C1-5	B-7	1	1:B = ~140 – ~3,200	-OH	Tol	10 min – 20 min (2 h)	50 – 70	640 – 15,000	1.01 – 1.19	$10^1 - 10^3$	[111]
C1-6	B-8	1	1:B = ~165 – ~690	-OH	Tol	10 min – 20 min (2 h)	50 – 70	770 – 3,230	1.02 – 1.03	$10^1 - 10^2$	[111]
C1-7	B-9	1	1:B = ~145 – ~690	-OH	Tol	10 min – 20 min (2 h)	50 – 70	680 – 3,220	1.04 – 1.17	$10^1 - 10^2$	[111]
C1-8	B-10	1	1:B = ~120 – ~1,800	-OH	Tol	10 min – 20 min (2 h)	50 – 70	565 – 8,410	1.01 – 1.02	$10^1 - 10^2$	[111]
C1-9	B-5	1/3 random copolymer	1:3:B = 120:60:1, 137:34:1, 135:22.5:1	-OH	THF	N/A	N/A	866 – 1,609	1.09 – 1.15	N/A	[116]
C1-10	B-5	1/4 random copolymer	1:4:B = ~50:10:1	-OH	THF	3 h (12 h)	50	1,808	1.13	$10^1 - 10^0$	[119]
C1-11	B-6 or B-7	1/5 random copolymer	1:5:B = 21:3:1, 30:3:1	-OH	DEE/Bz/Tol	1 h (~24 h)	60	445 – 874	1.02 – 1.06	$10^1 - 10^0$	[121]

Reaction condition = molar ratios of reagents; t_p = time for monomer conversion (time for B-C bond cleavage and ω -position functionalization reaction); Bz = benzene; DEE = diethyl ether; N/A = not available in literature; THF = tetrahydrofuran; Tol = toluene

2.4.5. Summary

Living polyhomologation allows for the production of extremely low molecular weight PEs and PE mimics with the best molecular weight distribution control out of the four polymerization systems discussed. Similar to living ROMP and CCTP, the reaction conditions for living polyhomologation is relatively mild. Further, living polyhomologation allows for the growth of three polymer chains from one catalyst.

The greatest challenge for living polyhomologation is the availability of raw materials. Not only is there a limited selection of suitable monomers and catalysts, these materials are not commercially available and must be synthesized. In addition, the pyrophoric nature of the organoborane catalysts poses a limitation for scale up applications.

It should be noted that living polyhomologation developments are far from mature. Living polyhomologation presents an opportunity to explore materials unobtainable via conventional olefin polymerization. Continuing research into new monomers and catalysts, optimization of monomer and catalyst preparation, and optimization of reaction conditions may yield living polyhomologation as a feasible and scalable process for the production of low molecular weight PEs and PE mimics with precise polydispersity and functionality control.

2.5. Application Concerns

The synthesis of low molecular weight PE and PE mimics with controlled molecular weight, chain-end functionalization, and in certain cases, backbone functionalization is possible with the polymerization systems discussed above. A summary of molecular weights and molecular weight distributions of the polymers produced by each reaction is given in **Table 2.16** and **Table 2.17**. Evidently, CCTP and polyhomologation yield products with the lowest molecular weights and polydispersities. As such, these two pathways appear to be optimal in the production of narrowly distributed low molecular weight polymers. However, in actual application, the ability to synthesize a desired product is only one of many concerns. Efficiency and safety of the system must also be considered.

Table 2.16. Polymer molecular weight produced via polymerization reactions.

System	M_n (g/mol)							
	< 1,000		1,000 – 10,000		10,000 – 100,000		> 100,000	
ROMP			ROMP-2	ROMP-10	ROMP-1	ROMP-10		
			ROMP-3	ROMP-12	ROMP-4	ROMP-11		
			ROMP-4	ROMP-13	ROMP-5	ROMP-12	ROMP-6	
			ROMP-5	ROMP-16	ROMP-6	ROMP-14	ROMP-7	
					ROMP-7	ROMP-15	ROMP-11	
					ROMP-8	ROMP-16	ROMP-12	
					ROMP-9	ROMP-17		
Metallocene					M-2	M-15		
					M-3	M-16		
					M-4	M-17		
			M-1	M-11	M-5	M-18	M-5	
			M-2	M-17	M-6	M-19	M-7	
			M-3	M-21	M-7	M-20	M-10	
			M-4	M-22	M-8	M-21	M-20	
			M-9	M-23	M-9	M-22	M-24	
					M-10	M-23	M-25	
					M-12	M-24		
					M-13	M-25		
					M-14			
	Non-metallocene					NM-1	NM-8	
						NM-2	NM-9	
					NM-3	NM-11	NM-2	
			NM-2		NM-4	NM-12	NM-8	
			NM-6		NM-5	NM-13	NM-9	
					NM-6	NM-14	NM-10	
					NM-7	NM-15		
CCTP			CCTP-1	CCTP-11		CCTP-4		
			CCTP-2	CCTP-12		CCTP-5		
			CCTP-3	CCTP-13				
			CCTP-4	CCTP-14		CCTP-10		
			CCTP-5	CCTP-15		CCTP-14		
			CCTP-6	CCTP-16		CCTP-15		
			CCTP-7	CCTP-17		CCTP-16		
			CCTP-8	CCTP-18				
			CCTP-9					
			CCTP-10					
C1	C1-1	C1-6	C1-1	C1-7		C1-3		
	C1-2	C1-7	C1-3	C1-8		C1-5		
	C1-3	C1-8	C1-4	C1-9				
	C1-4	C1-9	C1-5	C1-10				
	C1-5	C1-11	C1-6					

Table 2.17. Polydispersities of polymer produced via polymerization reactions.

System	PDI				
	< 1.10		1.10 – 1.50		> 2.00
ROMP	ROMP-1	ROMP-7	ROMP-3	ROMP-12	
	ROMP-2	ROMP-8	ROMP-4	ROMP-13	
	ROMP-3	ROMP-10	ROMP-5	ROMP-14	ROMP-6
	ROMP-6	ROMP-11	ROMP-6	ROMP-15	ROMP-16
		ROMP-12	ROMP-8	ROMP-16	
			ROMP-9	ROMP-17	
Metallocene	M-2	M-13	M-1	M-11	
	M-3	M-14	M-2	M-19	
	M-4	M-15	M-3	M-20	M-3
	M-5	M-16	M-6	M-21	M-10
	M-7	M-17	M-7	M-22	M-11
	M-12	M-18	M-8	M-23	M-24
		M-22	M-9	M-24	
			M-10	M-25	
Non-metallocene	NM-1	NM-6	NM-1	NM-8	
	NM-2	NM-7	NM-3	NM-9	
	NM-4	NM-8	NM-4	NM-10	
	NM-5	NM-11	NM-5	NM-13	
		NM-12	NM-6	NM-14	
		NM-7	NM-15		
CCTP			CCTP-1	CCTP-8	
	CCTP-3	CCTP-12	CCTP-2	CCTP-10	
	CCTP-9	CCTP-13	CCTP-3	CCTP-14	
	CCTP-10	CCTP-16	CCTP-4	CCTP-15	
	CCTP-11	CCTP-17	CCTP-5	CCTP-16	
			CCTP-6	CCTP-17	
			CCTP-7	CCTP-18	
CI	C1-1	C1-6	C1-1	C1-7	
	C1-2	C1-7	C1-2	C1-9	
	C1-3	C1-8	C1-3	C1-10	
	C1-4	C1-9	C1-5		
	C1-5	C1-11			

Efficiency of a polymerization system is often expressed by its turnover frequency (TOF). TOF is a measure of the amount of product obtained per amount of catalyst per unit of time. Units of $\text{mol}_{\text{polymer}} \text{mol}_{\text{catalyst}}^{-1} \text{h}^{-1}$ for liquid monomers and $\text{mol}_{\text{polymer}} \text{mol}_{\text{catalyst}}^{-1} \text{h}^{-1} \text{atm}_{\text{monomer}}^{-1}$ for gaseous monomers are used. The TOF of each polymerization reaction discussed are summarized in **Table 2.18**. They are classified using a ranking system similar to that described by Gibson et al. [123]: very high ($> 10,000$), high (1,000 – 10,000), moderate (100 – 1,000), low (10 – 100), and very low (< 10). It must be noted that TOF are influenced by factors, including but not limited to reactor size, stirring, solvent type, reaction temperature, reaction pressure, and reaction time. For example, for catalysts with high initial activities and fast deactivation, TOF expressed in units of $\text{mol mol}^{-1} \text{h}^{-1}$ can lead to artificially high values when short reaction times are extrapolated to one hour [123]. This effect is observed in the TOFs of several living coordination polymerization reactions via non-metallocene catalysts with short reaction times.

Table 2.18. Turnover frequency of polymerization reactions.

System	TOF ($\text{mol mol}^{-1} \text{h}^{-1}$ or $\text{mol mol}^{-1} \text{h}^{-1} \text{atm}^{-1}$)								
	Very low (< 10)	Low ($10 - 100$)	Moderate ($100 - 1,000$)	High ($1\,000 - 10,000$)	Very high ($> 10,000$)				
ROMP		ROMP-1 ROMP-2 ROMP-3 ROMP-4 ROMP-5 ROMP-12 ROMP-13 ROMP-15 ROMP-16	ROMP-6 ROMP-7 ROMP-8 ROMP-9 ROMP-10 ROMP-11 ROMP-16	ROMP-6 ROMP-7 ROMP-16	ROMP-7				
	Metallocene			M-3 M-5 M-8 M-11 M-12 M-13 M-16 M-17 M-18 M-19 M-20 M-23	M-12 M-19 M-20 M-23 M-24	M-23 M-24 M-25			
			M-1 M-2 M-9 M-22	M-3 M-4 M-6 M-7 M-11 M-14 M-15 M-21					
		Non-metallocene		NM-4 NM-5 NM-6 NM-7 NM-8	NM-1 NM-2 NM-4 NM-7 NM-8	NM-1 NM-3 NM-12 NM-14 NM-15	NM-9 NM-10 NM-11 NM-13		
			CCTP		CCTP-4 CCTP-6 CCTP-11 CCTP-12 CCTP-13	CCTP-6 CCTP-7 CCTP-17 CCTP-18	CCTP-1 CCTP-3 CCTP-7 CCTP-9 CCTP-10 CCTP-14 CCTP-15 CCTP-16 CCTP-17	CCTP-1 CCTP-2 CCTP-3 CCTP-8 CCTP-9	
					CCTP-5				
				C1		C1-1 C1-3 C1-5 C1-6 C1-7 C1-8	C1-1 C1-3 C1-5 C1-6 C1-7 C1-8	C1-5	
						C1-3 C1-4 C1-10 C1-11			

The efficiency of a polymerization system can also be judged by reactor volume and cost efficiencies. All of the systems discussed require the use of solvents, which takes up on average more than half of the reactor volume. The weight percent of polymer produced per reaction solution for each system is summarized in **Table 2.19**. Living ROMP, living coordination polymerization, and CCTP demonstrate the possibility for high reactor volume efficiency, where polymer product contributes to greater than 50 wt. % of the reactor solution in several cases. Polyhomologation shows the lowest reactor volume efficiency, where the reactor solution is 99 wt. % solvent. However, polyhomologation is a promising research area where most of the reported techniques are at their initial stages of development [109]. Upon optimization, improved reactor volume efficiency may be possible.

Cost efficiency considers various factors including but not limited to the cost of the raw materials (i.e. catalysts, co-catalysts, CTA, and monomers). For systems that require transition-metal-based catalysts, such as living ROMP, living coordination polymerization, and CCTP, the most expensive reagent is generally the catalyst. Although polyhomologation catalysts are not metal-based, they are homogeneous catalysts and are difficult to recycle for reuse after polymerization. It is, however, insufficient to solely consider catalyst cost in the analysis of catalyst cost efficiency. Evidently, the cost efficiency of a system which requires small amounts of expensive catalyst is comparable to that which requires large amounts of inexpensive catalyst. Thus, catalyst cost must be evaluated along with the amount of catalyst required. **Table 2.19** provides the catalyst

metal loading and the associated cost of catalyst metal per mass of polymer yield for living ROMP, living coordination polymerization, and CCTP. Since polyhomologation does not require the use of metal-based catalysts, the catalyst loading was determined based on catalyst mass and not catalyst metal mass. Also, the catalyst metal costs per polymer yield were given as zero. **Table 2.20** summarizes the cost of metals that are present in the catalysts discussed.

As expected from the living ROMP and living coordination polymerization mechanisms where one catalytic center yield one polymer chain, these two systems require high catalyst loadings. The simultaneous growth of three polymer chains from one catalytic center in polyhomologation addresses this issue. However, the low molecular weights of polyhomologation oligomers counteract this advantage, resulting in the need for very high catalyst loadings. The CCTP mechanism deals with the limitation of one polymer chain per catalytic center directly and efficiently. Polymer chain length is controlled by the loading of inexpensive CTA and not the loading of catalyst. Thus, CCTP demonstrates the lowest catalyst loadings of all the systems discussed. Of the metal-based catalysts discussed, ruthenium, with a price of approximately 4000 USD/kg, is the most expensive and titanium and iron, with prices of less than 10 USD/kg, are the least. As a result, living ROMP reactions involving ruthenium catalysts are the most cost inefficient while living coordination polymerization reactions involving titanium and iron catalysts are the most efficient.

In addition to the cost efficiency of catalysts, the availability of raw materials must also be considered. Several of the catalysts and monomers are commercially available, while all of the co-catalysts and CTA are readily available. Most of the living ROMP catalysts, some of the metallocene-based catalysts, and one of the CCTP catalysts are commercially available. However, the majority of the living coordination polymerization catalysts and all of the polyhomologation catalysts are not readily available. The majority of the monomers used in the reactions discussed are commercially available. Monomers used in living coordination polymerization and CCTP include olefins that are commonly used in olefin polymerization and that are readily available. Although most of the cyclic olefin monomers used for living ROMP are available, they are more expensive than olefin monomers. The monomers involved in polyhomologation are not commercially available, are difficult to synthesize, and have limited stability.

Further, it should be noted that all of the systems are air sensitive and must be carried in an inert atmosphere. Some systems are air sensitive not only in the aspect that catalyst poisoning may occur in ambient environment, but in the aspect that some raw materials are highly reactive in air. This is true for living coordination polymerization reactions involving alkylaluminum species as co-catalysts, CCTP reactions requiring the use of pyrophoric main-group metal alkyls, and living C1 polymerizations involving potentially explosive ylide monomers and pyrophoric organoborane catalysts.

Table 2.19. Comparison of reactor volume efficiency and catalyst cost efficiency of polymerization reactions.

	Ref. No.	Catalyst	Monomer	Polymer concentration ^a	Catalyst loading ^b	Catalyst metal cost/ polymer ^c
Living ROMP	ROMP-1	Mo-1	<i>f</i> -CPr	2.49	7,617	0.26
	ROMP-2	Mo-2	<i>f</i> -CPr	2.49	7,617	0.26
	ROMP-3	Mo-3	<i>f</i> -CPr	2.49	7,617	0.26
	ROMP-4	Ru-1	<i>f</i> -CB	0.92	12,810 – 76,679	50.06 – 320.40
	ROMP-5	Ru-2	<i>f</i> -CB	3.02 – 3.03	10,274 – 94,946	40.05 – 400.50
	ROMP-6	Ru-1	<i>t</i> -CO	5.28	2,541 – 5,069	9.83 – 19.66
	ROMP-7	Ru-1	<i>f-t</i> -Co	4.86	556 – 2,772	2.14 – 10.72
	ROMP-8	Mo-1	N	1.59 – 6.07	5,069 – 19,973	0.17 – 0.69
	ROMP-9	Mo-2	N	4.41	1,590	0.05
	ROMP-10	Ru-4	N	1.26	5,929 – 11,787	23.01 – 46.02
	ROMP-11	Ru-4	<i>f</i> -N	2.61	1,414 – 11,202	5.46 – 43.71
	ROMP-12	Mo-1	<i>f</i> -N	4.79 – 24.25	649 – 7,454	0.02 – 0.25
	ROMP-13	Ru-1	COD	6.82	10,274	40.05
	ROMP-14	Ru-4	<i>f</i> -CHp	38.33	5,550	21.53
	ROMP-15	Ru-4	CP	14.63	4,410	17.09
	ROMP-16	Ru-1	CP	0.93 – 6.95	1,558 – 1,851	6.02 – 7.16
	ROMP-17	Ru-4	<i>f</i> -CP	13.50	13,742	53.76
Living coordination polymerization	M-1	Zr-1	PL	0.02 – 0.08	267,343 – 645,953	9.62 – 48.11
	M-2	Zr-2	PL	0.24 – 1.19	23,749 – 108,442	0.64 – 3.21
	M-3	Zr-2	PL	0.71 – 8.10	3,306 – 39,385	0.09 – 1.08
	M-4	Hf-1	PL	0.70 – 4.95	10,865 – 75,043	8.85 – 65.37
	M-5	Hf-2	PL	4.90 – 18.95	2,439 – 10,982	1.97 – 8.95
	M-6	Zr-2	E/PL	4.15	6,712	0.18
	M-7	Hf-1	E/PL	4.14 – 10.27	4,968 – 13,049	4.02 – 10.65
	M-8	Hf-2	E/PL	14.92	3,249	2.63
	M-9	Zr-3	H	0.08 – 0.22	115,295 – 267,343	3.44 – 9.62
	M-10	Ti-3	H	0.01 – 0.48	502 – 24,574	0.01 – 0.19
	M-11	Ti-1	H	8.84	5,655	0.04
	M-12	Ti-2	H	8.84	5,655	0.04
	M-13	Zr-4	H	3.27	6,045	0.16
	M-14	Zr-4	VCH	4.27	4,586	0.12
	M-15	Zr-4	H/VCH	4.31	4,540	0.12
	M-16	Zr-5	H	3.27	6,045	0.16
	M-17	Zr-6	H	3.27	6,045	0.16
	M-18	Zr-7	H	1.00	19,869	0.53
	M-19	Zr-8	H	3.48 – 5.83	3,306 – 5,669	0.09 – 0.15
	M-20	Ti-4	PL	0.69 – 3.06	2,330 – 10,525	0.02 – 0.08
	M-21	Ti-4	PL	1.77	1,597	0.01
	M-22	Ti-4	H	2.47 – 9.21	4,333 – 17,108	0.03 – 0.13
	M-23	Ti-4	N	5.29 – 9.50	351 – 664	0.01
	M-24	Ti-4	E/N	2.84 – 20.61	142 – 1,258	0.01
	M-25	Ti-4	PL/N	2.25 – 12.10	267 – 1,593	0.01

Table 2.19. Continued

	Ref. No.	Catalyst	Monomer	Polymer concentration ^a	Catalyst loading ^b	Catalyst metal cost/ polymer ^c
Living coordination polymerization	NM-1	Ti-5	O or D	5.62 – 51.46	720 – 12,666	0.01 – 0.10
	NM-2	Ti-6	H, O, or D	0.76 – 15.16	4,258 – 7,925	0.03 – 0.06
	NM-3	Ti-6	PL	11.55	357	< 0.01
	NM-4	Ti-7	PL	0.03 – 0.07	1,712 – 6,300	0.01 – 0.05
	NM-5	Ti-8	PL	0.03 – 0.04	6,604 – 27,968	0.05 – 0.22
	NM-6	Ti-8	PL	0.02 – 0.04	5,204 – 67,276	0.04 – 0.55
	NM-7	Ti-9	PL	0.03 – 0.06	8,706 – 23,478	0.07 – 0.18
	NM-8	Ti-9	PL	0.19 – 3.93	338 – 19,163	0.01 – 0.15
	NM-9	Ti-8	E	0.07 – 0.10	254 – 1,209	< 0.01
	NM-10	Ti-10	E	0.02	827	0.01
	NM-11	Ti-11	E	0.02	4,145	0.03
	NM-12	Ti-12	E	0.01	8,951	0.07
	NM-13	Ti-13	E	0.06	1,974 – 1,990	0.02
	NM-14	Ti-14	E	0.01	9,483	0.07
	NM-15	Ti-15	E	0.02	5,535	0.04
CCTP	CCTP-1	Sm-1	E	0.69 – 17.66	162 – 4,987	0.02 – 0.75
	CCTP-2	Y-1	E	2.17 – 5.05	74 – 178	0.01 – 0.03
	CCTP-3	Y-2	E	0.53 – 1.91	202 – 740	0.03 – 0.12
	CCTP-4	Nd-1	St	45.84	3,871	1.15
	CCTP-5	La-1	St	35.21	5,796	0.36
	CCTP-6	Nd-2	IP	13.46 – 13.49	2,640 – 20,735	0.78 – 6.25
	CCTP-7	Zr-1	E	0.18	120,366	3.61
	CCTP-8	Fe-1	E	4.20 – 7.49	16 – 29	<< 0.01
	CCTP-9	Hf-3	E	0.60 – 3.26	1,523 – 8,428	1.23 – 6.85
	CCTP-10	Hf-3	PL	8.59 – 18.90	177 – 2,185	0.14 – 1.76
	CCTP-11	Hf-3	H	10.89 – 11.08	1,650 – 1,681	1.33 – 1.36
	CCTP-12	Hf-3	O	8.64	2,172	1.75
	CCTP-13	Hf-3	HD	8.16	2,313	1.87
	CCTP-14	Hf-3	E/H	7.45	639	0.52
	CCTP-15	Hf-3	E/O	6.97	686	0.55
	CCTP-16	Hf-3	E/HD	6.60	728	0.59
	CCTP-17	Hf-3	PL	6.47 – 83.54	41 – 2,966	0.03 – 2.4
	CCTP-18	Hf-3	PL/O	5.45	3,557	2.88
Polyhomologation	C1-1	B-5	1	0.68 – 0.95	11,050 – 49,291	0
	C1-2	B-5	2	N/A	N/A	0
	C1-3	B-6	1	N/A	244,513	0
	C1-4	B-6	1	N/A	244,513	0
	C1-5	B-7	1	0.83	212,216	0
	C1-6	B-8	1	0.83	133,859	0
	C1-7	B-9	1	0.80	175,433	0
	C1-8	B-10	1	0.53	497,058	0
	C1-9	B-5	1/3	N/A	N/A	0
	C1-10	B-5	1/4	0.36	85,934	0
	C1-11	B-6 or B-7	1/5	0.37 – 1.38	199,118 – 486,305	0

^a Mass of polymer produced per mass of reaction solution (wt. %)^b Mass of catalyst metal per mass of polymer produced (ppm) given for living ROMP, living coordination polymerization, and CCTP, and mass of catalyst per mass of polymer produced (ppm) given for polyhomologation^c Cost of catalyst metal per mass of polymer produced (USD/kg)

Table 2.20. Prices for transition metals present in catalysts.

Metal	USD/ kg	Ref.
Ruthenium	3,858	Johnson Matthey
Hafnium	806	Shanghai Metals Market
Neodymium	295	HEFA Rare Earth
Yttrium	165	HEFA Rare Earth
Samarium	150	HEFA Rare Earth
Lanthanum	62	HEFA Rare Earth
Molybdenum	34	London Metal Exchange
Zirconium	26	Shanghai Metals Market
Titanium	8	Shanghai Metals Market
Iron	0.12	The Steel Index

Prices reported between the years of 2009 to 2011.

2.6. Conclusions

Living ROMP, living coordination polymerization, CCTP, and living C1 polymerization are possible pathways to synthesize low molecular weight PE and PE mimics with narrow distributions and chain-end or backbone functionalization. With such a broad range of catalyst systems and monomers, it is possible to realise tailor-made materials with specific material performance.

The great success in bench scale production of narrowly distributed, low molecular weight PE and PE mimics with functionalization possibility was enabled by the extensive progress in novel catalyst and polymerization reaction development. Advancing catalyst and polymerization reaction research and development continues to push the current limits of monomer versatility, molecular weight distribution control, polymer architecture control, and catalyst activity. Each system discussed in the review has its advantages and disadvantages in the areas of cost, efficiency, and safety, with a common issue being the application in high efficiency and low cost polymer synthesis. As such, these systems are promising for specialty materials production, but their practical commercial applications continue to be challenging.

To enable viable practical applications of these polymerization systems, novel catalyst and polymerization reaction research must be followed closely by scale up development. The availability of raw materials and the optimization of polymerization systems are two

critical areas of focus. Many of the raw materials used in these systems, especially the catalysts, are not commercially available and require syntheses via multi-step processes. The development of more time efficient and cost effective catalyst and monomer syntheses is a possible route to enable the commercialization of the polymerization systems. In addition, the enhancement and optimization of catalyst systems, reaction conditions, and reaction process are often overlooked. There have been advancements in the development of supported catalysts for the systems discussed in the review, presenting possibilities in catalyst recycling and commercial polymerization process implementation. Optimization of polymerization systems for large scale production within current reactor technology limitations may allow for feasible commercial applications.

2.7. References

- [1] C. W. Bielawski and R. H. Grubbs, “Living Ring-Opening Metathesis Polymerization,” *Progress in Polymer Science*, vol. 32, pp. 1–29, 2007.
- [2] P. C. Hiemenz and T. P. Lodge, “Ring-Opening Metathesis Polymerization (ROMP),” in *Polymer Chemistry*, 2nd ed., Boca Raton: CRC Press, 2007, pp. 155–156.
- [3] P. Schwab, R. H. Grubbs, and J. W. Ziller, “Synthesis and Applications of $\text{RuCl}_2(\text{=CHR})(\text{PR}_3)_2$: The Influence of the Alkylidene Moiety on Metathesis Activity,” *Journal of the American Chemical Society*, vol. 118, pp. 100–110, 1996.
- [4] J. S. Murdzek and R. R. Schrock, “Low Polydispersity Homopolymers and Block Copolymers by Ring Opening of 5,6-Dicarbomethoxynorbornene,” *Macromolecules*, vol. 20, pp. 2640–2642, 1987.
- [5] J. H. Oskam et al., “Ligand Variation in Alkylidene Complexes of the Type $\text{Mo}(\text{CHR})(\text{NR}')(\text{OR})_2$,” *Journal of Organometallic Chemistry*, vol. 459, pp. 185–198, 1993.
- [6] C. Slugovc, “The Ring Opening Metathesis Polymerisation Toolbox,” *Macromolecular Rapid Communications*, vol. 25, pp. 1283–1297, 2004.
- [7] C. W. Bielawski and R. H. Grubbs, “Increasing the Initiation Efficiency of Ruthenium-Based Ring-Opening Metathesis Initiators: Effect of Excess Phosphine,” *Macromolecules*, vol. 34, pp. 8838–8840, 2001.
- [8] K. Matyjaszewski, S. Gaynor, D. Greszta, D. Mardare, and T. Shigemoto, “‘Living’ and Controlled Radical Polymerization,” *Journal of Physical Organic Chemistry*, vol. 8, pp. 306–315, 1995.
- [9] E. L. Dias, S. T. Nguyen, and R. H. Grubbs, “Well-Defined Ruthenium Olefin Metathesis Catalysts: Mechanism and Activity,” *Journal of the American Chemical Society*, vol. 119, pp. 3887–3897, 1997.
- [10] W. A. Herrmann and C. Kocher, “N-Heterocyclic Carbenes,” *Angewandte Chemie International Edition in English*, vol. 36, pp. 2162–2187, 1997.
- [11] J. Huang, H.-J. Schanz, E. D. Stevens, and S. P. Nolan, “Stereo-electronic Effects Characterizing Nucleophilic Carbene Ligands Bound to the Cp^*RuCl ($\text{Cp}^* = \eta^5$ -

- C5Me5) Moiety: A Structural and Thermochemical Investigation,” *Organometallics*, vol. 18, pp. 2370–2375, 1999.
- [12] A. Hejl, O. A. Scherman, and R. H. Grubbs, “Ring-Opening Metathesis Polymerization of Functionalized Low-Strain Monomers with Ruthenium-Based Catalysts,” *Macromolecules*, vol. 38, pp. 7214–7218, 2005.
- [13] S. B. Myers and R. A. Register, “Synthesis of Narrow-Distribution Polycyclopentene Using a Ruthenium Ring-Opening Metathesis Initiator,” *Polymer*, vol. 49, pp. 877–882, 2008.
- [14] C. Bielawski, D. Benitez, and R. H. Grubbs, “Synthesis of Cyclic Polybutadiene via Ring-Opening Metathesis Polymerization: The Importance of Removing Trace Linear Contaminants,” *Journal of the American Chemical Society*, vol. 125, pp. 8424–8425, 2003.
- [15] M. Rubin and V. Gevorgyan, “Simple Large-Scale Preparation of 3,3-Disubstituted Cyclopropenes: Easy Access to Stereodefined Cyclopropylmetals via Transition Metal-Catalyzed Hydrometalation,” *Synthesis*, vol. 5, pp. 796–800, 2004.
- [16] R. Singh, C. Czekelius, and R. R. Schrock, “Living Ring-Opening Metathesis Polymerization of Cyclopropenes,” *Macromolecules*, vol. 39, pp. 1316–1317, 2006.
- [17] B. R. Maughon and R. H. Grubbs, “Ruthenium Alkylidene Initiated Living Ring-Opening Metathesis Polymerization (ROMP) of 3-Substituted Cyclobutenes,” *Macromolecules*, vol. 30, pp. 3459–3469, 1997.
- [18] G. C. Bazan, S. R., H.-N. Cho, and V. C. Gibson, “Polymerization of Functionalized Norbornenes Employing $\text{Mo}(\text{CH-t-Bu})(\text{NAr})(\text{O-t-Bu})_2$ as the Initiator,” *Macromolecules*, vol. 24, pp. 4495–4502, 1991.
- [19] S. Kanaoka and R. H. Grubbs, “Synthesis of Block Copolymers of Silicon-Containing Norbornene Derivatives via Living Ring-Opening Metathesis Polymerization Catalyzed by a Ruthenium Carbene Complex,” *Macromolecules*, vol. 28, pp. 4707–4713, 1995.
- [20] K. Shea and J.-S. Kim, “Influence of Strain on Chemical Reactivity. Relative Reactivity of Torsionally Distorted Double Bonds in MCPBA Epoxidations,” *Journal of the American Chemical Society*, vol. 114, pp. 3044–3051, 1992.
- [21] R. Walker, R. M. Conrad, and R. H. Grubbs, “The Living ROMP of trans-Cyclooctene,” *Macromolecules*, vol. 42, pp. 599–605, 2009.

- [22] S. Inagaki, Y. Ishitani, and T. Kakefu, “Geminal Delocalization of σ -Electrons and Ring Strains,” *Journal of the American Chemical Society*, vol. 116, pp. 5954–5958, 1994.
- [23] N. Allinger and J. Sprague, “Conformational Analysis. LXXXIV. A Study of the Structures and Energies of Some Alkenes and Cycloalkenes by the Force Field Method,” *Journal of the American Chemical Society*, vol. 94, pp. 5734–5747, 1972.
- [24] L.-B. W. Lee, “Polymer Crystalline Texture Controlled Through Film Blowing and Block Copolymerization,” Princeton University, 2004.
- [25] L.-B. W. Lee and R. A. Register, “Hydrogenated Ring-Opened Polynorbornene : A Highly Crystalline Atactic Polymer,” *Macromolecules*, vol. 38, pp. 1216–1222, 2005.
- [26] T.-L. Choi and R. H. Grubbs, “Controlled Living Ring-Opening-Metathesis Polymerization by a Fast-Initiating Ruthenium Catalyst,” *Angewandte Chemie International Edition*, vol. 42, pp. 1743 – 1746, 2003.
- [27] G. C. Bazan et al., “Living Ring-Opening Metathesis Polymerization of 2,3-Difunctionalized Norbornenes by $\text{Mo}(\text{CH-t-Bu})(\text{N-2,6-C}_6\text{H}_3\text{-i-Pr}_2)(\text{O-t-Bu})_2$,” *Journal of the American Chemical Society*, vol. 112, pp. 8378–8387, 1990.
- [28] M. A. Hillmyer, S. T. Nguyen, and R. H. Grubbs, “Utility of a Ruthenium Metathesis Catalyst for the Preparation of End-Functionalized Polybutadiene,” *Macromolecules*, vol. 30, pp. 718–721, 1997.
- [29] A. Leitgeb, J. Wappel, and C. Slugovc, “The ROMP Toolbox Upgraded,” *Polymer*, vol. 51, pp. 2927–2946, 2010.
- [30] J. B. Matson and R. H. Grubbs, “Monotelechelic Poly(oxa)norbornenes by Ring-Opening Metathesis Polymerization using Direct End-Capping and Cross Metathesis,” *Macromolecules*, vol. 43, pp. 213–221, 2010.
- [31] J. E. Schwendeman and K. B. Wagener, “Synthesis of Amorphous Hydrophobic Telechelic Hydrocarbon Diols via ADMET Polymerization,” *Macromolecular Chemistry and Physics*, vol. 210, pp. 1818–1833, 2009.
- [32] M. P. McGrath, E. D. Sall, and S. J. Tremont, “Functionalization of Polymers by Metal-Mediated Processes,” *Chemical Reviews*, vol. 95, pp. 381–398, 1995.

- [33] K. D. Camm, N. M. Castro, Y. Liu, P. Czechura, J. L. Snelgrove, and D. E. Fogg, “Tandem ROMP-Hydrogenation with a Third-Generation Grubbs Catalyst,” *Journal of the American Chemical Society*, vol. 129, pp. 4168–4169, 2007.
- [34] O. J. Kwon, H. T. Vo, S. B. Lee, T. K. Kim, H. S. Kim, and H. Lee, “Ring-Opening Metathesis Polymerization and Hydrogenation of Ethyl-Substituted Tetracyclododecene,” *Bulletin of the Korean Chemical Society*, vol. 32, pp. 2737–2742, 2011.
- [35] T. Otsuki, K. Goto, and Z. Komiya, “Development of hydrogenated ring-opening metathesis polymers,” *Polymer Science Part A: Polymer*, vol. 38, pp. 4661–4668, 2000.
- [36] C. K. Santin, M. M. Jacobi, and R. H. Schuster, “Diimide Hydrogenation of Polydienes,” *Kautschuk, Gummi, Kunststoffe*, vol. 60, pp. 331–335, 2007.
- [37] K.-H. Yoon, K. O. Kim, M. Schaefer, and D. Y. Yoon, “Synthesis and Characterization of Hydrogenated Poly(norbornene endo-dicarboximide)s Prepared by Ring Opening Metathesis Polymerization,” *Polymer*, vol. 53, pp. 2290–2297, 2012.
- [38] R. H. Lambeth, S. J. Pederson, M. Baranoski, and A. M. Rawlett, “Methods for Removal of Residual Catalyst from Polymers Prepared by Ring Opening Metathesis Polymerization,” *Journal of Polymer Science Part A: Polymer Chemistry*, vol. 48, pp. 5752–5757, 2010.
- [39] S.-H. Lee, H.-J. Kim, D. H. Choi, S. S. Hwang, H. S. Chae, and K.-Y. Baek, “Highly Purified Cyclic Olefin Polymer by ROMP and In situ Hydrogenation with Ruthenium Supported Catalyst,” *Macromolecular Research*, vol. 20, pp. 777–779, Jun. 2012.
- [40] G. C. Vougioukalakis, “Removing Ruthenium Residues from Olefin Metathesis Reaction Products,” *Chemistry A European Journal*, vol. 18, pp. 8868–8880, Jul. 2012.
- [41] J. Okuda and R. Mulhaupt, “Transition Metal Catalyzed Olefin, Cycloolefin, and Styrene Polymerization,” in *Materials Science and Technology A Comprehensive Treatment*, R. W. Cahn, R. Haasen, and E. J. Kramer, Eds. New York: Wiley, 1999, pp. 123–162.
- [42] G. G. Odian, “Ionic and Coordination Polymerization,” in *Principles of Polymerization*, 2nd ed., New York: Wiley, 1981, pp. 587–591.

- [43] W. Kuran, “Coordination Homopolymerisation and Copolymerisation of Functionalised α -olefins with Ethylene and α -olefins,” in *Principles of Coordination Polymerisation*, Chichester: Wiley, 2001, pp. 200–203.
- [44] G. J. Domski, J. M. Rose, G. W. Coates, A. D. Bolig, and M. Brookhart, “Living Alkene Polymerization: New Methods for the Precision Synthesis of Polyolefins,” *Progress in Polymer Science*, vol. 32, pp. 30–92, 2007.
- [45] J.-Y. Dong and Y. Hu, “Design and Synthesis of Structurally Well-Defined Functional Polyolefins via Transition Metal-Mediated Olefin Polymerization Chemistry,” *Coordination Chemistry Reviews*, vol. 250, pp. 47–65, 2006.
- [46] T. Shiono, S. Yoshida, H. Hagihara, and T. Ikeda, “Additive Effects of Trialkylaluminum on Propene Polymerization with (t-BuNSiMe₂Flu)TiMe₂-Based Catalysts,” *Applied Catalysis A: General*, vol. 200, pp. 145–152, 2000.
- [47] Y. Fukui, M. Murata, and K. Soga, “Living Polymerization of Propylene and 1-Hexene using bis-Cp Type Metallocene Catalysts,” *Macromolecular Rapid Communications*, vol. 20, pp. 637–640, 1999.
- [48] Y. Fukui and M. Murata, “Living Polymerizations of Propylene and Syntheses of Atactic Metallocene Catalyst Systems,” *Applied Catalysis A: General*, vol. 237, pp. 1–10, 2002.
- [49] R. J. Keaton, K. C. Jayaratne, D. A. Henningsen, L. A. Koterwas, and L. R. Sita, “Dramatic Enhancement of Activities for Living Ziegler-Natta Polymerizations Mediated by ‘Exposed’ Zirconium Acetamidinate Initiators: The Isospecific Living Polymerization of Vinylcyclohexane,” *Journal of the American Chemical Society*, vol. 123, pp. 6197–6198, 2001.
- [50] K. C. Jayaratne and L. R. Sita, “Stereospecific Living Ziegler-Natta Polymerization of 1-Hexene,” *Journal of the American Chemical Society*, vol. 122, pp. 958–959, 2000.
- [51] K. Phomphrai et al., “Diverse Pathways of Activation and Deactivation of Half-Sandwich Aryloxy Titanium Polymerization Catalysts,” *Organometallics*, no. 25, pp. 214–220, 2006.
- [52] H. Hagihara, T. Shiono, and T. Ikeda, “Living Polymerization of Propene and 1-Hexene with the [t-BuNSiMe₂Flu]TiMe₂/B(C₆F₅)₃ Catalyst,” *Macromolecules*, vol. 31, pp. 3184–3188, 1998.

- [53] K. Nomura and A. Fudo, “Efficient Living Polymerization of 1-Hexene by Cp*TiMe₂(O-2,6-iPr₂C₆H₃)⁻-Borate Catalyst Systems at Low Temperature,” *Journal of Molecular Catalysis A: Chemical*, vol. 209, pp. 9–17, 2004.
- [54] K. Nishii, T. Shiono, and T. Ikeda, “A Novel Synthetic Procedure for Stereoblock Poly(propylene) with a Living Polymerization System,” *Macromolecular Rapid Communications*, vol. 25, pp. 1029–1032, May 2004.
- [55] T. Hasan, K. Nishii, T. Shiono, and T. Ikeda, “Living Polymerization of Norbornene via Vinyl Addition with ansa-Fluorenylamidodimethyltitanium Complex,” *Macromolecules*, vol. 35, pp. 8933–8935, 2002.
- [56] T. Hasan, T. Shiono, and T. Ikeda, “Living Random Copolymerization of Ethene and Norbornene Using ansa-Fluorenylamidodimethyltitanium Complex,” *Macromolecular Symposia*, vol. 213, pp. 123–129, 2004.
- [57] T. Hasan, T. Ikeda, and T. Shiono, “Random Copolymerization of Propene and Norbornene with ansa-Fluorenylamidodimethyltitanium-Based Catalysts,” *Macromolecules*, vol. 38, pp. 1071–1074, 2005.
- [58] L. Schock and T. J. Marks, “Organometallic Thermochemistry. Metal Hydrocarbyl, Hydride, Halide, Carbonyl, Amide, and Alkoxide Bond Enthalpy Relationships and Their Implications in Pentamethylcyclopentadienyl and Cyclopentadienyl Complexes of Zirconium and Hafnium,” *Journal of the American Chemical Society*, vol. 110, pp. 7701–7715, 1988.
- [59] P. Wolczanski and J. Bercaw, “Alkyl and Hydride Derivatives of (Pentamethylcyclopentadienyl)zirconium(IV),” *Organometallics*, vol. 1, pp. 793–799, 1982.
- [60] K. Nomura, N. Naga, M. Miki, and K. Yanagi, “Olefin Polymerization by (Cyclopentadienyl)(aryloxy)titanium (IV) Complexes-Cocatalyst Systems,” *Macromolecules*, vol. 31, pp. 7588–7597, 1998.
- [61] J. Okuda, F. Schattenmann, S. Wocadlo, and W. Massa, “Synthesis and Characterization of Zirconium Complexes Containing a Linked Amido-Fluorenyl Ligand,” *Organometallics*, vol. 14, pp. 789–795, 1995.
- [62] H. Hagimoto, T. Shiono, and T. Ikeda, “Living Polymerization of Propene with a Chelating Diamide Complex of Titanium Using Dried Methylaluminumoxane,” *Macromolecular Rapid Communications*, vol. 23, pp. 73–76, 2002.

- [63] J. D. Scollard and D. H. McConville, "Living Polymerization of α -Olefins by Chelating Diamide Complexes of Titanium," *Journal of the American Chemical Society*, vol. 118, pp. 10008–10009, 1996.
- [64] G. W. Coates, P. D. Hustad, and S. Reinartz, "Catalysts for the Living Insertion Polymerization of Alkenes: Access to New Polyolefin Architectures Using Ziegler-Natta Chemistry," *Angewandte Chemie International Edition*, vol. 41, pp. 2236–2257, 2002.
- [65] M. Mitani et al., "Fluorine- and Trimethylsilyl-Containing Phenoxy-Imine Ti Complex for Highly Syndiotactic Living Polypropylenes with Extremely High Melting Temperatures," *Journal of the American Chemical Society*, vol. 124, pp. 7888–7889, 2002.
- [66] J. Saito et al., "Microstructure of Highly Syndiotactic 'Living' Poly(propylene)s Produced from a Titanium Complex with Chelating Fluorine-Containing Phenoxyimine Ligands (an FI Catalyst)," *Macromolecular Rapid Communications*, vol. 22, pp. 1072–1075, 2001.
- [67] J. Tian, P. D. Hustad, and G. W. Coates, "A New Catalyst for Highly Syndiospecific Living Olefin Polymerization: Homopolymers and Block Copolymers from Ethylene and Propylene," *Journal of the American Chemical Society*, vol. 123, pp. 5134–5135, 2001.
- [68] M. Mitani et al., "Living Polymerization of Ethylene Catalyzed by Titanium Complexes Having Fluorine-Containing Phenoxy-Imine Chelate Ligands," *Journal of the American Chemical Society*, vol. 124, pp. 3327–3336, 2002.
- [69] J. D. Scollard, D. H. McConville, J. J. Vittal, and N. C. Payne, "Chelating Diamide Complexes of Titanium: New Catalyst Precursors for the Highly Active and Living Polymerization of α -Olefins," *Journal of Molecular Catalysis A: Chemical*, vol. 128, pp. 201–214, 1998.
- [70] T. Matsugi et al., "New Titanium Complexes Bearing Two Indolide-Imine Chelate Ligands for the Polymerization of Ethylene," *Macromolecules*, vol. 35, pp. 4880–4887, 2002.
- [71] E. F. Connor et al., "Linear Functionalized Polyethylene Prepared with Highly Active Neutral Ni(II) Complexes," *Journal of Polymer Science Part A: Polymer Chemistry*, vol. 40, pp. 2842–2854, 2002.
- [72] J. Merna, J. Cihlar, M. Kucera, A. Deffieux, and H. Cramail, "Polymerization of Hex-1-ene Initiated by Diimine Complexes of Nickel and Palladium," *European Polymer Journal*, vol. 41, pp. 303–312, 2005.

- [73] P. S. Umare, G. L. Tembe, and B. Trivedi, "Catalytic Synthesis of Low Molecular Weight Polyethylene by S-bridged Ti-Complexes," *Reaction Kinetics and Catalysis Letters*, vol. 91, pp. 45–51, 2007.
- [74] P. S. Umare, A. J. Tiwari, R. Antony, G. L. Tembe, and B. Trivedi, "Synthesis of Ultra-Low-Molecular-Weight Polyethylene Wax Using a Bulky Ti(IV) Aryloxide-Alkyl Aluminum Catalytic System," *Applied Organometallic Chemistry*, vol. 21, pp. 652–660, 2007.
- [75] T. R. Younkin, E. F. Connor, J. I. Henderson, S. K. Friedrich, R. H. Grubbs, and D. A. Bansleben, "Neutral, Single-Component Nickel (II) Polyolefin Catalysts That Tolerate Heteroatoms," *Science*, vol. 287, pp. 460–462, 2000.
- [76] K. Hakala, B. Löfgren, and T. Helaja, "Copolymerizations of Oxygen-Functionalized Olefins with Propylene Using Metallocene/Methylaluminoxane Catalyst," *European Polymer Journal*, vol. 34, pp. 1093–1097, 1998.
- [77] M. Atiqullah, M. Tinkl, R. Pfaendner, M. N. Akhtar, and I. Hussain, "Synthesis of Functional Polyolefins using Metallocenes: A Comprehensive Review," *Polymer Reviews*, vol. 50, pp. 178–230, 2010.
- [78] H. Hagihara, M. Murata, and T. Uozumi, "Alternating Copolymerization of Ethylene and 5-Hexen-1-ol [Ethylene(1-indenyl)(9-fluorenyl)]-zirconium Dichloride/Methylaluminoxane as the Catalyst," *Macromolecular Rapid Communications*, vol. 22, pp. 353–357, 2001.
- [79] N. Kawahara, J. Saito, S. Matsuo, H. Kaneko, T. Matsugi, and N. Kashiwa, "Polymer Hybrids Based on Polyolefins – Syntheses, Structures, and Properties," in *Advances in Polymer Science*, S. Kobayashi, Ed. Berlin: Springer, 2008, pp. 79–119.
- [80] H. Kaneyoshi and K. Matyjaszewski, "Synthesis of a Linear Polyethylene Macromonomer and Preparation of Polystyrene-graft-Polyethylene Copolymers via Grafting-Through Atom Transfer Radical Polymerization," *Journal of Applied Polymer Science*, vol. 105, pp. 3–13, 2007.
- [81] A. Amgoune, M. Krumova, and S. Mecking, "Nanoparticle-Supported Molecular Polymerization Catalysts," *Macromolecules*, vol. 41, pp. 8388–8396, 2008.
- [82] H. Makio, H. Terao, A. Iwashita, and T. Fujita, "FI Catalysts for Olefin Polymerization - A Comprehensive Treatment," *Chemical Reviews*, vol. 111, pp. 2363–2449, Mar. 2011.

- [83] Y. Choi and J. B. P. Soares, “Supported Single-Site Catalysts for Slurry and Gas-Phase Olefin Polymerisation,” *The Canadian Journal of Chemical Engineering*, vol. 90, pp. 646–671, Jun. 2012.
- [84] J. M. Campos, J. P. Lourenço, H. Cramail, and M. R. Ribeiro, “Nanostructured Silica Materials in Olefin Polymerisation: From Catalytic Behaviour to Polymer Characteristics,” *Progress in Polymer Science*, Mar. 2012.
- [85] W. Zhang, J. Wei, and L. R. Sita, “Living Coordinative Chain-Transfer Polymerization and Copolymerization of Ethene, α -Olefins, and α,ω -Nonconjugated Dienes using Dialkylzinc as ‘Surrogate’ Chain-Growth Sites,” *Macromolecules*, vol. 41, pp. 7829–7833, 2008.
- [86] P. Zinck, “Tuning Polyolefins and Polydienes Microstructure and Architecture via Coordinative Chain Transfer Polymerization,” *Polymer International*, vol. 61, pp. 2–5, 2012.
- [87] R. Kempe, “How to Polymerize Ethylene in a Highly Controlled Fashion?,” *Chemistry A European Journal*, vol. 13, pp. 2764–73, 2007.
- [88] J. Wei, W. Zhang, and L. R. Sita, “Aufbaureaktion Redux: Scalable Production of Precision Hydrocarbons from AlR_3 (R=Et or iBu) by Dialkyl Zinc Mediated Ternary Living Coordinative Chain-Transfer Polymerization,” *Angewandte Chemie International Edition*, vol. 49, pp. 1768–1772, 2010.
- [89] S. B. Amin and T. J. Marks, “Versatile Pathways for In Situ Polyolefin Functionalization with Heteroatoms: Catalytic Chain Transfer,” *Angewandte Chemie International Edition*, vol. 47, pp. 2006–2025, 2008.
- [90] J.-F. Pelletier, A. Mortreux, X. Olonde, and K. Bujadoux, “Synthesis of New Dialkylmagnesium Compounds by Living Transfer Ethylene Oligo- and Polymerization with Lanthanocene Catalysts,” *Angewandte Chemie International Edition in English*, vol. 35, pp. 1854–1856, 1996.
- [91] T. Tilley and R. A. Andersen, “Pentamethylcyclopentadienyl Derivatives of the Trivalent Lanthanide Elements Neodymium, Samarium, and Ytterbium,” *Inorganic Chemistry*, vol. 20, pp. 3267–3270, 1981.
- [92] W. P. Kretschmer, T. Bauer, B. Hessen, and R. Kempe, “An Efficient Yttrium Catalysed Version of the ‘Aufbaureaktion’ for the Synthesis of Terminal Functionalised Polyethylene,” *Dalton Transaction*, vol. 39, pp. 6576–88, 2010.
- [93] P. Zinck, A. Valente, A. Mortreux, and M. Visseaux, “In Situ Generated Half-Lanthanidocene Based Catalysts for the Controlled Oligomerisation of Styrene:

- Selectivity, Block Copolymerisation and Chain Transfer,” *Polymer*, vol. 48, pp. 4609–4614, 2007.
- [94] P. Zinck et al., “Reversible Coordinative Chain Transfer Polymerization of Styrene by Rare Earth Borohydrides, Chlorides/Dialkylmagnesium Systems,” *Journal of Polymer Science Part A: Polymer Chemistry*, vol. 48, pp. 802–814, 2010.
- [95] C. Fan, C. Bai, H. Cai, Q. Dai, X. Zhang, and F. Wang, “Preparation of High cis-1,4 Polyisoprene with Narrow Molecular Weight Distribution via Coordinative Chain Transfer Polymerization,” *Journal of Polymer Science Part A: Polymer Chemistry*, vol. 48, pp. 4768–4774, 2010.
- [96] G. J. P. Britovsek, S. A. Cohen, V. C. Gibson, P. J. Maddox, and M. van Meurs, “Iron-Catalyzed Polyethylene Chain Growth on Zinc: Linear α -Olefins with a Poisson Distribution,” *Angewandte Chemie International Edition*, vol. 114, pp. 507–509, 2002.
- [97] F. Rouholahnejad, D. Mathis, and P. Chen, “Narrowly Distributed Polyethylene via Reversible Chain Transfer to Aluminum by a Sterically Hindered Zirconocene/MAO,” *Organometallics*, vol. 29, pp. 294–302, 2010.
- [98] W. Zhang and L. R. Sita, “Highly Efficient, Living Coordinative Chain-Transfer Polymerization of Propene with ZnEt₂: Practical Production of Ultrahigh to Very Low Molecular Weight Amorphous Atactic Polypropenes of Extremely Narrow Polydispersity,” *Journal of the American Chemical Society*, vol. 130, pp. 442–443, 2008.
- [99] S. M. Cendrowski-Guillaume, G. Le Gland, M. Nierlich, and M. Ephritikhine, “Lanthanide Borohydrides as Precursors to Organometallic Compounds. Mono(cyclooctatetraenyl) Neodymium Complexes,” *Organometallics*, vol. 19, pp. 5654–5660, 2000.
- [100] F. Bonnet, M. Visseaux, D. Barbier-Baudry, A. Hafid, E. Vigier, and M. M. Kubicki, “Organometallic Early Lanthanide Clusters: Syntheses and X-ray Structures of New Monocyclopentadienyl Complexes,” *Inorganic Chemistry*, vol. 43, pp. 3682–3690, 2004.
- [101] A. Valente, P. Zinck, A. Mortreux, and M. Visseaux, “Catalytic Chain Transfer (co-)Polymerization: Unprecedented Polyisoprene CCG and a New Concept to Tune the Composition of a Statistical Copolymer,” *Macromolecular Rapid Communications*, vol. 30, pp. 528–531, 2009.

- [102] S. M. Guillaume, M. Schappacher, and A. Soum, “Polymerization of ϵ -Caprolactone Initiated by $\text{Nd}(\text{BH}_4)_3(\text{THF})_3$: Synthesis of Hydroxytelechelic Poly(ϵ -caprolactone),” *Macromolecules*, vol. 36, pp. 54–60, 2003.
- [103] J. Chen et al., “Syntheses of Iron, Cobalt, Chromium, Copper and Zinc Complexes with Bulky bis(Imino)Pyridyl Ligands and Their Catalytic Behaviors in Ethylene Polymerization and Vinyl Polymerization of Norbornene,” *Journal of Molecular Catalysis A: Chemical*, vol. 259, pp. 133–141, 2006.
- [104] J.-M. Qiu, L.-G. Sun, Y.-L. Hu, and Y.-F. Li, “The Behavior of Homogeneous Iron-Based Catalysts Bearing Pyridine Diimine Ligands for Ethylene Polymerization,” *Chinese Journal of Polymer Science*, vol. 18, pp. 509–513, 2000.
- [105] B. Bocharov, “Progress in the Chemistry of the Carbodiimides,” *Russian Chemical Reviews*, vol. 34, pp. 212–219, 1965.
- [106] G. J. P. Britovsek, S. A. Cohen, V. C. Gibson, and M. Van Meurs, “Iron Catalyzed Polyethylene Chain Growth on Zinc: A Study of the Factors Delineating Chain Transfer versus Catalyzed Chain Growth in Zinc and Related Metal Alkyl Systems,” *Journal of the American Chemical Society*, vol. 126, pp. 10701–10712, 2004.
- [107] Y. Zhao, L. Wang, A. Xiao, and H. Yu, “The Synthesis of Modified Polyethylene via Coordination Polymerization Followed by ATRP, RAFT, NMRP or ROP,” *Progress in Polymer Science*, vol. 35, pp. 1195–1216, 2010.
- [108] C.-Y. Guo, H. Xu, M. Zhang, H.-J. Yang, F. Yan, and G. Yuan, “Copolymerization of Ethylene and In situ-Generated α -Olefins to High-Performance Linear Low-Density Polyethylene with a Two-Catalyst System Supported on Mesoporous Molecular Sieves,” *Polymer International*, vol. 59, pp. 725–732, 2010.
- [109] E. Jellema, A. L. Jongerius, J. N. H. Reek, and B. D. Bruin, “C1 Polymerisation and Related C–C Bond Forming “Carbene InsertionI Reactions,” *Chemical Society Reviews*, vol. 39, pp. 1706–1723, 2010.
- [110] J. Luo and K. J. Shea, “Polyhomologation. A Living C1 Polymerization,” *Accounts of Chemical Research*, vol. 43, pp. 1420–1433, 2010.
- [111] B. B. Busch, C. L. Staiger, J. M. Stoddard, and K. J. Shea, “Living Polymerization of Sulfur Ylides. Synthesis of Terminally Functionalized and Telechelic Polymethylene,” *Macromolecules*, vol. 35, pp. 8330–8337, 2002.

- [112] W. J. Atkins, E. R. Burkhardt, and K. Matos, "Safe Handling of Boranes at Scale," *Organic Process Research & Development*, vol. 10, pp. 1292–1295, 2006.
- [113] C. E. Wagner, A. A. Rodriguez, and K. J. Shea, "Synthesis of Linear α -Olefins via Polyhomologation," *Macromolecules*, vol. 38, pp. 7286–7291, 2005.
- [114] H. C. Brown, *Hydroboration*. New York: Benjamin, 1962.
- [115] T. Onak, *Organooborane Chemistry*. New York: Academic Press, 1975.
- [116] X.-Z. Zhou and K. J. Shea, "Ersatz Ethylene-Propylene Copolymers: The Synthesis of Linear Carbon Backbone Copolymers One Carbon Atom at a Time," *Journal of the American Chemical Society*, vol. 122, pp. 11515–11516, 2000.
- [117] C. E. Wagner, J.-S. Kim, and K. J. Shea, "The Polyhomologation of 1-Boraadamantane: Mapping the Migration Pathways of a Propagating Macrotricyclic Trialkylborane," *Journal of the American Chemical Society*, vol. 125, pp. 12179–12195, 2003.
- [118] C. R. Johnson, M. Haake, and C. W. Schroeck, "Preparation and Synthetic Applications of (Dimethylamino)phenyloxosulfonium Methylide," *Journal of the American Chemical Society*, vol. 92, pp. 6594–6598, 1970.
- [119] R. Sulc, X. Zhou, and K. J. Shea, "Repetitive sp^3 - sp^3 Carbon-Carbon Bond-Forming Copolymerizations of Primary and Tertiary Ylides. Synthesis of Substituted Carbon Backbone Polymers: Poly (cyclopropylidene-co-methylidene)," *Macromolecules*, vol. 39, pp. 4948–4952, 2006.
- [120] K. J. Shea, J. W. Walker, H. Zhu, M. Paz, and J. Greaves, "Polyhomologation. A Living Polymethylene Synthesis," *Journal of the American Chemical Society*, vol. 119, pp. 9049–9050, 1997.
- [121] J. Bai and K. J. Shea, "Reaction of Boranes with TMS Diazomethane and Dimethylsulfoxonium Methylide. Synthesis of Poly(methylidene-co-TSMethylidene) Random Copolymers," *Macromolecular Rapid Communications*, vol. 27, pp. 1223–1228, 2006.
- [122] J. Luo, F. Lu, and K. J. Shea, "Hydrocarbon Waxes from a Salt in Water: The C1 Polymerization of Trimethylsulfoxonium Halide," *ACS Macro Letters*, vol. 1, no. 5, pp. 560–563, May 2012.
- [123] V. C. Gibson and S. K. Spitzmesser, "Advances in Non-Metallocene Olefin Polymerization Catalysis," *Chemical Reviews*, vol. 103, pp. 283–315, 2003.

3. Bulk Synthesis of Narrowly Distributed Low Molecular Weight Polymers via Living Ring Opening Metathesis Polymerization

This chapter is based on the manuscript authored by Lai Chi So, Santiago Faucher, and Shiping Zhu entitled “Bulk Synthesis and Modeling of Living ROMP of 1,5-Cyclooctadiene for Narrowly Distributed Low Molecular Weight Linear Polymers” prepared for submission for publication. Lai Chi So developed the experimental design and carried out the laboratory experimentation under the guidance of Dr. Faucher and Dr. Zhu. Dr. Faucher and Dr. Zhu aided in manuscript revision.

3.1. Introduction

Living ring opening metathesis polymerization (ROMP) has been selected for the study of the synthesis of narrowly distributed low molecular weight polyethylene (PE) mimics with functionalization possibilities. Living ROMP was developed from the industrially relevant ROMP process and requires the use of simple reaction setup (i.e. involving only non-gaseous reagents), mild reaction conditions (i.e. room temperature reaction process), and commercially available raw materials. In living ROMP, unsubstituted cycloolefins are polymerized to yield linear polymers with controlled molecular weights. The linear polymers contain periodic carbon-carbon double bond (C=C) unsaturations which can undergo post-polymerization hydrogenation or functionalization reactions to obtain polymers with controlled molecular weight and structures [1–3].

Living ROMP poses several advantages, including its relevance and importance in industry and academic fields, the availability of raw materials, the ease of polymerization reaction setup, and its efficiency in well-controlled high molecular production [4]. However, it has three major challenges for the efficient synthesis of well-defined low molecular weight polymers.

Firstly, one active center (i.e. catalyst) is responsible for the growth of one polymer chain and hence, large amounts of expensive catalyst are necessary for the production of low molecular weight products. Secondly, slow initiation and chain termination can result in molecular weight distribution broadening [5]. This non-ideality has a greater influence on the molecular weight distribution of low molecular weight products than that of high molecular weight products. Bielawski and Grubbs have reported the use of bulky labile phosphines in ruthenium catalyst based living ROMP to address this challenge. It was demonstrated that the much less expensive phosphines act as a polymerization regulator. The use of excess phosphines enhances initiation characteristics and attenuates chain propagation, which results in narrow distributions over a large molecular weight range [6]. Lastly, the majority of the reported living ROMP reactions are solution polymerization processes, which have poor reactor volume efficiencies, require the use of volatile organic compounds, and require energy intensive separation steps post polymerization. The polymer product generally contributes to less than 50 wt. % of the reactor solution, with the bulk of the reactor solution consisting of solvent [7–17]. Although there have been reports of successful bulk polymerizations of cyclopentene and

cycloheptene with various ruthenium catalysts, detailed studies of the behaviour and products of bulk living ROMP polymerizations have not been reported [7].

Herein, the synthesis of low molecular weight polymers with narrow distributions was studied via ROMP of a readily available 1,5-cyclooctadiene monomer via a commercially available Grubbs' "first generation" ruthenium catalyst in the absence and in the presence of the much less expensive polymerization regulator triphenylphosphine. The translation of ROMP from a solution polymerization system into a bulk polymerization system was investigated. Experimental results demonstrated that the bulk polymerization systems with and without triphenylphosphine yield similar, if not improved, molecular weight control compared to the solution polymerization systems. Studies into polymerization kinetics indicated that the bulk polymerization system exhibits living polymerization behaviour. The success of bulk living ROMP yields ROMP to be an efficient and viable polymerization pathway for the production of narrowly dispersed low molecular weight polymers.

3.2. Experimental

3.2.1. Materials

1,5-Cyclooctadiene (1,5-COD, $\geq 99\%$), triphenylphosphine (PPh₃, 99%), bis(tricyclohexylphosphine)benzylidene ruthenium(IV) dichloride (Grubbs' "first generation" ruthenium catalyst) (GI catalyst), ethyl vinyl ether (99%), 2,6-di-*tert*-butyl-4-methylphenol (butylated hydroxytoluene) (BHT, $\geq 99\%$), and anhydrous dichloromethane (DCM, $\geq 99.8\%$) were used as received from Sigma-Aldrich.

3.2.2. NMR Measurements

Chemical structures of polymers were characterized using nuclear magnetic resonance (NMR) spectroscopy. ¹H NMR spectra were recorded on a Bruker Avance 400 spectrometer at 298K using deuterated chloroform (CDCl₃) as a solvent and tetramethylsilane (TMS) as the reference. Data was recorded and analyzed using the Bruker TopSpin 3.0 software.

3.2.3. GPC Measurements

Gel permeation chromatography (GPC) was used to determine the number-average molecular weight (M_n), weight-average molecular weights (M_w), and reaction conversion (x). Conversions were determined based on the integral of the polymer peak and the

butylated hydroxytoluene (BHT) peak in the refractive index (RI) detector traces. GPC was carried out in tetrahydrofuran (THF) at a flow rate of 1 mL/min at 40°C with a Waters 2690 Separation Module, a Waters 410 Differential Refractometer, and five columns in series (Waters Styragel HR 1, 3, 4, 5 and 6). Molecular weights were reported relative to a calibration curve obtained using monodispersed polystyrene standards. Data was recorded and analyzed using the Waters Empower Pro software. Note that samples used for GPC analysis were directly withdrawn from the polymerization reaction flask to avoid the loss of low molecular weight product via subsequent precipitation, filtration, and washing steps.

3.2.4. DSC Measurements

The glass transition temperatures (T_g) and melting temperatures (T_m) of polymers were determined by differential scanning calorimetry (DSC) on a Thermal Analysis Q1000 Differential Scanning Calorimeter. Note that samples used for DSC analysis were precipitated, filtrated, and washed. As a result, the loss of low molecular weight product may be possible leading to slight discrepancies in DSC measurements.

3.2.5. Solution Polymerization

Two glass flasks were sealed with rubber septa and secured with wire. Five vacuum-nitrogen purge cycles were applied to the flasks, followed by heating via a heat gun and an additional purge with nitrogen for 15 min. Anhydrous DCM and 1,5-COD were transferred into the flasks via nitrogen purged stainless steel needles. DCM and 1,5-COD were bubbled with nitrogen for at least 30 min. PPh_3 (0.1565 g, 0.597 mmol) and GI catalyst (0.0838 g, 0.102 mmol) were added to two other flasks. The flasks were sealed with rubber septa and secured with wire. The flask containing catalyst also contained a magnetic stir bar and was sealed with a layer of Parafilm. The two flasks were purged with nitrogen for at least 30 min. 1,5-COD (2 mL, 0.0163 mol) and DCM (9 mL) were transferred into the flasks containing PPh_3 and GI catalyst, respectively, to allow for PPh_3 and GI catalyst dissolution. The 1,5-COD/ PPh_3 solution was transferred into the DCM/GI catalyst flask at room temperature with stirring and under positive nitrogen pressure. The reaction was terminated with ethyl vinyl ether (2 mL, 0.0208 mol, 200 eq. to catalyst) after 24 hours. THF was added to ensure polymer dissolution and BHT (5 g, 0.0227 mol, 1.3 eq. to monomer) was added to prevent polymer crosslinking. The mixture was stirred for at least 1 hour to ensure complete termination. Samples were withdrawn for GPC analysis to avoid the loss of low molecular weight product via subsequent precipitation, filtration, and washing steps. The polymer solution was then precipitated into approximately 1 L of methanol or methanol/isopropyl alcohol at 0°C. The polymer precipitate was washed at least three times with methanol and dried for DSC analysis.

3.2.6. Bulk Polymerization

The procedure used in bulk polymerization is similar to that used in solution polymerization. The only difference was that solvents were not used (i.e. DCM was not used).

3.2.7. Kinetic Studies

Parallel experiments were carried out to investigate the kinetics of bulk ROMP. Samples were withdrawn at various time intervals with nitrogen purged syringes and transferred into vials with known amounts of BHT and sufficient ethyl vinyl ether for reaction termination. The samples were diluted with THF and were analyzed using GPC.

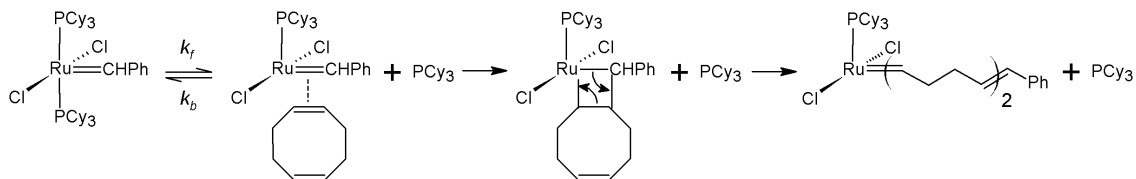
3.3. Results and Discussion

Scheme 3.1 shows the ROMP of 1,5-cyclooctadiene using a “Grubbs’ first generation” ruthenium catalyst. Initiation begins by the dissociation of a tricyclohexylphosphine (PCy_3) group from the ruthenium center of the metal alkylidene catalyst, creating a coordination site for the 1,5-COD monomer. The cycloolefin ring is opened and added onto the metal alkylidene. Propagation proceeds via the same steps as initiation. As previously discussed, the driving force of ROMP is the release of ring strain energy associated with ring opening. As such, ROMP can easily reach high conversion for highly strained cycloolefins such as norbornene. For low ring strain cycloolefins such as 1,5-COD, any monomer above the equilibrium monomer concentration ($[\text{M}]_{\text{eq}}$), which is 0.25 M at room temperature for 1,5-COD, can be converted into polymer. The amount of monomer above $[\text{M}]_{\text{eq}}$ is the effective monomer concentration ($[\text{M}]_{\text{eff}}$) that is available for polymerization. Finally, the reaction is terminated by deactivating and removing the metal catalyst from the polymer by the addition of ethyl vinyl ether.

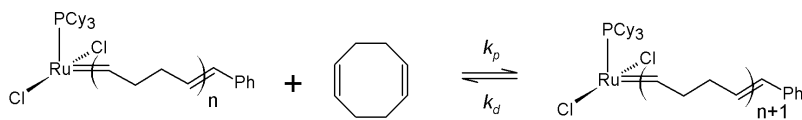
The reaction following **Scheme 3.1** has been reported to yield polymers with fairly well controlled molecular weight distributions. However, Bielawski and Grubbs demonstrated that the addition of bulky labile phosphines can enhance the living behaviour and hence the control of the chain polydispersity [6]. As discussed in **Chapter 2.1.2** and as shown in **Scheme 2.2**, the labile phosphine increases the initiation efficiency of the catalyst via a

fast phosphine exchange prior to monomer coordination and decreases the rate of propagation by competing with monomer for the catalyst metal center.

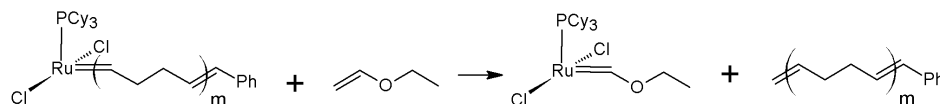
Initiation



Propagation



Termination



Scheme 3.1. Reaction scheme for living ROMP of 1,5-cyclooctadiene using a Grubbs' "first generation" ruthenium catalyst [9]. Note: k_f , k_b , k_p , and k_d are the rates of catalyst activation, catalyst deactivation, propagation, and depropagation, respectively.

3.3.1. Solution and Bulk Polymerization in the Absence of Phosphine

In preliminary experiments, the effects of monomer-to-catalyst ratios ($[M]_0/[I]$) and monomer concentration ($[M]_0$) were studied. For comparative purposes, solution polymerizations were carried out in parallel with bulk polymerizations. Three $[M]_0/[I]$ ratios of approximately 50, 150, and 250 were used in solution polymerization ($[M]_0 \cong 1.5$ M) and in bulk polymerization ($[M]_0 = 8.2$ M). The reaction ran 24 hours at room temperature.

To characterize the chemical structures of the synthesized poly(1,5-cyclooctadiene) (p(1,5-COD)), ^1H NMR spectra of the polymers were obtained. A representative spectra is given in **Figure 3.1**. The unsaturated double bond signal and the saturated single bond signal were observed at approximately 5.5 ppm and 2 ppm respectively. The signal at approximately 7.3 ppm is attributed to the phenyl functional group that results from the phenyl ligand on the GI catalyst.

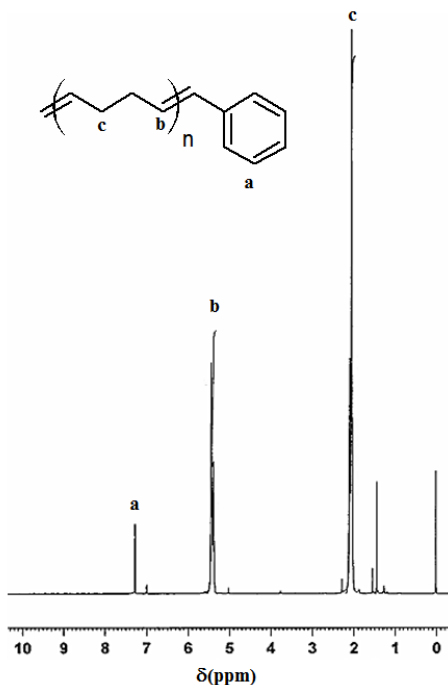


Figure 3.1. Representative ¹H NMR spectrum of poly(1,5-cyclooctadiene) synthesized via bulk polymerization.

Table 3.1 and **Figure 3.2** summarize the effect of increase in $[M]_0/[I]$ in both solution and bulk polymerization. As expected, an increase in $[M]_0/[I]$ resulted in an increase in polymer molecular weight. However, polydispersity was not significantly affected by changes in $[M]_0/[I]$.

A noticeable difference in viscosity between solution and bulk polymerization was visually observed. In solution polymerization, reaction solution viscosity did not increase significantly. The most noticeable viscosity increase was observed for $[M]_0/[I]$ ratio of approximately 50. However, for bulk polymerization, viscosity increased significantly.

For all values of $[M]_0/[I]$, viscosity increased such that the magnetic stir bar became immobile within the first two hours of reaction.

Despite the differences in viscosity increase, very little differences in polydispersity were found between solution and bulk polymerization with the same $[M]_0/[I]$ ratios. In general, bulk polymerization produced polymers with higher molecular weights and similar conversions as compared to solution polymerization. This observation is attributed to the equilibrium monomer concentration of 0.25 M for 1,5-COD. Bulk polymerization has a higher effective monomer concentration than solution polymerization independent of $[M]_0/[I]$ values. More monomer can be consumed prior to reaching the equilibrium monomer concentration. As a result, higher molecular weight polymers can be produced.

It is clear that living ROMP can allow for the synthesis of the desired low molecular weight polymers with molecular weights in the order of 10^3 g/mol. With a $[M]_0/[I]$ ratio of approximately 50, polymers with molecular weights of 9,200 g/mol and 15,000 g/mol were produced in solution and in bulk, respectively. By further increasing the catalyst loading, it would be possible to obtain polymers with shorter chain lengths. However, the increase in catalyst loading renders the reaction expensive and inefficient. Further, although the polymers have fairly narrow polydispersities, they do not satisfy the desired polydispersities of less than 1.20. Therefore, the use of excess phosphine in living ROMP to enhance molecular weight distribution control was studied.

Table 3.1. Solution and bulk ROMP of 1,5-cyclooctadiene with Grubbs’ “first generation” catalyst in the absence of phosphine.

Entry	$[M]_0$ (M)	$[M]_0/[I]$	$M_{n,th}^a$ (g/mol)	M_n (g/mol)	M_w (g/mol)	PDI	x^b	f^c	$T_{g, onset}$ (°C)	$T_{g, midpoint}$ (°C)	$T_{g, offset}$ (°C)	T_m (°C)
1-1 ^d	1.6	46	5,000	9,200	17,900	2.0	1.00	0.5	-	-	-	-
1-2 ^d	1.3	151	16,300	14,400	32,600	2.3	1.00	1.0	-28	-26	-23	13
1-3 ^d	1.5	250	27,000	19,500	46,300	2.4	1.00	1.0	-27	-25	-23	-2
1-4 ^e	8.2	53	5,400	15,000	30,100	2.0	1.00	0.4	-	-	-	-
1-5 ^e	8.2	146	15,800	19,500	39,000	2.0	1.00	0.8	-62	-50	-39	5
1-6 ^e	8.2	255	27,500	26,000	52,600	2.0	1.00	1.0	-60	-53	-45	-7

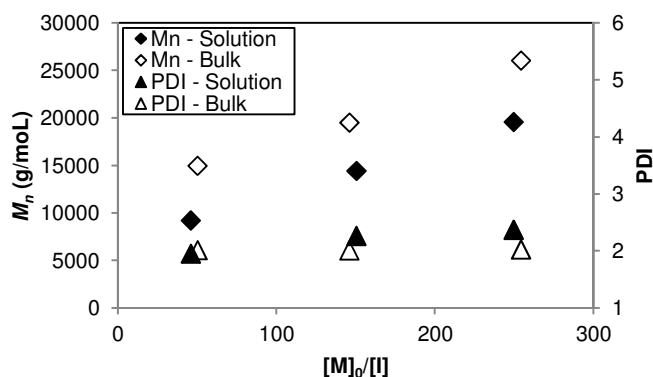
^aTheoretical M_n calculated as (monomer molecular weight) $\times x \times [M]_0/[I]$.

^bConversion determined by GPC.

^cInitiator efficiency, f , calculated as $([M]_0/[I]) \times (x / (M_n / (\text{monomer molecular weight})))$.

^dSolution polymerization.

^eBulk polymerization.

**Figure 3.2.** Comparison of the number average molecular weight (M_n) (diamond symbols) and polydispersities (PDI) (triangular symbols) of poly(1,5-cyclooctadiene) in solution ROMP (filled symbols) and bulk ROMP (empty symbols) via Grubbs’ “first generation” catalyst in the absence of phosphine.

3.3.2. Solution and Bulk Polymerization in the Presence of Phosphine

After the success of ROMP without phosphine, the effects of the addition of phosphine on molecular weight distribution control in ROMP was studied. For comparative purposes, solution polymerizations were carried out in parallel with bulk polymerizations. A $[M]_0/[I]$ ratio of approximately 150 was used in solution polymerization ($[M]_0 \cong 1.5$ M) and in bulk polymerization ($[M]_0 = 8.2$ M) with phosphine-to-catalyst ratios ($[P]_0/[I]$) ranging from 0 to 20. The reactions ran for 24 hours at room temperature. No increase in viscosity was observed for solution and bulk polymerizations conducted in the presence of phosphine. Slight viscosity increase was observed in the solution polymerization without phosphine and significant viscosity increase was observed in the bulk polymerization without phosphine.

As shown in **Table 3.2** and **Figure 3.3**, in solution and in bulk polymerization, an increase in $[P]_0/[I]$ resulted in a decrease in molecular weight, polydispersity, and conversion. At low $[P]_0/[I]$ ratios, there was limited control in the polymerization reaction and the polymer polydispersity is high (i.e. PDI ~ 2). As $[P]_0/[I]$ increases, the rate of initiation increased and the rate of propagation decreased. As a result, molecular weight, polydispersity, and conversion decreased. Polydispersities of lower than 1.5 were obtained in solution and in bulk polymerization with $[P]_0/[I]$ greater than 5. At a high $[P]_0/[I]$ ratio of 19.3 for bulk polymerization, no polymer was produced due to the excessively slow propagation rate [8].

At a short reaction time of 24 hours, polymers with similar molecular weights were produced at similar conversions via solution and bulk ROMP with the same triphenylphosphine loadings. However, bulk polymerization in the presence of triphenylphosphine consistently produced polymers with narrower molecular weight distributions at similar conversions. As previously mentioned, bulk polymerization has a higher effective monomer concentration than solution polymerization. Given similar conversions (prior to reaching the equilibrium monomer concentration), bulk polymerization maintains a higher monomer concentration from the equilibrium monomer concentration as compared to solution polymerization. By maintaining a monomer concentration further away from the equilibrium monomer concentration, the propagation-depropagation equilibrium that broadens the distribution can be limited.

Table 3.2. Solution and bulk ROMP of 1,5-cyclooctadiene with Grubbs’ “first generation” catalyst in the presence of triphenylphosphine.

Entry	$[M]_0$ (M)	$[M]_0/$ $[I]$	$[P]_0/$ $[I]$	$M_{n,th}^a$ (g/mol)	M_n (g/mol)	M_w (g/mol)	PDI	x^b	f^c	$T_{g, onset}$ (°C)	$T_{g, midpoint}$ (°C)	$T_{g, offset}$ (°C)	T_m (°C)
2-1 ^d	1.3	151	0	16,300	14,400	32,600	2.3	1.00	1.0	-28	-26	-23	13
2-2 ^d	1.5	160	5.9	2,600	4,200	5,700	1.4	0.15	0.6	-	-	-	-
2-3 ^d	1.6	160	11.3	2,200	2,700	3,600	1.4	0.13	0.8	-	-	-	-
2-4 ^d	1.5	155	14.4	1,200	2,300	2,800	1.2	0.07	0.5	-46	-43	-40	-24
2-5 ^e	8.2	146	0	15,800	19,500	39,000	2.0	1.00	0.8	-62	-50	-39	5
2-6 ^e	8.2	152	5.3	2,500	3,700	4,900	1.3	0.15	0.7	-30	-27	-24	4
2-7 ^e	8.2	151	10.8	1,000	2,100	2,500	1.2	0.06	0.5	-	-	-	-
2-8 ^e	8.2	151	15.1	200	2,000	2,200	1.1	0.01	0.1	-	-	-	-
2-9 ^e	8.2	140	19.3							No polymer			

^aTheoretical M_n calculated as (monomer molecular weight) $\times x \times [M]_0 / [I]$.

^bConversion determined by GPC.

^cInitiator efficiency, f , calculated as $([M]_0 / [I]) \times (x / (M_n / (\text{monomer molecular weight})))$.

^dSolution polymerization.

^eBulk polymerization.

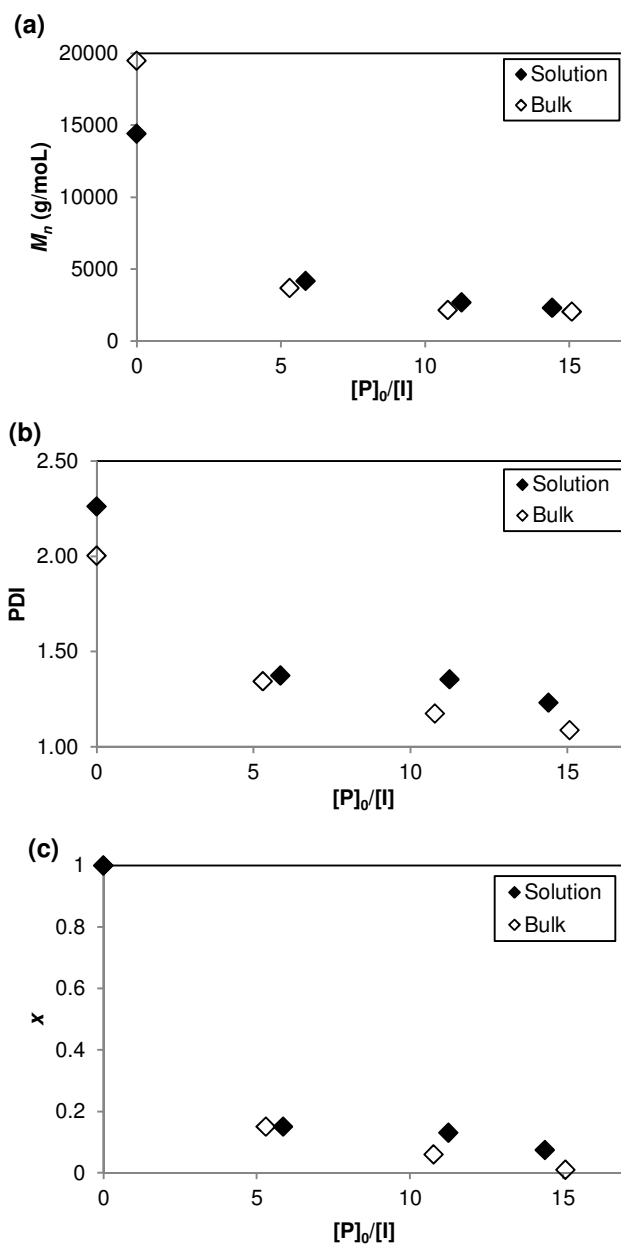


Figure 3.3. Comparison of (a) number average molecular weight (M_n), (b) polydispersity (PDI), and (c) conversion (x) of poly(1,5-cyclooctadiene) in solution ROMP (filled symbols) and bulk ROMP (empty symbols) with Grubbs' "first generation" catalyst in the presence of triphenylphosphine.

3.3.3. Living Behaviour of Bulk Polymerization in the Presence of Phosphine

Living behaviour in solution ROMP using GI catalyst have been demonstrated and reported in literature [9], [10], [12], [14], [16–18]. To demonstrate that bulk ROMP of 1,5-COD with GI catalyst in the presence of triphenylphosphine exhibits living feature, the time evolution of molecular weight distribution and conversion was studied. Bulk polymerizations with $[M]_0$ of 8.2 M, $[M]_0/[I]$ of 150, and $[P]_0/[I]$ of 10 were carried out at room temperature. Aliquots were terminated at various times over the course of 200 hours. No noticeable increase in viscosity was observed.

The time evolution of polymer molecular weight distribution is shown in **Figure 3.4**. The evolution of number-average molecular weight and polydispersity with respect to conversion and the first-order rate plot, shown in **Figure 3.5**, were also studied. As expected, the number-average molecular weight increased with reaction time. Polydispersity also increased with reaction time and remained below 2 even at high reaction times of 200 hours. It should be noted that at high reaction times of 200 hours, low conversion of less than 50% was obtained. High conversions were not achievable with high reaction times due to the attenuation of the rate of propagation as a result of the added triphenylphosphine. The general shape of the molecular weight distribution remained similar without significant broadening with increasing reaction time. This observation is in accordance to living polymerization features. Further, experimental data

demonstrated a near linear increase in number-average molecular weight with conversion and in the first-order rate plot, which is characteristic of a living system [19].

Slight broadening in the high molecular weight end of the distributions at high reaction times was observed. The increase in high molecular weight chains is likely due to intermolecular chain transfer reactions which occurred by the attack of active catalyst sites on the double bonds of polymer chains instead of monomers [8], [9]. The low molecular weight end of the distribution also showed slight broadening, which may be attributed to catalyst deactivation via thermalytic pathways and reactions with oxygen [20–22]. The random process of intermolecular chain transfer affects polymer chain length uniformity and the polydispersity is expected to increase to 2, as demonstrated by experimental data. Intermolecular chain transfer reactions do not create additional polymer chains nor change the number of chains with active catalyst centers. However, catalyst deactivation results in a decreasing number of chains with active catalyst centers as reaction time increases. The presence of catalyst deactivation in bulk ROMP act similarly to unimolecular chain termination in controlled living free radical polymerization and should result in a downward curvature in the first-order rate plot [19]. The near linear increase in the first-order rate plot is attributed to the slow rate of catalyst deactivation.

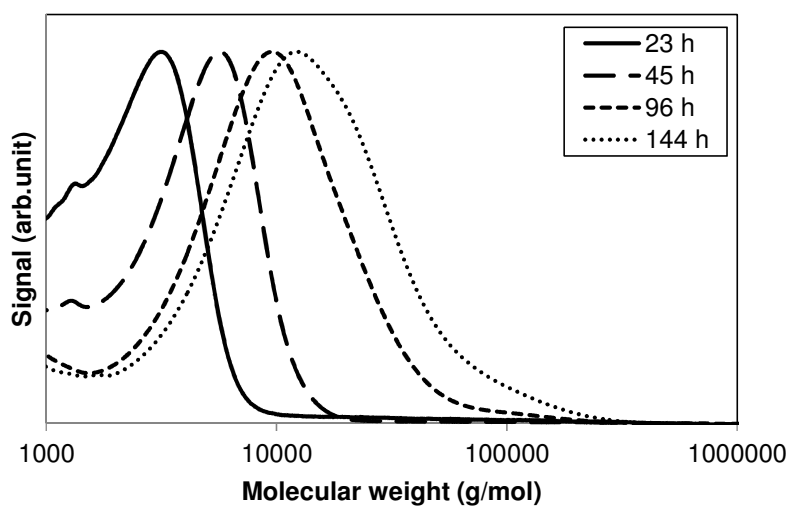


Figure 3.4. Time evolution of molecular weight distributions for room temperature bulk ROMP of 1,5-cyclooctadiene with Grubbs’ “first generation” catalyst in the presence of triphenylphosphine with $[M]_0$ of 8.2 M, $[M]_0/[I]$ of 150, and $[P]_0/[I]$ of 10.

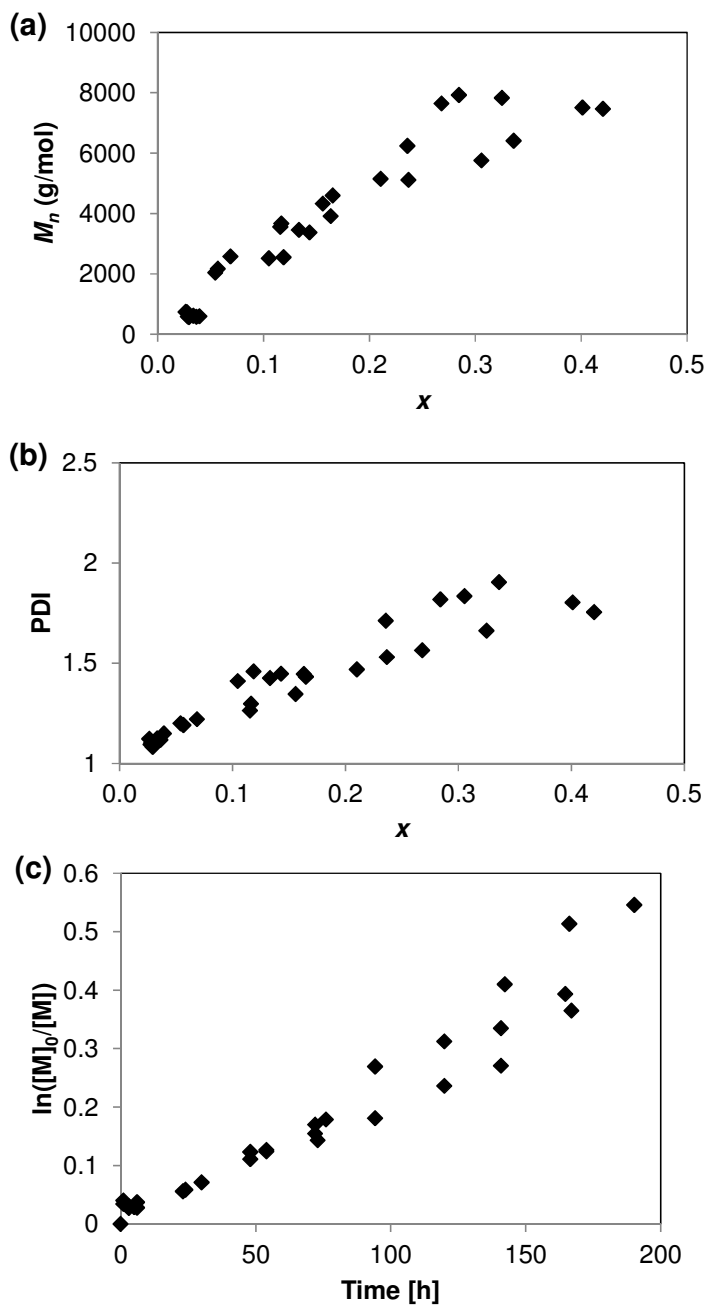


Figure 3.5. (a) Number-average molecular weight (M_n) versus conversion (x) plot, (b) polydispersity (PDI) versus conversion (x) plot, and (c) first-order rate plot for room temperature bulk ROMP of 1,5-cyclooctadiene with Grubbs' "first generation" catalyst in the presence of triphenylphosphine with $[M]_0$ of 8.2 M, $[M]_0/[I]$ of 150, and $[P]_0/[I]$ of 10. Conversion was determined by GPC.

3.4. Conclusions

The synthesis of narrowly distributed low molecular weight polymers via living ROMP of 1,5-COD via a ruthenium-based GI catalyst in the absence and in the presence of triphenylphosphine was studied. Living ROMP is usually carried out as solution polymerization processes with poor reactor volume efficiencies. As such, the possibility of bulk living ROMP was investigated.

At short reaction times, in the absence and in the presence of triphenylphosphine, bulk ROMP produced polymers with comparable or enhanced molecular weight distribution control and similar conversions as compared to solution ROMP. The monomer concentration in bulk can be maintained above the equilibrium monomer concentration more readily than in solution. Hence, molecular weight distribution can be better controlled in bulk polymerization.

In the presence of triphenylphosphine, the increase in phosphine loading resulted in a decrease in molecular weight, polydispersity, and conversion in bulk and solution polymerizations. This observation was in accordance to the increase in rate of initiation and the decrease in the rate of propagation that result from the use of excess phosphines. However, low conversions were obtained with phosphine due to the lowered rate of propagation.

Further, kinetics data demonstrated that bulk ROMP proceeded in a living manner. Deviations from ideal living polymerization behaviour were attributed to the presence intermolecular chain transfer reactions and catalyst deactivation.

The possibility and success of living ROMP as a bulk system has been demonstrated. The realization of bulk ROMP yields ROMP to be an efficient and viable polymerization pathway for the production of polymer with controlled molecular weight and structures.

3.5. References

- [1] M. A. Hillmyer, S. T. Nguyen, and R. H. Grubbs, “Utility of a Ruthenium Metathesis Catalyst for the Preparation of End-Functionalized Polybutadiene,” *Macromolecules*, vol. 30, pp. 718–721, 1997.
- [2] O. J. Kwon, H. T. Vo, S. B. Lee, T. K. Kim, H. S. Kim, and H. Lee, “Ring-Opening Metathesis Polymerization and Hydrogenation of Ethyl-Substituted Tetracyclododecene,” *Bulletin of the Korean Chemical Society*, vol. 32, pp. 2737–2742, 2011.
- [3] M. P. McGrath, E. D. Sall, and S. J. Tremont, “Functionalization of Polymers by Metal-Mediated Processes,” *Chemical Reviews*, vol. 95, pp. 381–398, 1995.
- [4] S. Sutthasupa, M. Shiotsuki, and F. Sanda, “Recent Advances in Ring-Opening Metathesis Polymerization, and Application to Synthesis of Functional Materials,” *Polymer Journal*, vol. 42, pp. 905–915, 2010.
- [5] K. Matyjaszewski, S. Gaynor, D. Greszta, D. Mardare, and T. Shigemoto, “‘Living’ and Controlled Radical Polymerization,” *Journal of Physical Organic Chemistry*, vol. 8, pp. 306–315, 1995.
- [6] C. W. Bielawski and R. H. Grubbs, “Increasing the Initiation Efficiency of Ruthenium-Based Ring-Opening Metathesis Initiators: Effect of Excess Phosphine,” *Macromolecules*, vol. 34, pp. 8838–8840, 2001.
- [7] A. Hejl, O. A. Scherman, and R. H. Grubbs, “Ring-Opening Metathesis Polymerization of Functionalized Low-Strain Monomers with Ruthenium-Based Catalysts,” *Macromolecules*, vol. 38, pp. 7214–7218, 2005.
- [8] S. B. Myers and R. A. Register, “Synthesis of Narrow-Distribution Polycyclopentene Using a Ruthenium Ring-Opening Metathesis Initiator,” *Polymer*, vol. 49, pp. 877–882, 2008.
- [9] C. W. Bielawski and R. H. Grubbs, “Living Ring-Opening Metathesis Polymerization,” *Progress in Polymer Science*, vol. 32, pp. 1–29, 2007.
- [10] G. C. Bazan et al., “Living Ring-Opening Metathesis Polymerization of 2,3-Difunctionalized Norbornenes by $\text{Mo}(\text{CH-t-Bu})(\text{N-2,6-C}_6\text{H}_3\text{-i-Pr}_2)(\text{O-t-Bu})_2$,” *Journal of the American Chemical Society*, vol. 112, pp. 8378–8387, 1990.

- [11] G. C. Bazan, S. R., H.-N. Cho, and V. C. Gibson, "Polymerization of Functionalized Norbornenes Employing $\text{Mo}(\text{CH-t-Bu})(\text{NAr})(\text{O-t-Bu})_2$ as the Initiator," *Macromolecules*, vol. 24, pp. 4495–4502, 1991.
- [12] T.-L. Choi and R. H. Grubbs, "Controlled Living Ring-Opening-Metathesis Polymerization by a Fast-Initiating Ruthenium Catalyst," *Angewandte Chemie International Edition*, vol. 42, pp. 1743 – 1746, 2003.
- [13] L.-B. W. Lee and R. A. Register, "Hydrogenated Ring-Opened Polynorbornene : A Highly Crystalline Atactic Polymer," *Macromolecules*, vol. 38, pp. 1216–1222, 2005.
- [14] B. R. Maughon and R. H. Grubbs, "Ruthenium Alkylidene Initiated Living Ring-Opening Metathesis Polymerization (ROMP) of 3-Substituted Cyclobutenes," *Macromolecules*, vol. 30, pp. 3459–3469, 1997.
- [15] J. S. Murdzek and R. R. Schrock, "Low Polydispersity Homopolymers and Block Copolymers by Ring Opening of 5,6-Dicarbomethoxynorbornene," *Macromolecules*, vol. 20, pp. 2640–2642, 1987.
- [16] R. Singh, C. Czekelius, and R. R. Schrock, "Living Ring-Opening Metathesis Polymerization of Cyclopropenes," *Macromolecules*, vol. 39, pp. 1316–1317, 2006.
- [17] R. Walker, R. M. Conrad, and R. H. Grubbs, "The Living ROMP of trans-Cyclooctene," *Macromolecules*, vol. 42, pp. 599–605, 2009.
- [18] G. J. Domski, J. M. Rose, G. W. Coates, A. D. Bolig, and M. Brookhart, "Living Alkene Polymerization: New Methods for the Precision Synthesis of Polyolefins," *Progress in Polymer Science*, vol. 32, pp. 30–92, 2007.
- [19] K. Matyjaszewski, "Introduction to Living Polymerization. Living and/or Controlled Polymerization," *Journal of Physical Organic Chemistry*, vol. 8, pp. 197–207, 1995.
- [20] S. H. Hong, A. G. Wenzel, T. T. Salguero, M. W. Day, and R. H. Grubbs, "Decomposition of Ruthenium Olefin Metathesis Catalysts," *Journal of the American Chemical Society*, vol. 129, pp. 7961–7968, 2007.
- [21] M. Ulman and R. H. Grubbs, "Ruthenium Carbene-Based Olefin Metathesis Initiators: Catalyst Decomposition and Longevity," *The Journal of Organic Chemistry*, vol. 64, pp. 7202–7207, 1999.

- [22] H. J. V. D. Westhuizen, A. Roodt, and R. Meijboom, “Kinetics of Thermal Decomposition and of the Reaction with Oxygen , Ethene and 1-Octene of First Generation Grubbs’ Catalyst Precursor,” *Polyhedron*, vol. 29, pp. 2776–2779, 2010.

4. Mathematical Modelling of Living Ring Opening Metathesis Polymerization

This chapter is based on the manuscript authored by Lai Chi So, Santiago Faucher, and Shiping Zhu entitled “Bulk Synthesis and Modeling of Living ROMP of 1,5-Cyclooctadiene for Narrowly Distributed Low Molecular Weight Linear Polymers” prepared for submission for publication. Lai Chi So developed the mathematical model with guidance from Dr. Zhu. Lai Chi So drafted the manuscript and Dr. Faucher and Dr. Zhu aided in manuscript revision.

4.1. Introduction

Research and development in living ring opening metathesis polymerization (ROMP) has been heavily focused on experimental studies with limited investigations into the modeling of living ROMP. Models of polymerization systems are essential in the development and the commercialization of polymerization systems. Not only can models yield new insights into polymerization mechanisms and be applied in experiment designs during the preliminary research phase, they can also be employed as predictive models and for process optimization once polymerization systems reach commercial implementation.

Trzaska et al. and Myers and Register have reported a simple kinetic model for the ROMP of cyclopentene (CP) using a ruthenium-based catalyst enhanced by the addition of tricyclohexylphosphine (PCy₃) as a polymerization regulator [1], [2]. The model assumed a first-order rate of monomer consumption with respect to monomer concentration and catalyst concentration. Hence, this highly simplistic model does not consider non-idealities, including but not limited to chain transfer reactions and catalyst decomposition, which are present in the real system and can significantly impact the molecular weight distribution of the final product. Furthermore, only number-average molecular weight (M_n) and conversion (x) can be obtained from this simple model.

To address the limited study into the modeling of ROMP, a model to describe the kinetics of phosphine-enhanced ruthenium-based living ROMP was developed using the method of moments. The model takes into consideration for non-idealities, including intermolecular chain transfer reactions and catalyst decomposition. The predictive model was validated with experimental data obtained for the bulk ROMP of 1,5-cyclooctadiene (1,5-COD) using Grubbs' "first generation" catalyst (GI catalyst) and triphenylphosphine (PPh₃) and published literature data obtained for the solution ROMP of CP using GI catalyst and PCy₃. The developed model can provide an enhanced understanding of the ROMP mechanism and guidance for new experiment designs.

4.2. Model Development

4.2.1. Reaction Scheme

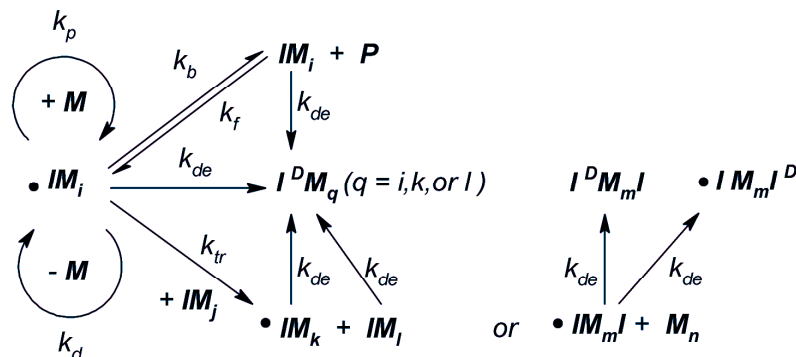
The general reaction mechanism for living ROMP with and without the use of excess phosphine was discussed in **Chapter 2.1.1**. In addition to the general reactions of initiation, propagation and depropagation, and catalyst activation and deactivation via phosphine dissociation or exchange, non-idealities such as chain transfer reactions and catalyst deactivation can occur. Disregarding the presence of impurities, the two dominant chain transfer reactions in the living ROMP system are intermolecular and intramolecular chain transfer reactions [3]. In an intermolecular chain transfer reaction, any carbon-carbon double bonds (C=C) on the backbone of a polymer chain can react with the metal center of an active catalyst of another polymer chain, resulting in two polymer chains with different chain lengths. In an intramolecular chain transfer reaction, the metal center of an active catalyst on a polymer chain can backbite with any C=C on its own polymer chain, forming a cyclic polymer species and a linear polymer chain. Catalyst deactivation can occur via thermalytic pathways and/or reactions with impurities [4–6].

The general reaction scheme for living ROMP in the presence of excess phosphine is given in **Scheme 4.1**, based on which the model was developed. A detailed reaction mechanism illustrating initiation, propagation and depropagation, catalyst activation and

deactivation, catalyst decomposition, and intermolecular chain transfer reactions between polymeric species is provided in **Appendix A.4.1**.

In this system, the following conditions and assumptions were applied:

- Reactions are carried out as a batch process.
- Reactions are carried out at constant temperature.
- Active catalyst centers deactivate into the dormant state quickly. Therefore, chain species bearing two active centers at any moment and the reactions between two active chain species are negligible.
- Intermolecular chain transfer reactions are considered. In practical systems where polymer concentration is high, it is more likely for polymer chains to experience chain transfer reactions with each other (i.e. intermolecular) than with itself (i.e. intramolecular) [3]. For simplicity, k_{tr} will be used hereafter to represent the rate of intermolecular chain transfer.
- Catalyst decomposition is considered due to catalyst sensitivity to air, moisture, and temperature [4–6].
- Controlled termination occurs only via the addition of a known reagent.
- Kinetics constants are not affected by polymer chain length.



$\bullet IM_i$	Chain species with i monomers and 1 active catalyst center
$\bullet IM_i I$	Chain species with i monomers, 1 active catalyst center, and 1 dormant catalyst center
$\bullet IM_i I^D$	Chain species with i monomers, 1 active catalyst center, and 1 decomposed catalyst center
IM_i	Chain species with i monomers and 1 dormant catalyst center
$IM_i I^D$	Chain species with i monomers, 1 dormant catalyst center, and 1 decomposed catalyst center
$I^D M_i$	Chain species with i monomers and 1 decomposed catalyst center
M_i	Chain species with i monomers and no catalyst centers
M	Monomer species
P	Phosphine species
k_b	Rate constant for catalyst deactivation
k_d	Rate constant for depropagation
k_{de}	Rate constant for catalyst decomposition
k_f	Rate constant for catalyst activation
k_p	Rate constant for propagation
$k_{tr, inter}$	Rate constant for intermolecular chain transfer

Scheme 4.1. General living ROMP reaction scheme used in model development [3], [7].

4.2.2. Mass Balance Equations

Model derivation was based on the first principle of mass balances. Considering a batch process in which initiation, propagation and depropagation, catalyst activation and deactivation, catalyst decomposition, and intermolecular chain transfer reactions between polymeric species can occur, the formation of nine types of chain species is possible. The nine types of chain species are listed in **Table 4.1** and their mass balance equations are provided in **Appendix A.4.2**.

Table 4.1. Chain species resulting from the living ROMP mechanism used in model development.

Species	Description
$\bullet\text{IM}_i$	Chain species with i monomers and 1 active catalyst center
$\bullet\text{IM}_i\text{I}$	Chain species with i monomers, 1 active catalyst center, and 1 dormant catalyst center
$\bullet\text{IM}_i\text{I}^{\text{D}}$	Chain species with i monomers, 1 active catalyst center, and 1 decomposed catalyst center
IM_i	Chain species with i monomers and 1 dormant catalyst center
IM_iI	Chain species with i monomers and 2 dormant catalyst centers
$\text{IM}_i\text{I}^{\text{D}}$	Chain species with i monomers, 1 dormant catalyst center, and 1 decomposed catalyst center
$\text{I}^{\text{D}}\text{M}_i$	Chain species with i monomers and 1 decomposed catalyst center
$\text{I}^{\text{D}}\text{M}_i\text{I}^{\text{D}}$	Chain species with i monomers and 2 decomposed catalyst centers
M_i	Chain species with i monomers and no catalyst centers

4.2.3. Method of Moments

The method of moments is very powerful tool in modeling and reduces the large number of mass balance equations (i.e. that for chain species with chain length i from 1 to theoretically infinite) to a small number of moment equations. It should be noted that as a trade-off, the method of moments allows for the determination of various average molecular weights and polydispersities but not the full molecular weight distribution. **Eq. (A.4.2.1.) to (A.4.2.9)** in **Appendix A.4.2** are the mass balance equations for each type of chain species defined in **Table 4.1**. In theory, this set of ordinary differential equations (ODEs) is sufficient to give the molecular weight distribution of each chain type. However, solving such a large number of ODEs is practically impossible. As such, one must resort to the use of the method of moments. The moments of the zeroth, first, and second order for the different chain species can be defined as follow:

For the moment of the zeroth order:

$$Q_0 = \sum_{i=1}^{\infty} i^0 [M_i] \quad (4.1)$$

For the moment of the first order:

$$Q_1 = \sum_{i=1}^{\infty} i^1 [M_i] \quad (4.2)$$

For the moment of the second order:

$$Q_2 = \sum_{i=1}^{\infty} i^2 [M_i] \quad (4.3)$$

where Q_j is the moment of a given chain species of the j^{th} order and $[M_i]$ is the concentration of a given chain species with chain length i .

The zeroth order moment is the concentration of the given chain species, the first order moment is related to the concentration of monomer units on the chains, and the second order moment reflects the average of the concentration of monomers with larger chain being more heavily weighted [8]. From the definitions of the moments, it is possible to define the number-average molecular weight, weight-average molecular weight (M_w), and polydispersity (PDI).

For number-average molecular weight:

$$M_n = MW \left(\frac{Q_1}{Q_0} \right) \quad (4.4)$$

For weight-average molecular weight:

$$M_w = MW \left(\frac{Q_2}{Q_1} \right) \quad (4.5)$$

For polydispersity:

$$PDI = \frac{\bar{M}_w}{\bar{M}_n} \quad (4.6)$$

where MW is the molecular weight of the monomer.

Using **Eq. (4.1)** to **(4.3)**, the moment equations of the j^{th} order for each chain species can be expressed from the mass balance equations of **Eq. (A.4.2.1)** to **(A.4.2.9)** in **Appendix A.4.2**. The mathematical approximations used to obtain the moment equations of the j^{th} order are provided in **Appendix A.4.3** and **Appendix A.4.4**. The moment equations of the j^{th} order for each chain species are given in **Table 4.2**. Please refer to **Appendix A.4.4** for the definition of the shorthand notation f .

Table 4.2. j^{th} order moment equations for chain species in living ROMP.

Species	j^{th} order moment equation
$\bullet\text{IM}_i$	$\begin{aligned} \frac{d[\bullet IQ_j]}{dt} = & k_p \sum_{k=0}^{j-1} \binom{j}{k} [\bullet IQ_k][M] - k_d \sum_{k=0}^{j-1} \binom{j}{k} [\bullet IQ_k] + k_f [IQ_j] - \\ & k_b [\bullet IQ_j] ([P]_0 - [IQ_0] - [\bullet IQ_0 I] - 2[IQ_0 I] - [IQ_0 I^D]) - \\ & k_{de} [\bullet IQ_j] - k_{tr} [\bullet IQ_j] N([IQ_1] + \frac{1}{2}[IQ_1 I] + \frac{1}{2}[Q_1] + [I^D Q_1] + \\ & [IQ_1 I^D] + \frac{1}{2}[I^D Q_1 I^D]) + k_{tr} \left(\frac{1}{j+1}\right) \left(\frac{1}{2}\right) ([\bullet IQ_0] + [\bullet IQ_0 I] + \\ & [\bullet IQ_0 I^D]) ([IQ_{j+1}] + [Q_{j+1}] + [I^D Q_{j+1}]) \end{aligned} \quad (4.7)$
$\bullet\text{IM}_i\text{I}$	$\begin{aligned} \frac{d[\bullet IQ_j I]}{dt} = & k_p \sum_{k=0}^{j-1} \binom{j}{k} [\bullet IQ_k I][M] - k_d \sum_{k=0}^{j-1} \binom{j}{k} [\bullet IQ_k I] + 2k_f [IQ_j I] - \\ & k_b [\bullet IQ_j I] ([P]_0 - [IQ_0] - [\bullet IQ_0 I] - 2[IQ_0 I] - [IQ_0 I^D]) - \\ & 2k_{de} [\bullet IQ_j I] - k_{tr} [\bullet IQ_j I] ([IQ_1] + \frac{1}{2}[IQ_1 I] + \frac{1}{2}[Q_1] + [I^D Q_1] + \\ & [IQ_1 I^D] + \frac{1}{2}[I^D Q_1 I^D]) + k_{tr} \left(\frac{1}{j+1}\right) \left(\frac{1}{2}\right) ([\bullet IQ_0] + [\bullet IQ_0 I] + \\ & [\bullet IQ_0 I^D]) ([IQ_{j+1}] + [IQ_{j+1} I] + [IQ_{j+1} I^D]) \end{aligned} \quad (4.8)$
$\bullet\text{IM}_i\text{I}^D$	$\begin{aligned} \frac{d[\bullet IQ_j I^D]}{dt} = & k_p \sum_{k=0}^{j-1} \binom{j}{k} [\bullet IQ_k I^D][M] - k_d \sum_{k=0}^{j-1} \binom{j}{k} [\bullet IQ_k I^D] + k_f [IQ_j I^D] - \\ & k_b [\bullet IQ_j I^D] ([P]_0 - [IQ_0] - [\bullet IQ_0 I] - 2[IQ_0 I] - [IQ_0 I^D]) + \\ & k_{de} [\bullet IQ_j I] - k_{de} [\bullet IQ_j I^D] - k_{tr} [\bullet IQ_j I^D] ([IQ_1] + \frac{1}{2}[IQ_1 I] + \frac{1}{2}[Q_1] + \\ & [I^D Q_1] + [IQ_1 I^D] + \frac{1}{2}[I^D Q_1 I^D]) + k_{tr} \left(\frac{1}{j+1}\right) \left(\frac{1}{2}\right) ([\bullet IQ_0] + [\bullet IQ_0 I] + \\ & [\bullet IQ_0 I^D]) ([I^D Q_{j+1}] + [IQ_{j+1} I^D] + [I^D Q_{j+1} I^D]) \end{aligned} \quad (4.9)$

Table 4.2. Continued

Species	j^{th} order moment equation
IM_i	$\begin{aligned} \frac{d[IQ_j]}{dt} = & -k_f[IQ_j] + k_b[\bullet IQ_j]([P]_0 - [IQ_0] - [\bullet IQ_0I] - 2[IQ_0I] - [IQ_0I^D]) - \\ & k_{de}[IQ_j] - k_{tr}[IQ_{j+1}]([\bullet IQ_0] + [\bullet IQ_0I] + [\bullet IQ_0I^D]) + \\ & k_{tr}\left(\frac{1}{2}\right)\{f(j, [\bullet IM], [IM]) + f(j, [\bullet IM], [IMI]) + \\ & f(j, [\bullet IM], [IMI^D]) + f(j, [\bullet IMI], [IM]) + f(j, [\bullet IMI], [M]) + \\ & f(j, [\bullet IMI], [I^D M])\} \end{aligned} \quad (4.10)$
IM_iI	$\begin{aligned} \frac{d[IQ_jI]}{dt} = & -2k_f[IQ_jI] + k_b[\bullet IQ_jI]([P]_0 - [IQ_0] - [\bullet IQ_0I] - 2[IQ_0I] - \\ & [IQ_0I^D]) - 2k_{de}[IQ_jI] - k_{tr}\left(\frac{1}{2}\right)[IQ_{j+1}I]([\bullet IQ_0] + [\bullet IQ_0I] + \\ & [\bullet IQ_0I^D]) + k_{tr}\left(\frac{1}{2}\right)\{f(j, [\bullet IMI], [IM]) + f(j, [\bullet IMI], [IMI]) + \\ & f(j, [\bullet IMI], [IMI^D])\} \end{aligned} \quad (4.11)$
IM_iI^D	$\begin{aligned} \frac{d[IQ_jI^D]}{dt} = & -k_f[IQ_jI^D] + k_b[\bullet IQ_jI^D]([P]_0 - [IQ_0] - [\bullet IQ_0I] - 2[IQ_0I] - \\ & [IQ_0I^D]) + k_{de}[\bullet IQ_jI] + 2k_{de}[IQ_jI] - k_{de}[IQ_jI^D] - \\ & k_{tr}[IQ_{j+1}I^D]([\bullet IQ_0] + [\bullet IQ_0I] + [\bullet IQ_0I^D]) + \\ & k_{tr}\left(\frac{1}{2}\right)\{f(j, [\bullet IMI], [I^D M]) + f(j, [\bullet IMI], [IMI^D]) + \\ & f(j, [\bullet IMI], [I^D MI^D]) + f(j, [\bullet IMI^D], [IM]) + f(j, [\bullet IMI^D], [IMI]) + \\ & f(j, [\bullet IMI^D], [IMI^D])\} \end{aligned} \quad (4.12)$
$I^D M_i$	$\begin{aligned} \frac{d[I^D Q_j]}{dt} = & k_{de}[IQ_j] + k_{de}[\bullet IQ_j] - k_{tr}[I^D Q_{j+1}]([\bullet IQ_0] + [\bullet IQ_0I] + [\bullet IQ_0I^D]) + \\ & k_{tr}\left(\frac{1}{2}\right)\{f(j, [\bullet IM], [I^D M]) + f(j, [\bullet IM], [IMI^D]) + \\ & f(j, [\bullet IM], [I^D MI^D]) + f(j, [\bullet IMI^D], [IM]) + f(j, [\bullet IMI^D], [M]) + \\ & f(j, [\bullet IMI^D], [I^D M])\} \end{aligned} \quad (4.13)$
$I^D M_iI^D$	$\begin{aligned} \frac{d[I^D Q_jI^D]}{dt} = & k_{de}[\bullet IQ_jI^D] + k_{de}[IQ_jI^D] - k_{tr}\left(\frac{1}{2}\right)[I^D Q_{j+1}I^D]([\bullet IQ_0] + [\bullet IQ_0I] + \\ & [\bullet IQ_0I^D]) + k_{tr}\left(\frac{1}{2}\right)\{f(j, [\bullet IMI^D], [I^D M]) + f(j, [\bullet IMI^D], [IMI^D]) + \\ & f(j, [\bullet IMI^D], [I^D MI^D])\} \end{aligned} \quad (4.14)$
M_i	$\begin{aligned} \frac{d[Q_j]}{dt} = & -k_{tr}\left(\frac{1}{2}\right)[Q_{j+1}]([\bullet IQ_0] + [\bullet IQ_0I] + [\bullet IQ_0I^D]) + \\ & k_{tr}\left(\frac{1}{2}\right)\{f(j, [\bullet IM], [IM]) + f(j, [\bullet IM], [M]) + f(j, [\bullet IM], [I^D M])\} \end{aligned} \quad (4.15)$

The zeroth, first, and second order moment equations can be obtained by setting $j = 0, 1,$ and $2,$ respectively, in **Eq. (4.7) to Eq. (4.15)**. Note that there exists terms for moments of the third order in the second order moment equations. For closure purposes, the expression of the third order moment of a given chain species, $Q_3,$ as a function of the first and second order moment of the given chain species, Q_1 and $Q_2,$ respectively, was adopted [9]:

$$Q_3 = \frac{3}{2} \left(\frac{Q_2^2}{Q_1} \right) \quad (4.16)$$

In addition to the system of 27 differential equations formed by the zeroth, first, and second moment equations for each chain species, three additional equations are necessary to create the basis of the model.

Firstly, the rate of monomer consumption is required and can be expressed as:

$$\begin{aligned} \frac{d[M]}{dt} = & -k_p([\bullet IQ_0] + [I Q_0 I] + [I Q_0 I^D])[M] \\ & + k_d([\bullet IQ_0] + [I Q_0 I] + [I Q_0 I^D]) \end{aligned} \quad (4.17)$$

In addition, the following conservation equations for catalyst concentration, $[I]_0,$ and added phosphine concentration, $[P]_0,$ apply:

$$\begin{aligned} [I]_0 = & [\bullet IQ_0] + [I Q_0] + 2[\bullet IQ_0 I] + 2[I Q_0 I] + [I^D Q_0] \\ & + 2[I Q_0 I^D] + 2[\bullet IQ_0 I^D] + 2[I^D Q_0 I^D] \end{aligned} \quad (4.18)$$

$$[P]_0 = [P] + [IQ_0] + [\bullet IQ_0I] + 2[IQ_0I] + [IQ_0I^D] \quad (4.19)$$

The system of 28 differential equation resulting from the zeroth, first, and second moment equations of **Eq. (4.7)** to **(4.15)** along with **Eq. (4.17)** were solved numerically using the MATLAB ode45 solver, which is based on an explicit Runge-Kutta (4,5) formula. The following initial conditions were used:

$$\begin{array}{lll}
 [\bullet IQ_0] = 10^{-8} & [IQ_0] = [I]_0 & [I^D Q_0] = 10^{-8} \\
 [\bullet IQ_1] = 10^{-8} & [IQ_1] = 10^{-8} & [I^D Q_1] = 10^{-8} \\
 [\bullet IQ_2] = 10^{-8} & [IQ_2] = 10^{-8} & [I^D Q_2] = 10^{-8} \\
 [\bullet IQ_0I] = 10^{-8} & [IQ_0I] = 10^{-8} & [IQ_0I^D] = 10^{-8} \\
 [\bullet IQ_1I] = 10^{-8} & [IQ_1I] = 10^{-8} & [IQ_1I^D] = 10^{-8} \\
 [\bullet IQ_2I] = 10^{-8} & [IQ_2I] = 10^{-8} & [IQ_2I^D] = 10^{-8} \\
 [\bullet IQ_0I^D] = 10^{-8} & [Q_0] = 10^{-8} & [I^D Q_0I^D] = 10^{-8} \\
 [\bullet IQ_1I^D] = 10^{-8} & [Q_1] = 10^{-8} & [I^D Q_1I^D] = 10^{-8} \\
 [\bullet IQ_2I^D] = 10^{-8} & [Q_2] = 10^{-8} & [I^D Q_2I^D] = 10^{-8} \\
 & & x = 10^{-8}
 \end{array} \quad (4.20)$$

Values of 10^{-8} were used in lieu of zeroes to avoid division by zero.

To determine reaction kinetics and average molecular weight distribution, the solution for the system of differential equations was applied in the following expressions.

For conversion:

$$x = 1 - \frac{[M]}{[M]_0} \quad (4.21)$$

For number-average chain length:

$$r_n = \frac{[•IQ_1] + [•IQ_1I] + [•IQ_1I^D] + [IQ_1] + [IQ_1I] + [Q_1] + [I^DQ_1] + [IQ_1I^D] + [I^DQ_1I^D]}{[•IQ_0] + [•IQ_0I] + [•IQ_0I^D] + [IQ_0] + [IQ_0I] + [Q_0] + [I^DQ_0] + [IQ_0I^D] + [I^DQ_0I^D]} \quad (4.22)$$

For weight-average chain length:

$$r_w = \frac{[•IQ_2] + [•IQ_2I] + [•IQ_2I^D] + [IQ_2] + [IQ_2I] + [Q_2] + [I^DQ_2] + [IQ_2I^D] + [I^DQ_2I^D]}{[•IQ_1] + [•IQ_1I] + [•IQ_1I^D] + [IQ_1] + [IQ_1I] + [Q_1] + [I^DQ_1] + [IQ_1I^D] + [I^DQ_1I^D]} \quad (4.23)$$

For polydispersity:

$$PDI = \frac{r_w}{r_n} \quad (4.24)$$

4.3. Model Validation

To validate the model developed in **Chapter 4.2**, model predictions obtained from the model were compared to experimental data obtained for two contrasting living ROMP systems. Solution and bulk living ROMP processes with various reagents were modeled to demonstrate the applicability of the model in polymerization systems with different reagents, monomer concentrations, and degrees of intermolecular chain transfer reactions.

4.3.1. Case I: Bulk Polymerization of 1,5-Cyclooctadiene via Grubbs' "First Generation" Catalyst and Triphenylphosphine

The developed model was used to describe the synthesis of poly(1,5-cyclooctadiene) (p(1,5-COD)) using GI catalyst as catalyst, and PPh_3 as a polymerization regulator. The experimental data used is the same as that presented in **Chapter 3.3.3**. Reaction conditions used to obtain the experimental data and for simulation are summarized in **Table 4.3**.

To understand the effects of intermolecular chain transfer reactions and catalyst decomposition on the kinetics and development of molecular weight distribution, four model simulations were explored:

- (1) Presence of intermolecular chain transfer reactions and catalyst decomposition
- (2) Absence of intermolecular chain transfer reactions
- (3) Absence of catalyst decomposition
- (4) Absence of intermolecular chain transfer reactions and catalyst decomposition

Kinetic parameters used for model simulations are provided in **Table 4.4**.

Table 4.3. Reaction conditions used for reactions and in simulated model for bulk living ROMP of 1,5-cyclooctadiene.

Parameter	Value	Unit	Ref.
$[I]_0$	0.054	mol L ⁻¹	-
$[M]_0$	8.15	mol L ⁻¹	-
$[P]_0$	0.54	mol L ⁻¹	-
$[M]_{eq}$	0.25	mol L ⁻¹	[10]
T_R	23	°C	-

Table 4.4. Kinetic parameters used in simulated models for bulk living ROMP of 1,5-cyclooctadiene.

Simulation	1	2	3	4		
Chain Transfer	Yes	No	Yes	No		
Catalyst Decomposition	Yes	Yes	No	No		
Parameter	Value				Unit	Ref.
k_f			7.5		s ⁻¹	[11]
k_b			$100 \times k_f^a$		s ⁻¹	-
k_p			10^{-3}^b		L mol ⁻¹ s ⁻¹	[7]
k_d			$k_p \times [M]_{eq}$		s ⁻¹	[12], [13]
k_{tr}	$2 \times 10^{-4}^c$	10^{-8}	$2 \times 10^{-4}^c$	10^{-8}	L mol ⁻¹ s ⁻¹	-
k_{de}	10^{-6}	10^{-6}	10^{-8}	10^{-8}	s ⁻¹	[4], [6]

^a The catalyst was assumed to be dominantly in the dormant state and not in the active state. Hence, a value satisfying the following relationship was used: $k_b > k_f$.

^b 1,5-COD consists of two active C=C. Therefore, the value of used here is equivalent to $2 \times k_p$. Bielawski and Grubbs reported values of k_p ranging from 10^{-3} to 10^{-5} L mol⁻¹ s⁻¹ [7]. A value close to the upper limit value was used.

^c Chain transfer was assumed to be slower than propagation. Hence, a value satisfying the following relationship was used: $k_{tr} < k_p$.

Experimental and simulated molecular weight, polydispersity, conversion, and first-order rate plots are compared in **Figure 4.1**. The experimental data showed a near linear increase in molecular weight with conversion. The four model simulations yielded the same linear trend, which is expected of a living system and which coincided well with experimental data.

Significant differences in the four simulations were observed in the polydispersity versus conversion plots. In the ideal case where intermolecular chain transfer reactions and catalyst decomposition were considered to be negligible (i.e. Simulation 4), the model showed a decrease in polydispersity towards the ideal value of 1. However, this behaviour was not representative of that of the real system. When only catalyst decomposition was considered (i.e. Simulation 2), the model demonstrated an initial decrease in polydispersity followed by a slight gradual increase. Although a similar trend was observed in the real system, the model prediction greatly underestimated the polydispersity at high conversions. When only intermolecular chain transfer reactions were considered (i.e. Simulation 3), the model prediction yielded a better fit to experimental data, especially at high conversions. The best fit was obtained when intermolecular chain transfer reactions and catalyst decomposition were considered (i.e. Simulation 1).

As discussed in **Chapter 3.3.3**, the presence of intermolecular chain transfer reactions in real systems can lead to the formation of high molecular weight polymers. Further,

catalyst deactivation is present in real systems and decreases the number of chains with active catalyst centers. Hence, a broadening of polydispersity with reaction time was observed in the experimental data. It is clear that when intermolecular chain transfer reactions were considered to be negligible, the model prediction was unable to capture the broadening of polydispersity at higher conversions. Although the absence of catalyst decomposition in the simulations resulted in a similar underestimation of polydispersity, its effects on polydispersity were less severe. The model simulation that considered the non-idealities of intermolecular chain transfer reactions and catalyst decomposition demonstrated showed the same fast initial decrease in polydispersity followed by a gradual increase and gave the best fit to the experimental data.

Slight differences between the model simulations were also observed in the first-order rate plots. When catalyst deactivation was considered to be negligible (i.e. Simulations 3 and 4), the first-order rate plots showed a linear relationship. However, when catalyst deactivation was assumed to be present (i.e. Simulations 1 and 2), a downward curvature was observed. For an ideal living polymerization system, a linear relationship should be observed in the first-order rate plot [14]. As discussed in **Chapter 3.3.3**, the deviation from ideality was due to catalyst deactivation. Although these reactions occur at a slower rate than the rate of reaction with monomers, they decrease the number of chains with active catalyst centers as the reaction progresses and result in a downward curvature in the first-order rate plot [14]. Simulations 1 and 2 provided a more representative fit to the

experimental data, indicating that catalyst deactivation played an influential role in the rate of monomer consumption.

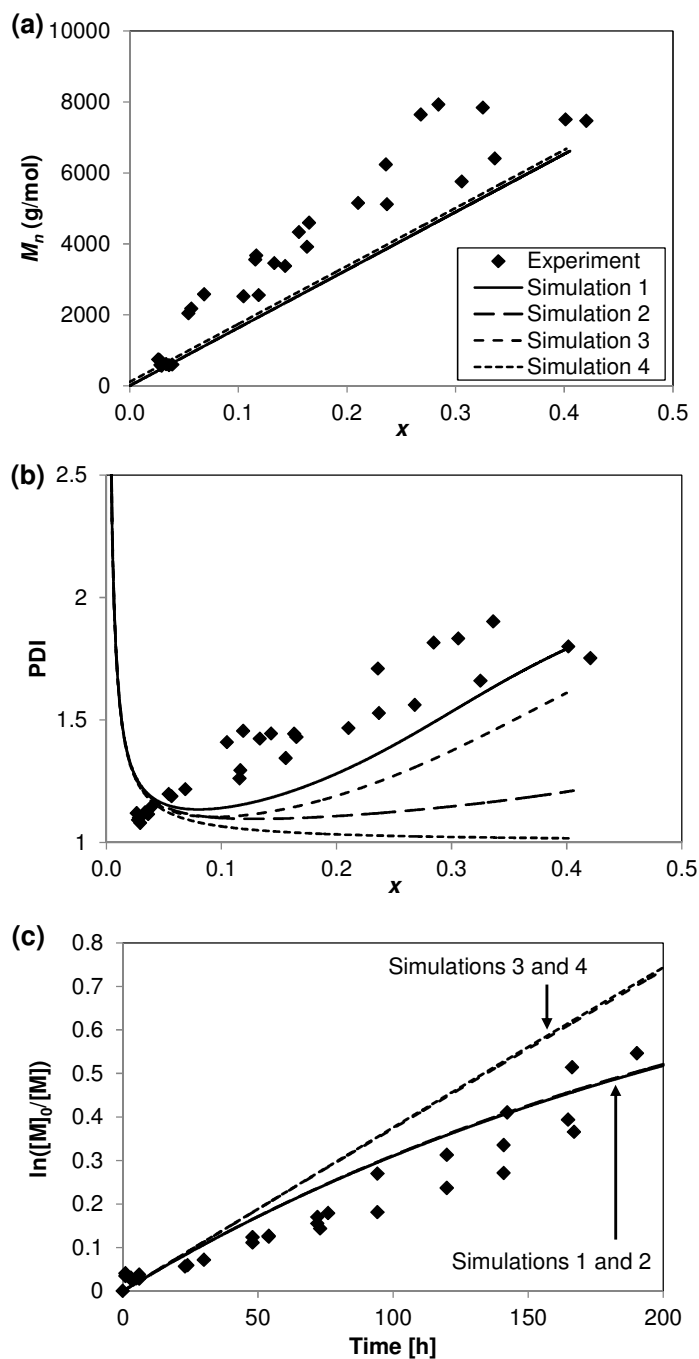


Figure 4.1. Comparison of experimentally determined (filled symbols) and model simulations (solid and dashed lines) of (a) number-average molecular weight (M_n) versus conversion (x) plot, (b) polydispersity (PDI) versus conversion (x) plot, and (c) first-order rate plot for bulk ROMP of 1,5-cyclooctadiene.

4.3.2. Case II: Solution Polymerization of Cyclopentene via Grubbs' "First Generation" Catalyst and Tricyclohexylphosphine

The model demonstrated excellent representation of the reaction kinetics and molecular weight distributions of a bulk living ROMP process in which the monomer concentration is high, the degree of intermolecular chain transfer reactions is high, and the rate of polymerization is fairly low. It is also of interest to investigate the ability of the model to describe a contrasting polymerization process, specifically a solution polymerization process in which different reagents are used, monomer concentration is low, the presence of intermolecular chain transfer is less significant, and the rate of polymerization is fast.

The model was used to describe the synthesis of polycyclopentene (p(CP)) via ROMP using GI catalyst as catalyst, PCy₃ as a polymerization regulator, and toluene as solvent. Simulation results were compared with experimental data reported by Myers and Register [1]. Reaction conditions used in experimental work and in simulation are provided in **Table 4.5**. Kinetic parameters used in simulation are also listed in **Table 4.5**.

Table 4.5. Reaction conditions used for reactions and in simulated model, and kinetic parameters used in simulated model for solution living ROMP of cyclopentene.

	Parameter	Value	Unit	Ref.
Reaction conditions	$[I]_0$	0.001	mol L ⁻¹	[1]
	$[M]_0$	3	mol L ⁻¹	[1]
	$[P]_0$	0.004	mol L ⁻¹	[1]
	$[M]_{eq}$	1.3	mol L ⁻¹	[1]
	T_R	23	°C	[1]
Kinetic parameters	k_f	0.13	s ⁻¹	[11]
	k_b	$100 \times k_f^a$	s ⁻¹	-
	k_p	$7 \times 10^{-2}{}^b$	L mol ⁻¹ s ⁻¹	[7]
	k_d	$k_p \times [M]_{eq}$	s ⁻¹	[12], [13]
	k_{tr}	$2 \times 10^{-3}{}^c$	L mol ⁻¹ s ⁻¹	-
	k_{de}	10^{-6}	s ⁻¹	[6], [15]

^a The catalyst was assumed to be dominantly in the dormant state and not in the active state. Hence, a value satisfying the following relationship was used: $k_b > k_f$.

^b Bielawski and Grubbs reported values of k_p ranging from 10^{-3} to 10^{-5} L mol⁻¹ s⁻¹ [7]. A value close to the upper limit value was used.

^c Chain transfer was assumed to be slower than propagation. Hence, a value satisfying the following relationship was used: $k_{tr} < k_p$.

Figure 4.2 and **Figure 4.3** give a comparison of experimentally determined and simulated molecular weight, polydispersity, and conversion. The simulated results were in excellent agreement with experimental results. The model and experimental data demonstrated increases in both molecular weight and apparent conversion, which was determined from the number-average molecular weight assuming that each catalyst results in the growth of one chain. This observation is in accordance to a living polymerization system. The simulated polydispersity and conversion also demonstrated good agreement with the experimental polydispersity and true conversion, which was determined from gel permeation chromatography (GPC). Polydispersity first decreased to a minimum and then gradually increased with time, while conversion increased with time. Simulated results

fitted experimental results well at low reaction time but under-predicted experimental results at high reaction time. This discrepancy may be attributed to the presence of chain transfer reactions.

Myers and Register reported that two types of chain transfer reactions were present in the system – intermolecular chain transfer between polymer chains and chain transfer of polymers to contaminants in the monomer supply. In the presence of intermolecular chain transfer reaction between polymer chains, an active catalyst on a polymer chain attacks a double bond in another polymer chain instead of a double bond in a monomer. The uniformity of polymer chain length is affected and the polydispersity is expected to increase to approximately 2 in this random process. Since the model considered intermolecular chain transfer reactions between polymer chains, it was able to capture the time evolution of polydispersity accurately. However, intermolecular chain transfer reactions between polymer chains do not create additional polymer chains (i.e. each catalyst results in the growth of one polymer chain). As such, the true conversion should not continue to increase considerably with time at high reaction times. The more significant increase in true conversion as compared to apparent conversion is the result of chain transfer of polymers to contaminants in the monomer supply. It has been reported that multiple polymer chains can be created by one catalyst via chain transfer to contaminants. The progressive increase in the number of polymer chains results in an increase in monomer consumption and conversion. Since the model did not consider

chain transfer to contaminants, the simulated conversion did not fully capture the time evolution of true conversion.

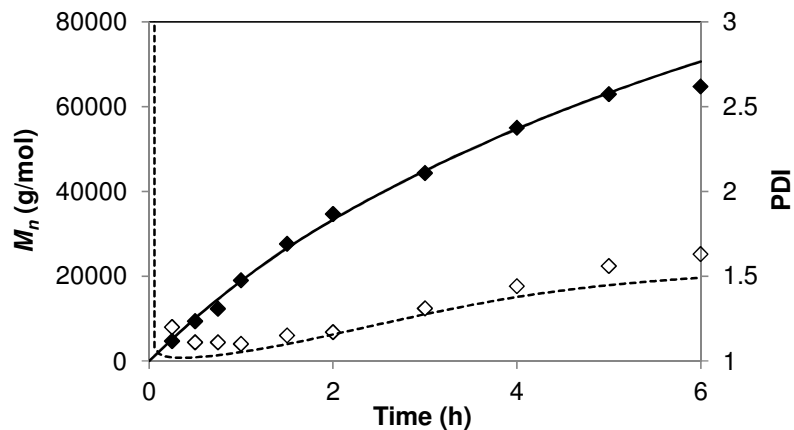


Figure 4.2. Comparison of time evolution of experimentally determined molecular weight (M_n) (filled symbols) and polydispersity (PDI) (empty symbols) with model predictions of M_n (solid line) and PDI (dashed line) for the polymerization of cyclopentene. Experimental data was reported by Myers and Register [1].

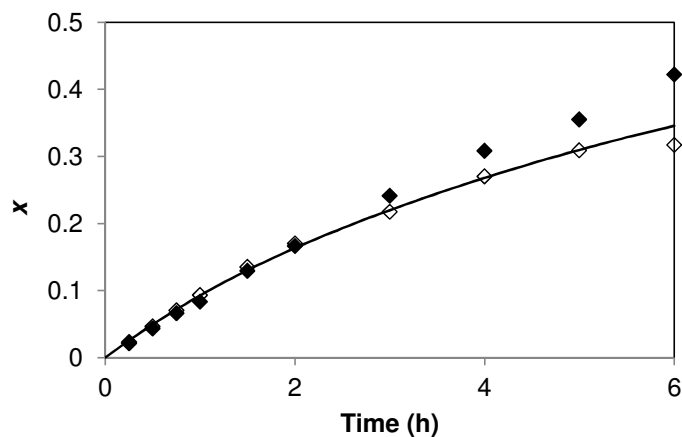


Figure 4.3. Comparison of time evolution of experimentally determined true conversion (filled symbols) and apparent conversion (empty symbols) with model predictions (solid line) for the polymerization of cyclopentene. True conversion was determined by GPC and apparent conversion was calculated from M_n assuming that each catalyst results in the growth of one chain. Experimental data was reported by Myers and Register [1].

As shown by the good fit of model simulations to the two contrasting sets of living ROMP experimental results, it is evident that the model is able to describe living ROMP systems with various reagents, monomer concentrations, degrees of chain transfer reactions, and rates of polymerization. Firstly, the model provided a good prediction of kinetic behaviour of two ROMP systems based on two different monomers. With the use of different monomers, the reaction kinetics is affected due to the difference in equilibrium monomer concentration. CP has a higher $[M]_{eq}$ than 1,5-COD and will be more impacted by the propagation-depropagation equilibrium. Also, maximum conversion is reached at higher monomer concentration for CP than for 1,5-COD.

Secondly, the simulations of solution and bulk processes demonstrated that the model is able to describe processes with various initial monomer concentration and degrees of intermolecular chain transfer reactions. In a bulk process where initial monomer concentration is high, the concentration of polymer chains throughout the reaction is also high. Therefore, intermolecular chain transfer reactions are more dominant in bulk processes than in solution processes. As demonstrated in the simulations above, the model provided excellent predictions of processes in which intermolecular chain transfer is of high significance (i.e. bulk polymerization of 1,5-COD with k_p/k_{tr} ratio of 5) and of low significance (i.e. solution polymerization of CP with k_p/k_{tr} ratio of 35).

Furthermore, the model was representative of processes with different phosphine compounds as polymerization regulators and hence different rates of polymerization.

Bielawski and Grubbs reported that the use of phosphines with Grubbs' "first generation" catalyst enhances initiation characteristics and attenuates propagation, resulting in a system with increased living behaviour. In addition, the influence on the initiation and propagation rates increases with phosphine loading. The use of PPh_3 and PCy_3 yield similar enhancement in initiation characteristics. However, the decrease in propagation rate is higher when PPh_3 is used [7]. As expected and as demonstrated by experimental and simulation results, the polymerization of 1,5-COD in the presence of PPh_3 with $[\text{P}]_0/[\text{I}]_0$ ratio of 10 was slower than the polymerization CP in the presence of PCy_3 with $[\text{P}]_0/[\text{I}]_0$ ratio of 4.

4.4. Results and Discussion

Upon model validation, the model can be used in a detailed examination of the effects of various factors related to reagent type, reagent concentrations, and polymerization process conditions on reaction kinetics and molecular weight distribution. For example, the use of different types and concentrations of catalysts and/or monomers can yield different chain propagation and intermolecular chain transfer rates, the use of different types or concentrations of phosphines can result in different catalyst activation and deactivation rates, and the purity of the polymerization system can affect the catalyst decomposition rates. Thus, the influences of catalyst decomposition, catalyst activation and deactivation, and intermolecular chain transfer reactions on polymerization behaviour are studied.

The reaction conditions used in the following simulation study follow those listed in **Table 4.4**. The kinetic parameters used also follow those listed for Simulation 1 in **Table 4.5**, except the rate of intermolecular chain transfers (a value of 10^{-4} s^{-1} is used for k_{tr}) and unless otherwise stated. The rate of propagation was assumed to be faster than the rate of intermolecular chain transfer, which was assumed to be faster than the rate of catalyst decomposition (i.e. $k_p > k_{tr} > k_{de}$). Hence, catalyst deactivation occurs slower than intermolecular chain transfer and propagation, and intermolecular chain transfer occurs slower than propagation. As such, it would be possible to study the effects of catalyst deactivation and intermolecular chain transfer separately and independently. In

accordance to a living polymerization system, catalyst deactivation was assumed to occur at a faster rate than catalyst activation (i.e. $k_b/k_f > 1$).

4.4.1. Effects of Catalyst Decomposition

The effects of catalyst decomposition on polymerization kinetics and the resulting polymer products are shown in **Figure 4.4**. As indicated by **Figure 4.4 (a)**, different catalyst decomposition rates (with all other factors held constant) yielded the same initial rate of increase in conversion and molecular weight. As the catalyst decomposition rate increased, the increase in conversion and molecular weight tapered at lower reaction times and lower maximum conversion and molecular weight value were reached. **Figure 4.4 (b)** also shows that different catalyst decomposition rates resulted in similar trends in polydispersity. A gradual increase in polydispersity was observed. The tapering of conversion, molecular weight, and polydispersity increase was observed at approximately the same reaction time for each individual simulation.

When catalyst decomposition occurs, chain species with active and/or dormant catalyst centers become dead chain species. The dead chains species is unable to participate in chain propagation and intermolecular chain transfer reactions. Shorter polymer chains are formed by the dead chain species, while the remaining chain species with active and/or dormant catalyst continue to propagate. As a result, polydispersity is broadened with the presence of catalyst decomposition. When the catalyst decomposition rate is high, the increase in chain species with decomposed catalyst centers and the decrease in chain species with active and/or dormant catalyst centers are rapid. Propagation reactions are limited at a faster rate and hence, the maximum amount of converted monomer is lowered

and is reached at shorter reaction times. Chain transfer reactions, which occur at a slower rate than chain propagation, are also limited when catalyst decomposition is fast.

As shown by the time evolution of polydispersity with a catalyst decomposition rate of 10^{-6} s^{-1} , polydispersity was initially lowest compared to all of the simulations. At high reaction times when near complete catalyst decomposition is reached by simulations with catalyst decomposition rates of 10^{-4} s^{-1} and 10^{-5} s^{-1} , the simulation with catalyst decomposition rate of 10^{-6} s^{-1} still consists of chains with active and/or dormant catalysts. The continuing presence of intermolecular chain transfer reactions lead to further broadening of polydispersity at high reaction times.

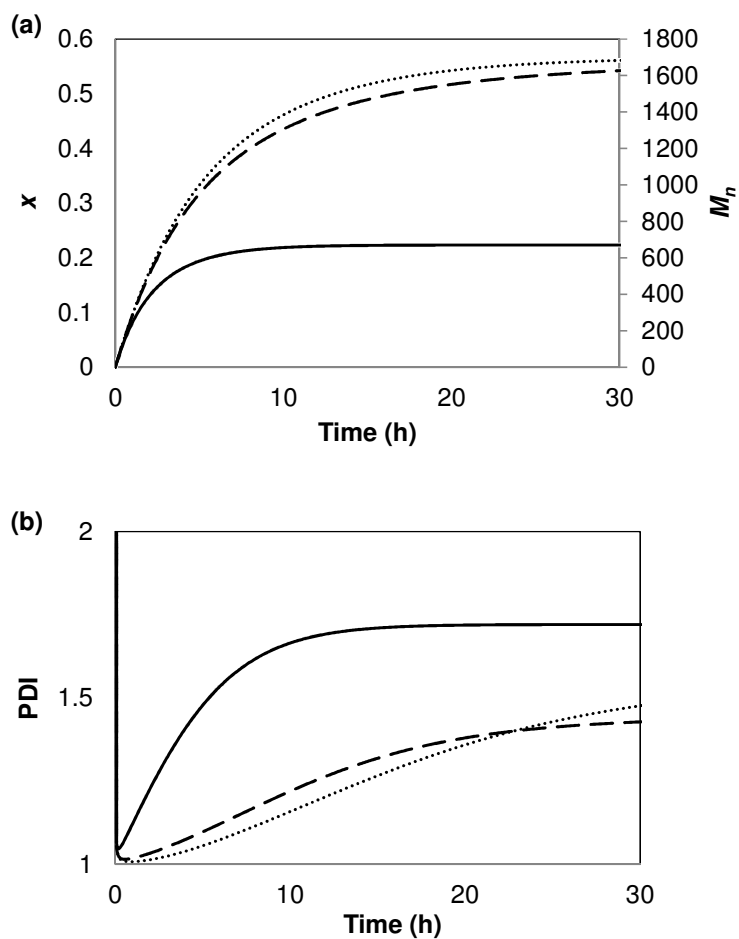


Figure 4.4. Effects of catalyst decomposition on the time evolution of (a) conversion and number-average molecular weight and (b) polydispersity in living ROMP. k_{de} values of 10^{-4} s^{-1} (solid line), 10^{-5} s^{-1} (dashed line), and 10^{-6} s^{-1} (dotted line) were used in simulation.

4.4.2. Effects of Catalyst Activation and Deactivation

Figure 4.5 illustrates the effects of catalyst activation and deactivation on polymerization kinetics and molecular weight distribution. Various ratios between the rates of catalyst deactivation and catalyst activation (i.e. k_b/k_f ratio) were used while all other factors were held constant. When catalyst deactivation is much faster than catalyst activation, the chain species are predominantly in the dormant state and not in the active state. Chain propagation (which leads to the formation of monodispersed polymers in a living polymerization system) and intermolecular chain transfer reactions (which leads to polydispersity broadening) can only occur when the chain species are in the active state and are limited.

As indicated in **Figure 4.5 (a)**, the slower overall propagation rate of simulations with fast catalyst deactivation resulted in a slower rate of increase in conversion and molecular weight. In addition, as shown in **Figure 4.5 (b)**, the slow overall propagation rate led to a slow rate of initial polydispersity decrease (i.e. prior to reaction time of 3 hours). However, due to the slower overall intermolecular chain transfer rate when catalyst deactivation is fast, the rate of increase in polydispersity was slower at long reaction times.

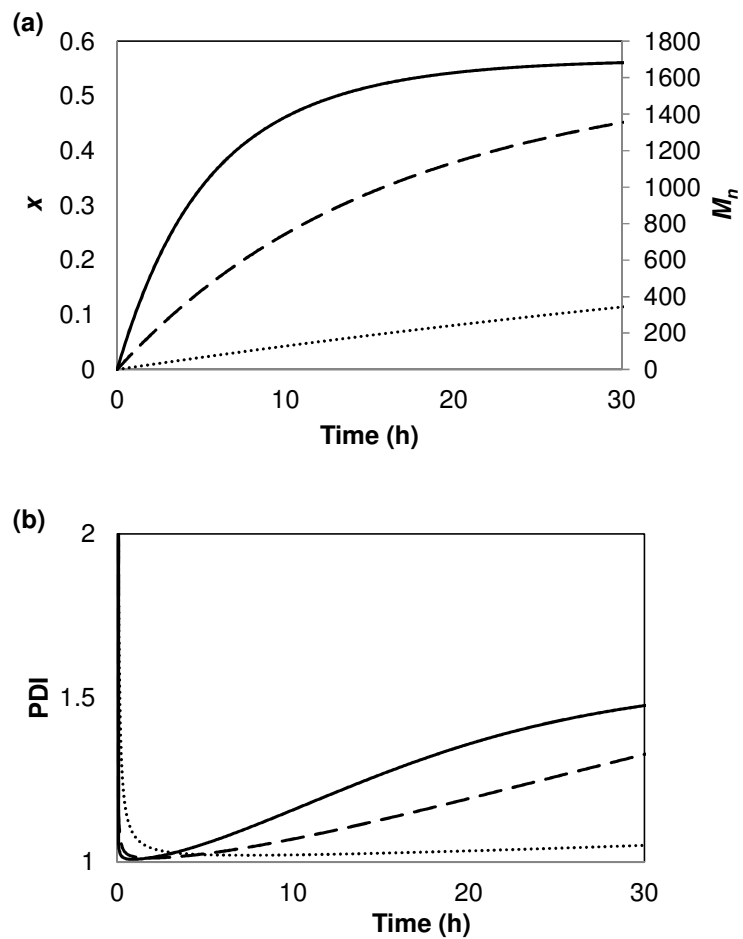


Figure 4.5. Effects of catalyst activation and deactivation on the time evolution of (a) conversion and number-average molecular weight and (b) polydispersity in living ROMP. k_b/k_f values of 100 (solid line), 1000 (dashed line), and 10,000 (dotted line) were used in simulation.

4.4.3. Effects of Intermolecular Chain Transfer Reactions

The effects of intermolecular chain transfer reactions on polymerization behaviour are provided in **Figure 4.6**. There were limited influences on the time evolution of conversion and molecular weight when the rate of intermolecular chain transfer reactions was varied. Chain species with active and/or dormant catalyst centers can participate in propagation, intermolecular chain transfer, or catalyst decomposition reactions. When the rate of intermolecular chain transfer increased (with all other factors are held constant), chain species with active and/or dormant catalyst centers were able to participate in intermolecular chain transfer reactions at earlier reaction times and at higher frequency. Thus, the overall propagation rate was lowered leading to a slightly slower increase in conversion and molecular weight, as indicated in **Figure 4.6 (a)**. Further, the increased intermolecular chain transfer reactions resulted in faster and more significant polydispersity broadening, as shown in **Figure 4.6 (b)**.

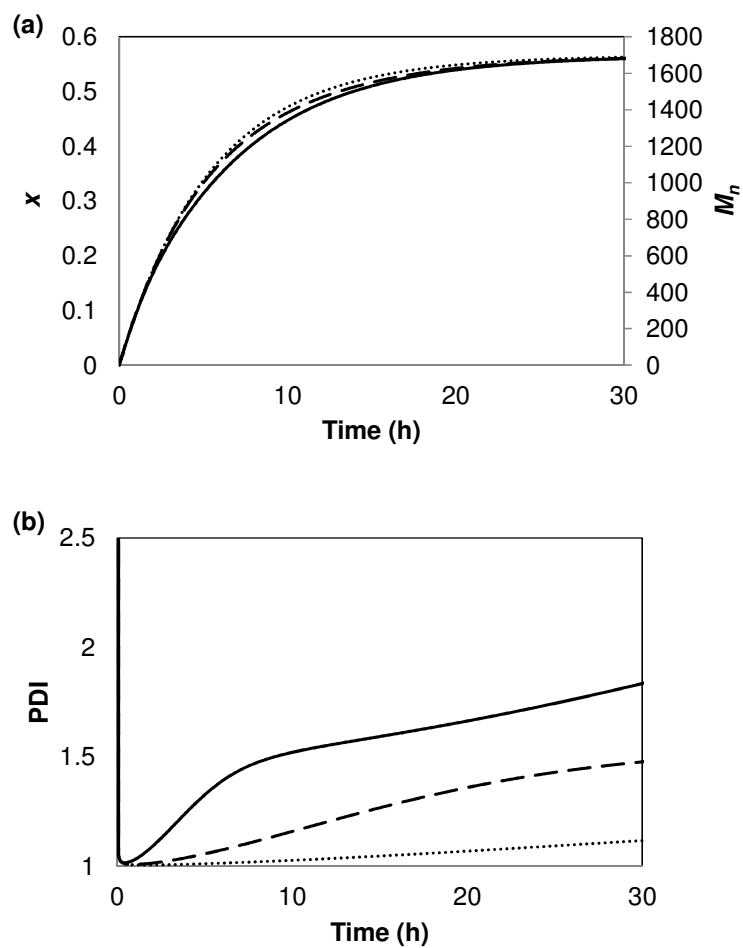


Figure 4.6. Effects of intermolecular chain transfer reactions on the time evolution of (a) conversion and number-average molecular weight and (b) polydispersity in living ROMP. $k_{tr, inter}$ values of 10^{-3} L mol⁻¹ s⁻¹ (solid line), 10^{-4} L mol⁻¹ s⁻¹ (dashed line), and 10^{-5} L mol⁻¹ s⁻¹ (dotted line) were used in simulation.

4.5. Conclusions

A model was developed using method of moments to describe the polymerization kinetics and the development of molecular weight distribution of ROMP. The model considered catalyst initiation, polymer chain propagation and depropagation, and catalyst activation and deactivation, along with non-idealities, including catalyst decomposition and intermolecular chain transfer reactions. Excellent representations of two contrasting ROMP processes were demonstrated in comparisons of simulated results with experimental data.

The model provided a good fit of experimental results obtained for the bulk ROMP of 1,5-COD via GI catalyst and PPh_3 when the non-idealities of intermolecular chain transfer reactions and catalyst decomposition were considered in the model. When the non-ideality of catalyst decomposition was considered negligible, the simulations failed to yield a representative model of monomer conversion and polydispersity at high conversions. When the non-ideality of intermolecular chain transfer reactions was considered negligible, the simulations greatly underestimated polydispersity at high conversions. The inclusion of intermolecular chain transfer reactions and catalyst decomposition were critical in obtaining a representative model of the kinetics and development of molecular weight distribution of the ROMP of 1,5-COD.

The model was also compared to published literature results obtained for the solution living ROMP of CP via GI catalyst and PCy₃. Compared to the bulk ROMP system, the solution ROMP system consisted of different monomer and initial monomer concentration. As a result, the significance of intermolecular chain transfer reactions was different. In addition, a different phosphine compound was used in the solution ROMP system, resulting in different chain propagation kinetics. However, the model demonstrated an overall good fit for this contrasting system. The time evolution of number-average molecular weight and the initial changes in polydispersities and conversions were well-described by the model. Polydispersity and conversions at higher reaction times were underestimated by the model due to chain transfer reactions to contaminants, which was not considered in the developed model.

The validated model was also used to study the effects of factors including reagent type, reagent concentrations, and polymerization process conditions on polymerization behaviour. An enhanced understanding of the impacts of catalyst decomposition, catalyst activation and deactivation, and intermolecular chain transfer reactions on ROMP behaviour was obtained. The validity and versatility of the model in describing ROMP not only yielded the model as a useful tool in gaining new insights into the ROMP mechanism, but also yielded the model as a valuable aid and as a potential predictive model in new experiment design and in process optimization.

4.6. References

- [1] S. B. Myers and R. A. Register, “Synthesis of Narrow-Distribution Polycyclopentene Using a Ruthenium Ring-Opening Metathesis Initiator,” *Polymer*, vol. 49, pp. 877–882, 2008.
- [2] S. T. Trzaska, L. W. Lee, and R. A. Register, “Synthesis of Narrow-Distribution ‘Perfect’ Polyethylene and Its Block Copolymers by Polymerization of Cyclopentene,” *Macromolecules*, vol. 33, pp. 9215–9221, 2000.
- [3] C. W. Bielawski and R. H. Grubbs, “Living Ring-Opening Metathesis Polymerization,” *Progress in Polymer Science*, vol. 32, pp. 1–29, 2007.
- [4] M. Ulman and R. H. Grubbs, “Ruthenium Carbene-Based Olefin Metathesis Initiators: Catalyst Decomposition and Longevity,” *The Journal of Organic Chemistry*, vol. 64, pp. 7202–7207, 1999.
- [5] S. H. Hong, A. G. Wenzel, T. T. Salguero, M. W. Day, and R. H. Grubbs, “Decomposition of Ruthenium Olefin Metathesis Catalysts,” *Journal of the American Chemical Society*, vol. 129, pp. 7961–7968, 2007.
- [6] H. J. V. D. Westhuizen, A. Roodt, and R. Meijboom, “Kinetics of Thermal Decomposition and of the Reaction with Oxygen, Ethene and 1-Octene of First Generation Grubbs’ Catalyst Precursor,” *Polyhedron*, vol. 29, pp. 2776–2779, 2010.
- [7] C. W. Bielawski and R. H. Grubbs, “Increasing the Initiation Efficiency of Ruthenium-Based Ring-Opening Metathesis Initiators: Effect of Excess Phosphine,” *Macromolecules*, vol. 34, pp. 8838–8840, 2001.
- [8] K. Seavey and Y. A. Liu, “Functional-Group Approach and the Method of Moments,” in *Step-Growth Polymerization Process Modeling and Product Design*, New Jersey: Hoboken, 2008, pp. 137–138.
- [9] S. Zhu, “Advances in Free-Radical Polymerization Kinetics,” McMaster University, 1991.
- [10] C. Bielawski, D. Benitez, and R. H. Grubbs, “Synthesis of Cyclic Polybutadiene via Ring-Opening Metathesis Polymerization: The Importance of Removing Trace Linear Contaminants,” *Journal of the American Chemical Society*, vol. 125, pp. 8424–8425, 2003.

- [11] J. A. Love, M. S. Sanford, M. W. Day, and R. H. Grubbs, “Synthesis, Structure, and Activity of Enhanced Initiators for Olefin Metathesis,” *Journal of the American Chemical Society*, vol. 125, pp. 10103–10109, 2003.
- [12] A. Duda and A. Kowalski, “Thermodynamics and Kinetics of Ring-Opening Polymerization,” in *Handbook of Ring-Opening Polymerization*, P. Dubois, O. Coulembier, and J.-M. Raquez, Eds. Weinheim: Wiley, 2009, pp. 1–51.
- [13] S. Penczek, M. Cypryk, A. Duda, P. Kubisa, and S. Słomkowski, “Living Ring-Opening Polymerization of Heterocyclic Monomers,” in *Controlled and Living Polymerizations: From Mechanisms to Applications*, A. H. E. Muller and K. Matyjaszewski, Eds. Weinheim: Wiley, 2009, pp. 241–295.
- [14] K. Matyjaszewski, “Introduction to Living Polymerization. Living and/or Controlled Polymerization,” *Journal of Physical Organic Chemistry*, vol. 8, pp. 197–207, 1995.
- [15] M. S. Sanford, M. Ulman, and R. H. Grubbs, “New Insights into the Mechanism of Ruthenium-Catalyzed Olefin Metathesis Reactions,” *Journal of the American Chemical Society*, vol. 123, pp. 749–750, 2001.

Appendices to Chapter 4

A.4.1. Reaction Mechanism

A detailed living ROMP reaction mechanism used for model development is given in **Table A.4.1.1**. A Grubbs' "first generation" catalyst is used as the catalyst and triphenylphosphine is used as the polymerization regulator. L_n , M , and R represents the $(Cl)_2PCy_3$ ligand, metal center, and Ph pendant group of the catalyst. I^D represents a decomposed catalyst. k_f , k_b , k_p , k_d , $k_{tr, inter}$, and k_{de} are the rates of catalyst activation, catalyst deactivation, propagation, depropagation, intermolecular chain transfer, and catalyst decomposition, respectively. A simplified symbolic representation of the reaction mechanism is shown beside the chemical structures. Refer to **List of Abbreviations and Symbols** for symbol details.

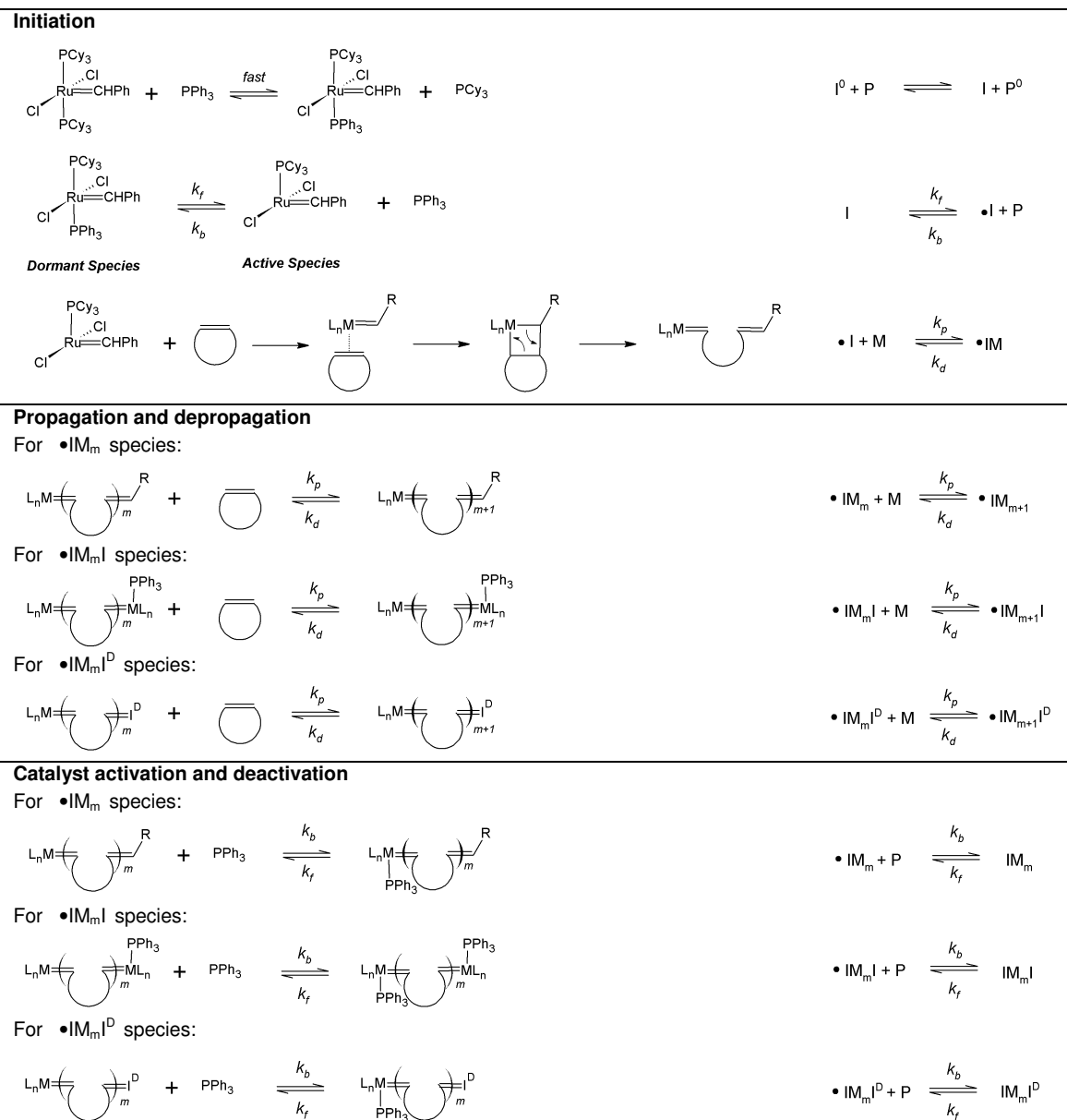
Table A.4.1.1. Detailed living ROMP mechanism used in model development [3], [7].

Table A.4.1.1. Continued

Intermolecular chain transfer reactions

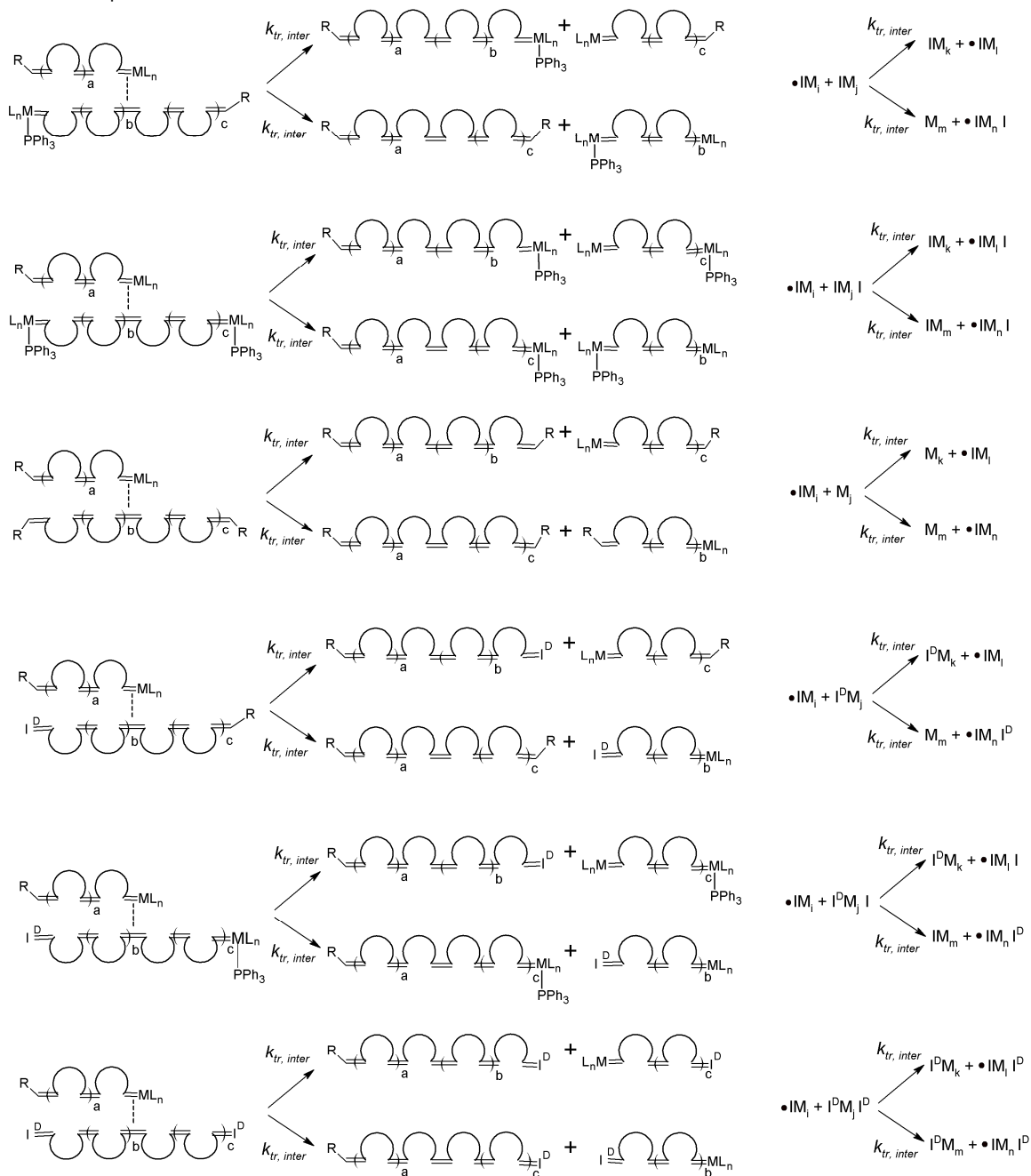
For $\bullet\text{IM}_m$ species:

Table A.4.1.1. Continued

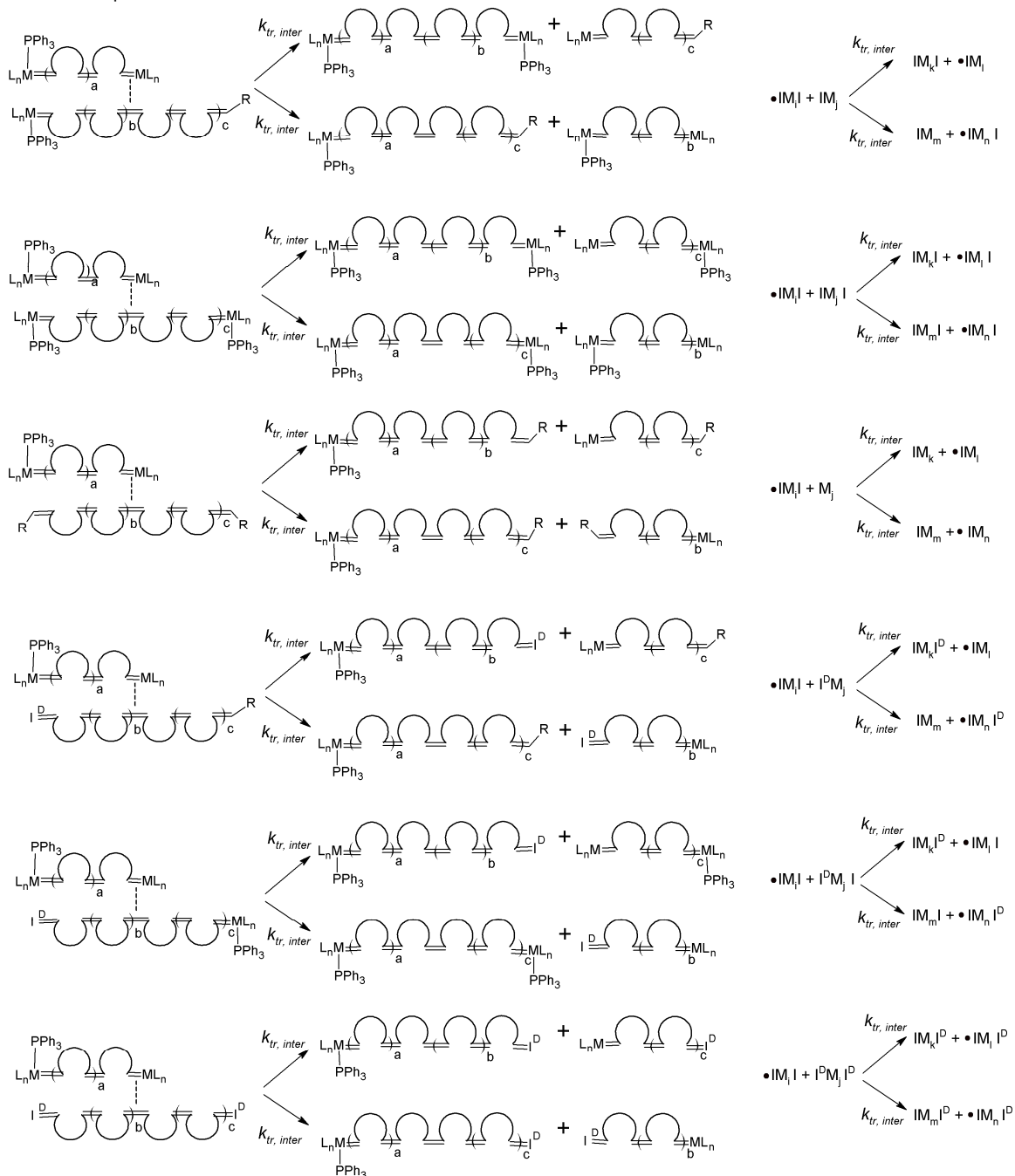
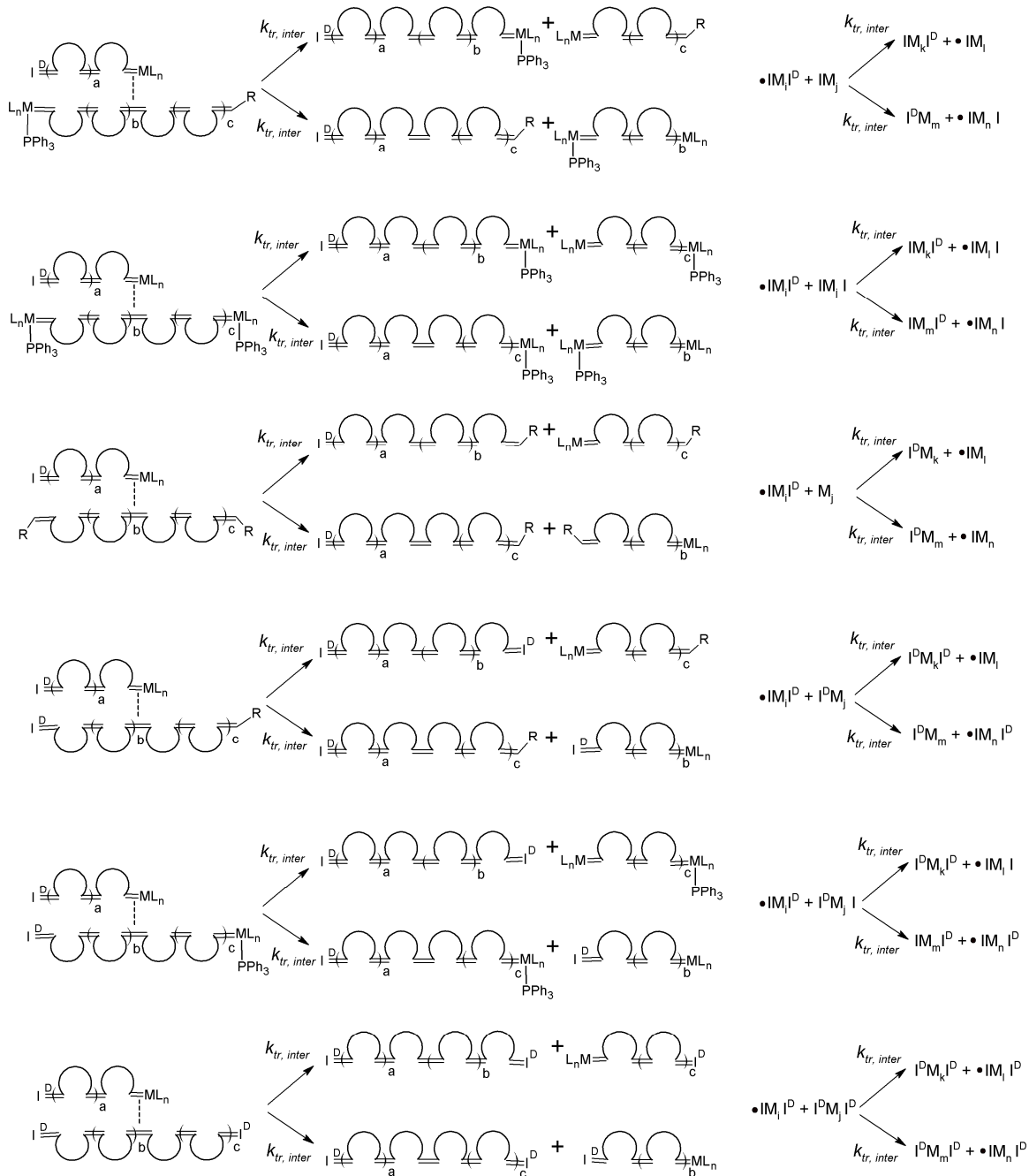
For $\bullet\text{IM}_m\text{I}$ species:

Table A.4.1.1. Continued

For $\bullet\text{IM}_m\text{I}^{\text{D}}$ species:

A.4.2. Mass Balance Equations

The mass balance equations for the formation of the nine chain species resulting from the living ROMP reaction mechanism used in model development are summarized in **Table A.4.2.1**.

A.4.2.1.

Table A.4.2.1. Mass balance equations for chain species formation in living ROMP.

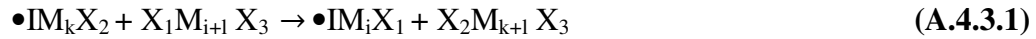
Species	Mass balance equation
$\bullet IM_i$	$\begin{aligned} \frac{d[\bullet IM_i]}{dt} = & k_p[\bullet IM_{i-1}][M] - k_p[\bullet IM_i][M] + k_d[\bullet IM_{i+1}] - k_d[\bullet IM_i] + k_f[IM_i] - \\ & k_b[\bullet IM_i][P] - k_{de}[\bullet IM_i] - k_{tr}[\bullet IM_i]([IQ_1] + \frac{1}{2}[IQ_1I] + \frac{1}{2}[Q_1] + \\ & [I^D Q_1] + [IQ_1I^D] + \frac{1}{2}[I^D Q_1I^D]) + k_{tr}(\frac{1}{2})(\sum_{k=1}^{\infty}[\bullet IM_k] \sum_{l=1}^{\infty}[IM_{i+l}] + \\ & \sum_{k=1}^{\infty}[\bullet IM_k] \sum_{l=1}^{\infty}[M_{i+l}] + \sum_{k=1}^{\infty}[\bullet IM_k] \sum_{l=1}^{\infty}[I^D M_{i+l}] + \\ & \sum_{k=1}^{\infty}[\bullet IM_k I] \sum_{l=1}^{\infty}[IM_{i+l}] + \sum_{k=1}^{\infty}[\bullet IM_k I] \sum_{l=1}^{\infty}[M_{i+l}] + \\ & \sum_{k=1}^{\infty}[\bullet IM_k I] \sum_{l=1}^{\infty}[I^D M_{i+l}] + \\ & \sum_{k=1}^{\infty}[\bullet IM_k I^D] \sum_{l=1}^{\infty}[IM_{i+l}] + \sum_{k=1}^{\infty}[\bullet IM_k I^D] \sum_{l=1}^{\infty}[M_{i+l}] + \\ & \sum_{k=1}^{\infty}[\bullet IM_k I^D] \sum_{l=1}^{\infty}[I^D M_{i+l}]) \end{aligned} \quad (A.4.2.1)$
$\bullet IM_i I$	$\begin{aligned} \frac{d[\bullet IM_i I]}{dt} = & k_p[\bullet IM_{i-1} I][M] - k_p[\bullet IM_i I][M] + k_d[\bullet IM_{i+1} I] - k_d[\bullet IM_i I] + \\ & 2k_f[IM_i I] - k_b[\bullet IM_i I][P] - 2k_{de}[\bullet IM_i I] - k_{tr}[\bullet IM_i I]([IQ_1] + \\ & \frac{1}{2}[IQ_1I] + \frac{1}{2}[Q_1] + [I^D Q_1] + [IQ_1I^D] + \frac{1}{2}[I^D Q_1I^D]) + \\ & k_{tr}(\frac{1}{2})(\sum_{k=1}^{\infty}[\bullet IM_k] \sum_{l=1}^{\infty}[IM_{i+l}] + \sum_{k=1}^{\infty}[\bullet IM_k] \sum_{l=1}^{\infty}[IM_{i+l}I] + \\ & \sum_{k=1}^{\infty}[\bullet IM_k] \sum_{l=1}^{\infty}[IM_{i+l}I^D] + \sum_{k=1}^{\infty}[\bullet IM_k I] \sum_{l=1}^{\infty}[IM_{i+l}] + \\ & \sum_{k=1}^{\infty}[\bullet IM_k I] \sum_{l=1}^{\infty}[IM_{i+l}I] + \sum_{k=1}^{\infty}[\bullet IM_k I] \sum_{l=1}^{\infty}[IM_{i+l}I^D] + \\ & \sum_{k=1}^{\infty}[\bullet IM_k I^D] \sum_{l=1}^{\infty}[IM_{i+l}] + \sum_{k=1}^{\infty}[\bullet IM_k I^D] \sum_{l=1}^{\infty}[IM_{i+l}I] + \\ & \sum_{k=1}^{\infty}[\bullet IM_k I^D] \sum_{l=1}^{\infty}[IM_{i+l}I^D]) \end{aligned} \quad (A.4.2.2)$

Table A.4.2.1. Continued

Species	Mass balance equation
$\bullet IM_i I^D$	$\begin{aligned} \frac{d[\bullet IM_i I^D]}{dt} = & k_p[\bullet IM_{i-1} I^D][M] - k_p[\bullet IM_i I^D][M] + k_d[\bullet IM_{i+1} I^D] - k_d[\bullet IM_i I^D] + \\ & k_f[IM_i I^D] - k_b[\bullet IM_i I^D][P] + k_{de}[\bullet IM_i I] - k_{de}[\bullet IM_i I^D] - \\ & k_{tr}[\bullet IM_i I^D]N([IQ_1] + \frac{1}{2}[IQ_1 I] + \frac{1}{2}[Q_1] + [I^D Q_1] + [IQ_1 I^D] + \\ & \frac{1}{2}[I^D Q_1 I^D]) + \\ & k_{tr}(\frac{1}{2})(\sum_{k=1}^{\infty}[\bullet IM_k] \sum_{l=1}^{\infty}[I^D M_{i+l}] + \sum_{k=1}^{\infty}[\bullet IM_k] \sum_{l=1}^{\infty}[IM_{i+l} I^D] + \\ & \sum_{k=1}^{\infty}[\bullet IM_k] \sum_{l=1}^{\infty}[I^D M_{i+l} I^D] + \sum_{k=1}^{\infty}[\bullet IM_k I] \sum_{l=1}^{\infty}[I^D M_{i+l}] + \\ & \sum_{k=1}^{\infty}[\bullet IM_k I] \sum_{l=1}^{\infty}[IM_{i+l} I^D] + \sum_{k=1}^{\infty}[\bullet IM_k I] \sum_{l=1}^{\infty}[I^D M_{i+l} I^D] + \\ & \sum_{k=1}^{\infty}[\bullet IM_k I^D] \sum_{l=1}^{\infty}[I^D] + \sum_{k=1}^{\infty}[\bullet IM_k I^D] \sum_{l=1}^{\infty}[IM_{i+l} I^D] + \\ & \sum_{k=1}^{\infty}[\bullet IM_k I^D] \sum_{l=1}^{\infty}[I^D M_{i+l} I^D]) \end{aligned} \quad (\text{A.4.2.3})$
IM_i	$\begin{aligned} \frac{d[IM_i]}{dt} = & -k_f[IM_i] + k_b[\bullet IM_i][P] - k_{de}[IM_i] - k_{tr}[IQ_{j+1}]([\bullet IQ_0] + [\bullet IQ_0 I] + \\ & [\bullet IQ_0 I^D]) + \\ & k_{tr}(\frac{1}{2})\{\sum_{k=1}^i\{[\bullet IM_k] \sum_{l=1}^{\infty}[IM_{l+i-k}]\} + \sum_{k=1}^i\{[\bullet IM_k] \sum_{l=1}^{\infty}[IM_{l+i-k} I]\} + \\ & \sum_{k=1}^i\{[\bullet IM_k] \sum_{l=1}^{\infty}[IM_{l+i-k} I^D]\} + \sum_{k=1}^i\{[\bullet IM_k I] \sum_{l=1}^{\infty}[IM_{l+i-k}]\} + \\ & \sum_{k=1}^i\{[\bullet IM_k I] \sum_{l=1}^{\infty}[M_{l+i-k}]\} + \sum_{k=1}^i\{[\bullet IM_k I] \sum_{l=1}^{\infty}[I^D M_{l+i-k}]\}\} \end{aligned} \quad (\text{A.4.2.4})$
$IM_i I$	$\begin{aligned} \frac{d[IM_i I]}{dt} = & -2k_f[IM_i I] + k_b[\bullet IM_i I][P] - 2k_{de}[IM_i I] - k_{tr}(\frac{1}{2})[IQ_{j+1} I]([\bullet IQ_0] + \\ & [\bullet IQ_0 I] + [\bullet IQ_0 I^D]) + k_{tr}(\frac{1}{2})\{\sum_{k=1}^i\{[\bullet IM_k I] \sum_{l=1}^{\infty}[IM_{l+i-k}]\} + \\ & \sum_{k=1}^i\{[\bullet IM_k I] \sum_{l=1}^{\infty}[IM_{l+i-k} I]\} + \sum_{k=1}^i\{[\bullet IM_k I] \sum_{l=1}^{\infty}[IM_{l+i-k} I^D]\}\} \end{aligned} \quad (\text{A.4.2.5})$
$IM_i I^D$	$\begin{aligned} \frac{d[IM_i I^D]}{dt} = & -k_f[IM_i I^D] + k_b[\bullet IM_i I^D][P] + k_{de}[\bullet IM_i I] + 2k_{de}[IM_i I] - \\ & k_{de}[IM_i I^D] - k_{tr}[IQ_{j+1} I^D]([\bullet IQ_0] + [\bullet IQ_0 I] + [\bullet IQ_0 I^D]) + \\ & k_{tr}(\frac{1}{2})\{\sum_{k=1}^i\{[\bullet IM_k I] \sum_{l=1}^{\infty}[I^D M_{l+i-k}]\} + \\ & \sum_{k=1}^i\{[\bullet IM_k I] \sum_{l=1}^{\infty}[IM_{l+i-k} I^D]\} + \sum_{k=1}^i\{[\bullet IM_k I] \sum_{l=1}^{\infty}[I^D M_{l+i-k} I^D]\} + \\ & \sum_{k=1}^i\{[\bullet IM_k I^D] \sum_{l=1}^{\infty}[IM_{l+i-k}]\} + \sum_{k=1}^i\{[\bullet IM_k I^D] \sum_{l=1}^{\infty}[IM_{l+i-k} I]\} + \\ & \sum_{k=1}^i\{[\bullet IM_k I^D] \sum_{l=1}^{\infty}[IM_{l+i-k} I^D]\}\} \end{aligned} \quad (\text{A.4.2.6})$
$I^D M_i$	$\begin{aligned} \frac{d[I^D M_i]}{dt} = & k_{de}[IM_i] + k_{de}[\bullet IM_i] - k_{tr}[I^D Q_{j+1}]([\bullet IQ_0] + [\bullet IQ_0 I] + [\bullet IQ_0 I^D]) + \\ & k_{tr}(\frac{1}{2})\{\sum_{k=1}^i\{[\bullet IM_k] \sum_{l=1}^{\infty}[I^D M_{l+i-k}]\} + \\ & \sum_{k=1}^i\{[\bullet IM_k] \sum_{l=1}^{\infty}[IM_{l+i-k} I^D]\} + \sum_{k=1}^i\{[\bullet IM_k] \sum_{l=1}^{\infty}[I^D M_{l+i-k} I^D]\} + \\ & \sum_{k=1}^i\{[\bullet IM_k I^D] \sum_{l=1}^{\infty}[IM_{l+i-k}]\} + \sum_{k=1}^i\{[\bullet IM_k I^D] \sum_{l=1}^{\infty}[M_{l+i-k}]\} + \\ & \sum_{k=1}^i\{[\bullet IM_k I^D] \sum_{l=1}^{\infty}[I^D M_{l+i-k}]\}\} \end{aligned} \quad (\text{A.4.2.7})$
$I^D M_i I^D$	$\begin{aligned} \frac{d[I^D M_i I^D]}{dt} = & k_{de}[\bullet IM_i I^D] + k_{de}[IM_i I^D] - k_{tr}(\frac{1}{2})[I^D Q_{j+1} I^D]([\bullet IQ_0] + [\bullet IQ_0 I] + \\ & [\bullet IQ_0 I^D]) + \\ & k_{tr}(\frac{1}{2})\{\sum_{k=1}^i\{[\bullet IM_k I^D] \sum_{l=1}^{\infty}[I^D M_{l+i-k}]\} + \\ & \sum_{k=1}^i\{[\bullet IM_k I^D] \sum_{l=1}^{\infty}[IM_{l+i-k} I^D]\} + \sum_{k=1}^i\{[\bullet IM_k I^D] \sum_{l=1}^{\infty}[I^D M_{l+i-k} I^D]\}\} \end{aligned} \quad (\text{A.4.2.8})$
M_i	$\begin{aligned} \frac{d[M_i]}{dt} = & -k_{tr}(\frac{1}{2})[Q_{j+1}]([\bullet IQ_0] + [\bullet IQ_0 I] + [\bullet IQ_0 I^D]) + \\ & k_{tr}(\frac{1}{2})\{\sum_{k=1}^i\{[\bullet IM_k] \sum_{l=1}^{\infty}[IM_{l+i-k}]\} + \\ & \sum_{k=1}^i\{[\bullet IM_k] \sum_{l=1}^{\infty}[M_{l+i-k}]\} + \sum_{k=1}^i\{[\bullet IM_k] \sum_{l=1}^{\infty}[I^D M_{l+i-k}]\}\} \end{aligned} \quad (\text{A.4.2.9})$

A.4.3. Mathematical Approximations for Generation of Species with Active Catalyst Centers via Chain Transfer Reactions

As shown in **Appendix A.4.1**, the generation of species with active catalyst centers ($\bullet\text{IM}_i$, $\bullet\text{IM}_i\text{I}$, and $\bullet\text{IM}_i\text{I}^{\text{D}}$) via chain transfer reactions follow the general reaction scheme below:



where X_1 , X_2 , and X_3 can be the pendant group from the catalyst (R), a dormant catalyst (I), or a decomposed catalyst (I^{D}), and i , k , and l are the number of monomers on the chains.

The generation of species $\bullet\text{IM}_i\text{X}_1$ with respect to time as a result of reaction (A.4.3.1) is given by:

$$\frac{d[\bullet\text{IM}_i\text{X}_1]}{dt} = k_{tr} \sum_{k=1}^{\infty} [\bullet\text{IM}_k\text{X}_2] \sum_{l=1}^{\infty} [\text{X}_1\text{M}_{i+l}\text{X}_3] \quad (\text{A.4.3.2})$$

The moment equation of the j^{th} order for the above expression is given by:

$$\begin{aligned} \frac{d[\bullet\text{I}Q_j\text{X}_1]}{dt} &= \sum_{i=1}^{\infty} \{i^j k_{tr} \sum_{k=1}^{\infty} [\bullet\text{IM}_k\text{X}_2] \sum_{l=1}^{\infty} [\text{X}_1\text{M}_{i+l}\text{X}_3]\} \\ &= k_{tr} [\bullet\text{I}Q_0\text{X}_2] \sum_{i=1}^{\infty} (i^j \sum_{l=1}^{\infty} [\text{X}_1\text{M}_{i+l}\text{X}_3]) \\ &= k_{tr} [\bullet\text{I}Q_0\text{X}_2] \sum_{m=2}^{\infty} ([\text{X}_1\text{M}_m\text{X}_3] \sum_{i=1}^{m-1} i^j) \end{aligned} \quad (\text{A.4.3.3.a})$$

Using the approximation:

$$\sum_{i=1}^{m-1} i^j \doteq \int_0^m i^j di = \frac{m^{j+1}}{j+1}, \quad (\text{A.4.3.4})$$

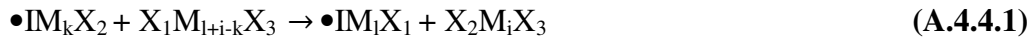
Eq. (A.4.3.3.a) becomes:

$$\begin{aligned} \frac{d[\bullet I Q_j X_1]}{dt} &= k_{tr} [\bullet I Q_0 X_2] \sum_{m=2}^{\infty} \left\{ [X_1 M_m X_3] \frac{m^{j+1}}{j+1} \right\} \\ &= \frac{1}{j+1} k_{tr} [\bullet I Q_0 X_2] [X_1 Q_{j+1} X_3] \end{aligned} \quad (\text{A.4.3.3.b})$$

Eq. (A.4.3.3.b) is used in the moment equations for chain species $\bullet IM_i$, $\bullet IM_i I$, and $\bullet IM_i I^D$.

A.4.4. Mathematical Approximations for Generation of Species without Active Catalyst Centers via Chain Transfer Reactions

As shown in **Appendix A.4.1**, the generation of species without active catalyst centers (IM_i , IM_iI , M_i , $I^D M_i$, $IM_i I^D$, and $I^D M_i I^D$) via chain transfer reactions follow the general reaction scheme below:



where X_1 , X_2 , and X_3 can be the pendant group from the catalyst (R), a dormant catalyst (I), or a decomposed catalyst (I^D), and i , k , and l are the number of monomers on the chains.

The generation of species $X_2 M_i X_3$ with respect to time as a result of reaction (A.4.4.1) is given by:

$$\frac{d[X_2 I M_i X_3]}{dt} = k_{tr} \sum_{k=1}^i \{ [\bullet I M_k X_2] \sum_{l=1}^{\infty} [X_1 M_{l+i-k} X_3] \} \quad (\text{A.4.4.2})$$

The moment equation of the j^{th} order for the above expression is given by:

$$\frac{d[X_2 I Q_j X_3]}{dt} = \sum_{i=1}^{\infty} \{ i^j k_{tr} \sum_{k=1}^i ([\bullet I M_k X_2] \sum_{l=1}^{\infty} [X_1 M_{l+i-k} X_3]) \} \quad (\text{A.4.4.3.a})$$

which can be expanded into:

$$\begin{aligned}
 \frac{d[X_2IQ_jX_3]}{dt} &= k_{tr}[\bullet IM_1X_2] \sum_{m=1}^{\infty} \{ [X_1M_mX_3] \sum_{i=1}^m i^j \} \\
 &+ k_{tr}[\bullet IM_2X_2] \sum_{m=1}^{\infty} \{ [X_1M_mX_3] \sum_{i=2}^{m+1} i^j \} \\
 &+ k_{tr}[\bullet IM_3X_2] \sum_{m=1}^{\infty} \{ [X_1M_mX_3] \sum_{i=3}^{m+2} i^j \} + \dots
 \end{aligned} \tag{A.4.4.3.b}$$

Using the approximation:

$$\begin{aligned}
 \sum_{i=s}^{m+s-1} i^j &\doteq \sum_{i=s}^{m+s} i^j \\
 &\doteq \int_s^{m+s} i^j di \\
 &= \frac{(m+s)^{j+1} - s^{j+1}}{j+1} \\
 &= \frac{\sum_{r=0}^{j+1} \binom{j+1}{r} (m^{j+1-r} (s^r) - s^{j+1})}{j+1} \\
 &= \frac{\sum_{r=0}^j \binom{j+1}{r} (m^{j+1-r} (s^r))}{j+1}
 \end{aligned} \tag{A.4.4.4}$$

Eq. (A.4.4.3.b) becomes:

$$\begin{aligned}
 \frac{d[X_2IQ_jX_3]}{dt} &= k_{tr}[\bullet IM_1X_2] \sum_{m=1}^{\infty} \left\{ [X_1M_mX_3] \frac{\sum_{r=0}^j \binom{j+1}{r} (m^{j+1-r})}{j+1} \right\} \\
 &+ k_{tr}[\bullet IM_2X_2] \sum_{m=1}^{\infty} \left\{ [X_1M_mX_3] \frac{\sum_{r=0}^j \binom{j+1}{r} (m^{j+1-r})(2^r)}{j+1} \right\} \\
 &+ k_{tr}[\bullet IM_3X_2] \sum_{m=1}^{\infty} \left\{ [X_1M_mX_3] \frac{\sum_{r=0}^j \binom{j+1}{r} (m^{j+1-r})(3^r)}{j+1} \right\} + \dots
 \end{aligned}$$

$$\begin{aligned}
&= k_{tr}[\bullet IM_1 X_2] \sum_{m=1}^{\infty} \left\{ \frac{m}{j+1} [X_1 M_m X_3] \sum_{r=0}^j \binom{j+1}{r} (m^{j-r}) \right\} \\
&\quad + k_{tr}[\bullet IM_2 X_2] \sum_{m=1}^{\infty} \left\{ \frac{m}{j+1} [X_1 M_m X_3] \sum_{r=0}^j \binom{j+1}{r} (m^{j-r})(2^r) \right\} \\
&\quad + k_{tr}[\bullet IM_3 X_2] \sum_{m=1}^{\infty} \left\{ \frac{m}{j+1} [X_1 M_m X_3] \sum_{r=0}^j \binom{j+1}{r} (m^{j-r})(3^r) \right\} + \dots \\
&= k_{tr} \left\{ \sum_{m=1}^{\infty} [\bullet IM_m X_2] \right\} \left\{ \frac{\sum_{m=1}^{\infty} [X_1 M_m X_3] (m^{j+1})}{j+1} \right\} \\
&\quad + k_{tr} \left\{ \sum_{m=1}^{\infty} m [\bullet IM_m X_2] \right\} \left\{ \sum_{m=1}^{\infty} [X_1 M_m X_3] (m^j) \right\} \\
&\quad + k_{tr} \left\{ \sum_{m=1}^{\infty} m^2 [\bullet IM_m X_2] \right\} \left\{ \sum_{m=1}^{\infty} [X_1 M_m X_3] (m^{j-1}) \right\} \left[\frac{\binom{j+1}{2}}{j+1} \right] + \dots \\
&\quad + k_{tr} \left\{ \sum_{m=1}^{\infty} m^t [\bullet IM_m X_2] \right\} \left\{ \sum_{m=1}^{\infty} [X_1 M_m X_3] (m^{j-t+1}) \right\} \left[\frac{\binom{j+1}{t}}{j+1} \right]
\end{aligned} \tag{A.4.4.3.c}$$

where $t = 0, 1, 2, 3, \dots, j$

The following shorthand notation for **Eq. (A.4.4.3.c)** will be used:

$$\frac{d[X_2 I Q_j X_3]}{dt} = f(j, [\bullet IM X_2], [X_1 M X_3]) \tag{A.4.4.3.d}$$

The zeroth, first, and second order moments are necessary to obtain monomer conversion and average molecular weight distribution. The moments of the zeroth, first, and second order of **Eq. (A.4.4.3.c)** has the form:

$$\begin{aligned}\frac{d[X_2IQ_0X_3]}{dt} &= f(0, [IMX_2], [X_1MX_3]) \\ &= k_{tr}[IQ_0X_2][X_1Q_1X_3]\end{aligned}\quad (\text{A.4.4.5})$$

$$\begin{aligned}\frac{d[X_2IQ_1X_3]}{dt} &= f(1, [IMX_2], [X_1MX_3]) \\ &= k_{tr}\left\{\frac{1}{2}[IQ_0X_2][X_1Q_2X_3] + [IQ_1X_2][X_1Q_1X_3]\right\}\end{aligned}\quad (\text{A.4.4.6})$$

$$\begin{aligned}\frac{d[X_2IQ_2X_3]}{dt} &= f(2, [IMX_2], [X_1MX_3]) \\ &= k_{tr}\left\{\frac{1}{3}[IQ_0X_2][X_1Q_3X_3] + [IQ_1X_2][X_1Q_2X_3] \right. \\ &\quad \left. + [IQ_2X_2][X_1Q_3X_3]\right\}\end{aligned}\quad (\text{A.4.4.7})$$

Eq. (A.4.4.5) to **(A.4.4.7)** are used in the moment equations for chain species IM_i , IM_iI , M_i , $I^D M_i$, $IM_i I^D$, and $I^D M_i I^D$.

5. Conclusions and Recommendations

5.1. Conclusions

The purpose of this work was to study the synthesis of low molecular weight polyethylenes (PE) and PE mimics with narrow distributions and controlled structures and functionalization. Low molecular weight polymeric materials have vast applications. To ensure consistent materials performance, polymers with narrow distributions and controlled structures are necessary. To allow for polymer processing and application in various media, tunable polymer functionalization is required. Thus, simple PEs and PE mimics with molecular weights in the order of 10^3 g/mol, with polydispersities of less than 1.20, and that allow for chain-end and/or backbone functionalization were the focus.

Various polymerization systems exist for the production of low molecular weight PE and PE mimics with narrow polydispersities and functionalization possibilities. **Chapter 2** summarized four promising polymerization systems, including living ring-opening metathesis polymerization (ROMP), living coordination polymerization, coordinative chain transfer polymerization (CCTP), and living C1 polymerization via polyhomologation. Analysis and comparisons of polymeric product, reaction efficiency, cost, and safety for each polymerization system indicated that each system has its respective advantages and disadvantages. CCTP and C1 polymerization yield product with the lowest molecular weights and polydispersities. However, the applications of

CCTP and C1 polymerization are limited by the availability of CCTP and C1 polymerization raw materials and the low turnover frequencies of C1 polymerization. ROMP and living coordination polymerization yield product with slightly higher molecular weights and polydispersities, but require raw materials that are readily available. Due to the industrial relevance of ROMP polymers, the availability of raw materials, and the ease of polymerization system setup, living ROMP was selected for study.

The experimental study of the synthesis of narrowly distributed low molecular weight polymers via living ROMP was summarized in **Chapter 3**. The efficient synthesis of narrowly distributed low molecular product via living ROMP faces several challenges. Firstly, polydispersity broadening is observed due to slow initiation and chain termination. Also, living ROMP is generally carried out as solution polymerization processes, which require large volumes of solvents and energy intensive post-polymerization separation processes. The two challenges were addressed by the use of excess phosphines as a polymerization regulator and the implementation of bulk polymerization.

A ROMP system consisting of 1,5-cyclooctadiene (1,5-COD) as the monomer, Grubbs' "first generation" ruthenium catalyst (GI catalyst) as the catalyst, and triphenylphosphine (PPh₃) as the polymerization regulator was used in the experimental study. Bulk ROMP in the absence of phosphine was demonstrated to yield product with similar and/or

improved molecular weight control and at similar conversions compared to solution ROMP. In bulk polymerization, the monomer concentration remains above the equilibrium monomer concentration over a larger concentration range. As a result, polydispersity is not broadened through propagation-depropagation equilibrium. In the presence of phosphine, similar observations were made. In addition, with increasing phosphine loading, a decrease in molecular weight, polydispersity, and conversion was observed in solution and bulk systems. Kinetic study of bulk ROMP confirmed living polymerization features. The success of ROMP as a bulk process yield ROMP as a promising and viable polymerization pathway for the production of narrowly distributed low molecular weight polymers with functionalization possibilities.

To further the potential for commercial application of ROMP, a model of ROMP was developed and was presented in **Chapter 4**. The method of moments was applied in the development of a realistic model that considered non-idealities, including intermolecular chain transfer reactions and catalyst decomposition. Validation with experimental data obtained for the bulk ROMP of 1,5-COD and published literature data obtained for the solution ROMP of cyclopentene (CP) confirmed the ability of the model to correctly represent ROMP systems with various reagents, kinetic parameters, and polymerization process conditions. The model was demonstrated to be a useful tool in providing an enhanced understanding of living ROMP and may also be applied in new experiment design and in process optimization during commercial implementation.

5.2. Recommendations

Living ROMP, living coordination polymerization, CCTP, and living C1 polymerization have been highlighted as promising pathways for the synthesis of narrowly distributed low molecular weight PEs and PE mimics with various chain-end and backbone functionalization. With such a diverse range of catalyst systems and monomers, it is possible to realise polymeric materials with tailored material performance.

As a result of the extensive progress in new catalyst and polymerization reaction development, there has been great success in bench scale production of narrowly distributed, low molecular weight polymers with functionalization possibility. While advancing research and development continues to open new possibilities in molecular weight distribution control and polymer architecture control, scale up development must follow to enable viable practical applications of these new technologies.

From the four highlighted polymerization pathways, living ROMP and living coordination polymerization are two pathways where many or most of the raw materials are commercially available. However, these two pathways yield polymers with molecular weights and polydispersities that are in the upper limit of the desired range. As demonstrated in this work, the transformation of living ROMP from a solution process into a bulk process is a preliminary optimization step in enabling practical application of living ROMP. Under the reaction conditions studied, polymers with molecular weights in

the range of 10^3 g/mol and polydispersities of under 1.50 can be produced at room temperature within 24 hours. However, low conversions of less than 20% were obtained. Various counteracting processes occur in the bulk ROMP process. One catalyst is responsible for the growth of one polymer chain in ROMP. To obtain polymeric product with low molecular weight at high conversion, a high catalyst to monomer ratio is necessary. However, the cost of operation would increase with catalyst loading. Furthermore, to enable the production of narrowly distributed product, the use of excess phosphines was demonstrated to be a promising solution. Excess phosphines enhances initiation behaviour and attenuates propagation rate. Although product with low polydispersities can be produced, long reaction times are necessary. As such, optimization of bulk ROMP, which can be aided by the developed mathematical model, is necessary to yield this polymerization system as a commercially viable process. Similarly, optimization of living coordination polymerization may yield current catalyst systems to be commercially applicable.

In contrast to living ROMP and living coordination polymerization, CCTP and living C1 polymerization yield low molecular weight product with extremely narrow polydispersities, but require the use of raw materials that are not readily available. As such, the syntheses of catalysts and monomers should be studied. The scale-up development of time efficient and cost effective catalyst and monomer syntheses will address the current limitations and may yield CCTP and living C1 polymerization as

viable and practical processes for the synthesis of well-defined low molecular weight polymers in the future.